Current Nanoscience, 2020, *16*, 321-362

REVIEW ARTICLE

A Review on Electrospun Luminescent Nanofibers: Photoluminescence Characteristics and Potential Applications

Gibin George[1] and Zhiping Luo[1,*]

[1]*Department of Chemistry and Physics, Fayetteville State University, Fayetteville, NC, USA*

Abstract: ***Background*:** Photoluminescent materials have been used for diverse applications in the fields of science and engineering, such as optical storage, biological labeling, noninvasive imaging, solid-state lasers, light-emitting diodes, theranostics/theragnostics, up-conversion lasers, solar cells, spectrum modifiers, photodynamic therapy remote controllers, optical waveguide amplifiers and temperature sensors. Nanosized luminescent materials could be ideal candidates in these applications.

***Objective*:** This review is to present a brief overview of photoluminescent nanofibers obtained through electrospinning and their emission characteristics.

***Methods*:** To prepare bulk-scale nanosized materials efficiently and cost-effectively, electrospinning is a widely used technique. By the electrospinning method, a sufficiently high direct-current voltage is applied to a polymer solution or melt; and at a certain critical point when the electrostatic force overcomes the surface tension, the droplet is stretched to form nanofibers. Polymer solutions or melts with a high degree of molecular cohesion due to intermolecular interactions are the feedstock. Subsequent calcination in air or specific gas may be required to remove the organic elements to obtain the desired composition.

***Results*:** The luminescent nanofibers are classified based on the composition, structure, and synthesis material. The photoluminescent emission characteristics of the nanofibers reveal intriguing features such as polarized emission, energy transfer, fluorescent quenching, and sensing. An overview of the process, controlling parameters and techniques associated with electrospinning of organic, inorganic and composite nanofibers are discussed in detail. The scope and potential applications of these luminescent fibers also conversed.

***Conclusion*:** The electrospinning process is a matured technique to produce nanofibers on a large scale. Organic nanofibers have exhibited superior fluorescent emissions for waveguides, LEDs and lasing devices, and inorganic nanofibers for high-end sensors, scintillators, and catalysts. Multifunctionalities can be achieved for photovoltaics, sensing, drug delivery, magnetism, catalysis, and so on. The potential of these nanofibers can be extended but not limited to smart clothing, tissue engineering, energy harvesting, energy storage, communication, safe data storage, *etc.* and it is anticipated that in the near future, luminescent nanofibers will find many more applications in diverse scientific disciplines.

ARTICLE HISTORY

Received: July 23, 2018
Revised: September 23, 2018
Accepted: January 1, 2019

DOI:
10.2174/1573413715666190112121113

CrossMark

Keywords: Application, electrospinning, polymer nanofibers, ceramic nanofibers, photoluminescence, fluorescent probe.

1. INTRODUCTION

The boundless search for better properties and performances substituted many conventional materials with nanostructured materials since the latter surpasses the former as their structure and properties fall between that of atoms and materials in bulk. High-aspect-ratio nanofibers are preferred over nanoparticles and thin films because of the anisotropy in their length. The super elongated nanostructures have enhanced performances regarding charge and energy transport compared to bulk materials or two-dimensional systems. Consequently, luminescent organic/inorganic nanofibers are enticing a growing demand on the development of nanoscale light-emitting devices with high efficiency, highly sensitive optical sensors, optical filters, waveguides, and novel laser architectures. Both organic, inorganic and hybrid nanowires are crucial candidates for active and passive nanophotonic circuits as several studies reveal the strong potential of electrospun nanofibers as a light and energy propagation matrix in the light-emitting and photovoltaic devices. By proper design and manipulation of the nanowire assembly, they can

*Address correspondence to this author at the Department of Chemistry and Physics, Fayetteville State University, Fayetteville, NC 28301, USA;
Tel: +1-910-672-2647; Fax: +1-910-672- 2110; E-mail: zluo@uncfsu.edu

1875-6786/20 $65.00+.00

be utilized in complementary to photonic band-gap structures and plasmonic-based devices in nanophotonics [1].

The quantum confinement in nanostructured architectures below Bohr radius leads to exceptional photonic, and optoelectronic properties; therefore, one can tailor the optical and transport properties by controlling the size/shape of the materials at the nanoscale by fine-tuning the electronic band-gap.

The effect of quantum confinement in organic materials are insignificant than inorganic nanomaterials, and the nanostructures of inorganic semiconductors exhibit enhanced performances than their bulk counterparts. However, confining the natural materials to 1D nanostructures redefines arrangement of supramolecules along the axis; as a result, they can exhibit a well-defined polarization, spontaneous emission, enhanced charge mobilities, and non-radiative energy transfer and control on the energy transfer and migration [2].

1D nanomaterials are conventionally fabricated through template-based synthesis, laser ablation, mechanical milling, chemical route, and vapor deposition techniques. The low throughput of these techniques and unavailability of a clear methodology on controlling structural heterogeneities and uniformity for a range of materials make them inappropriate for large-scale production. Nonetheless, electrospinning is exceptional with high throughput, versatile, cost-effective and easy control of the shape and size. Electrospun ceramic nanofibers exhibit some unique qualities such as 1D morphology, extraordinary length, high surface area, and hierarchically porous structure. In addition to that, through electrospinning, nanofibers can be easily tailored as a simple membrane or any other intricate shapes as demanded by the application, by the desired selection of collector geometry.

Electrospinning works on the principle that if a sufficiently high direct-current voltage is applied to a polymer solution or melt held by its surface tension, charges are induced on the droplet's surface, and at a certain critical point when the electrostatic force overcomes the surface tension, the droplet is stretched to form nanofibers. Polymer solutions or melts with a high degree of molecular cohesion due to intermolecular interactions are the feedstock. The precursor solution is prepared in agreement with the morphology and composition of the final nanofibrous structure. Electrospinning can be exploited for the fabrication of not only polymeric nanofibers but also ceramic, carbon and metallic nanofibers. A typical electrospinning unit (Fig. **1**) has three major components, they are: (1) syringe pump, which feeds the polymer solution or melt with the help of a syringe or any other means, (2) a high voltage DC supply and (3) a collector plate, on which the nanofibers are collected. A representative SEM image of electrospun nanofibers is shown in Fig. (**2**).

The spinneret can be of any shape and be able to deliver the solution at a controlled rate. The high voltage unit must be able to supply a DC voltage ranging from 1 to 100 kV. The collector plate geometry is varied to meet the specific product requirements. Besides a static collector plate, a rotating drum collector is also commonly used to collect aligned nanofibers. Generally, the spinneret is given a high positive charge, and the collector is grounded.

The shape and stability of the droplet at the needle tip is dictated by its surface tension, which is in turn controlled by the concentration of the polymer solution. The charged jet coming off the spinneret becomes unstable due to electrostatic forces at close premises of the collector plate, which leads to the whipping of large fibers. Whipping reduces diameters of fibers further to ~30 nm. In atmospheric conditions, the solvents are evaporated before the arrival of fibers at the collector plate.

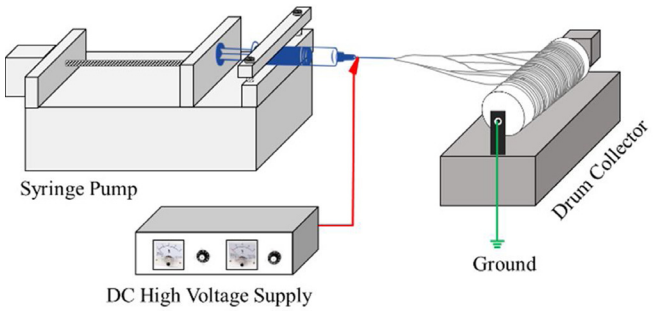

Fig. (1). Schematic of a simple electrospinning unit.

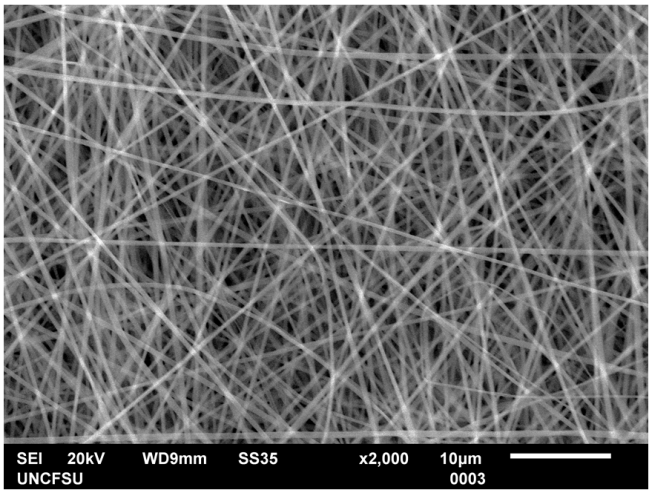

Fig. (2). SEM image of electrospun polyvinyl pyrrolidone nanofibers.

The electrospinning technique is highly versatile. The morphology of the electrospun nanofibers can be controlled by the appropriate modifications in the spinneret or the collector assemblies. For instance, hollow/core-shell [3] or multi-channel nanofibers [4] can be obtained by a coaxial spinneret and nanofiber yarns by the modification of the electrostatic field and the collector elements [5]. The nanofibers can be deposited on different templates based on the applications, *e.g*., depositing nanofibers around a conducting carbon fiber to form a nano-solenoid [6], direct deposit of nanofibers on surface acoustic wave (SAW) devices to form SAW sensor [7], *etc*. Moreover, the post-processing of electrospun nanofibers can yield nanofibers with stipulated morphology and enhanced properties. ZnO nanorods grown on electrospun nanofibers are suitable for flexible supercapaci-

tor electrodes [8], and SnO_2 Nanoflowers grown on electrospun carbon nanofibers are potential candidates for Li-ion battery anode [9].

The control of fiber morphology and diameter in electrospinning is not a trivial task, and several synergic factors impact the fiber size and morphology. The careful control of the electrospinning parameters is essential to produce defect-free nanofibers from various polymeric and precursor solutions. Many factors significantly affect the electrospinning process and the fiber diameter, which can be classified into three major categories as (1) material parameters, (2) process parameters and (3) atmospheric parameters. Among these parameters, the solution concentration, applied electric voltage, and solution flow-rate are most significant. At many instances, there is a connection between above parameters; for example, as the solution concentration is increased, the viscosity of the solution can be improved, along with the surface tension, dielectric constant and the conductivity. The atmospheric parameters are crucial in some instances; when solvents with high boiling point or water are used, then the humidity plays a significant role in the obtention of the fibers. Therefore, while preparing the spinnable solution, one must consider all these possible aspects, to obtain bead free fibers.

Electrospun nanofibers are promising for a myriad of applications starting from filtration [10] to energy storage [11] and production [12]. Photoluminescence is a characteristic of specific materials, and at several instances, their electrospun nanofibrous structure outperforms the conventional bulk structures. These luminescent nanofibrous materials can be potentially used in biomedical engineering, solar cells, cancer treatment, drug delivery, sensing, lasing, optical storage, and data transfer, LEDs, displays, *etc*.

The luminescent nanofibers obtained by electrospinning can be broadly classified into organic, inorganic, hybrid and composite nanofibers, as in Fig. (**3**). Each classification has unique luminescent characteristics and functionalities. This review discusses the luminescent electrospun nanofibrous materials under the classification above and their functionalities towards, sensing, waveguiding, *etc*.

2. ORGANIC LUMINESCENT NANOFIBERS

The term 'organic luminescent nanofibers' used here is to represent the nanofibers with its principal part is a polymer/organic material. They can be further classified as electrospun luminescent conjugated polymers, polymer blends containing a spinnable non-luminescent polymer and a conjugated polymer, a non-luminescent polymer containing a

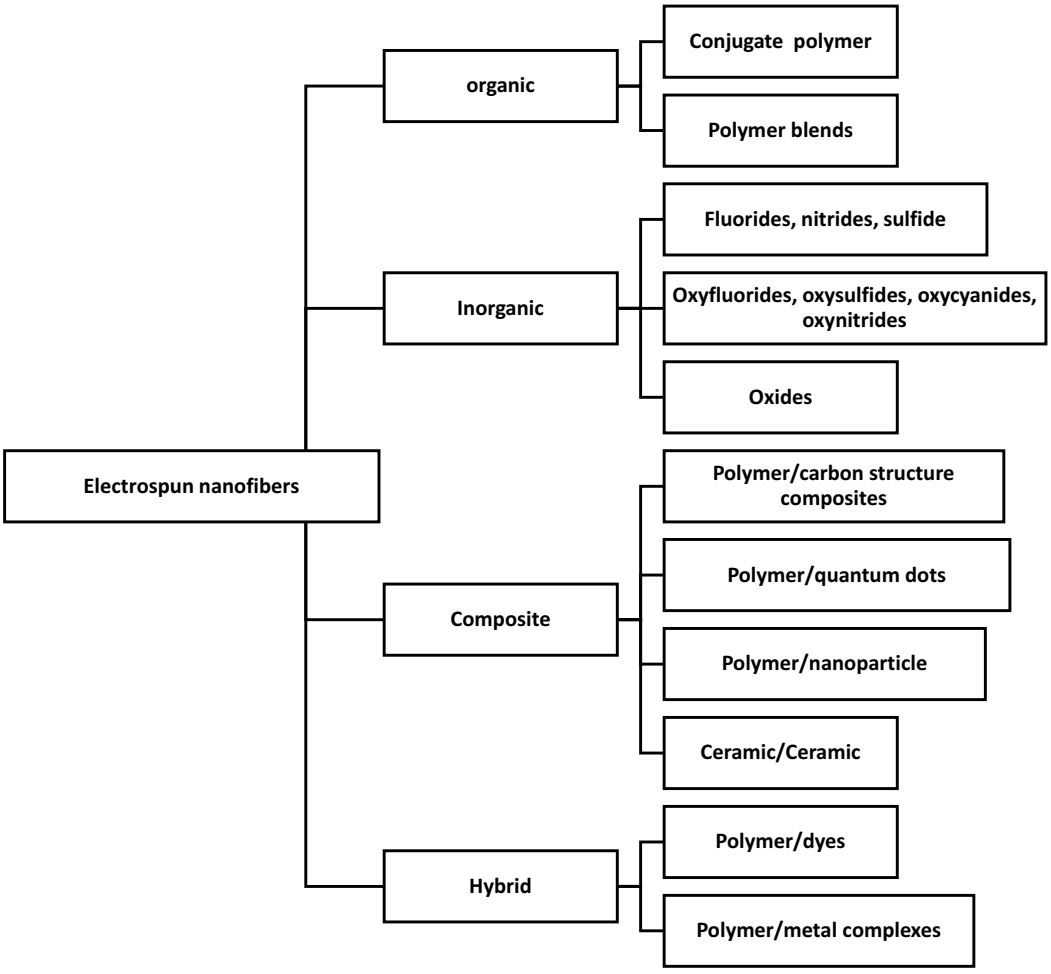

Fig. (3). Classification of electrospun luminescent fibers.

luminescent complex, such as rare earth metal salt or a metal complex or a dye. The significant advantage of these nanofibers is their flexibility, and most of the fibers exhibit anisotropic emission along their axis as compared to the direction perpendicular to the axis. Moreover, organic polymeric fibers can be easily tuned as luminescent probes for the sensing of harsh chemicals and molecules. The thermal and photostability of the luminescent emission from these nanofibers are very poor as compared to the inorganic nanofibers.

2.1. Conjugated Polymer Nanofibers

Conjugated polymers are the class of polymers with good mechanical, thermal, optical, and electrical properties. Many conjugated polymers often exhibit electro or photoluminescent (PL) characteristics. The most renowned classes of luminescent polymers are Poly(*p*-phenylene vinylene) (PPV) ((λ_{max} = 551 nm and a secondary peak at 520 nm), and its derivatives such as Alkoxy-, Thioalkyl-, and Alkylamino-Substituted PPVs (*e.g*., poly(*2,5*-dialkoxy-*1,4*-phenylene vinylene)s (RO-PPVs), poly[*2*-methoxy-*5*-(*2*-ethylhexyl)-*1,4*-phenylene vinylene] (MEH-PPV), Alkyl- and Silyl-Substituted PPVs (*e.g*., butyl-ethylhexyl-PPV (BuEH-PPV)), Aryl-Substituted PPVs (*e.g*., poly(*2*-phenylphenylene vinylene) (PPPV), Poly(arylene ethynylene)s, poly (phenylene ethynylene)s (PPEs), Poly(*para*-phenylene) (PPP), polythiophenes (PTs), poly(*9,9*-dialkylfluorene)s (PDAFs) [13], *etc*. exhibit properties favorable for optoelectronic applications such as LEDs and photovoltaic devices.

Nanowires or nanofibers made of conjugated polymers are ideal for charge transport and luminescence in one-dimensional (lD) systems and hold promise as the building blocks for flexible nanoelectronics. Luminescent emission from conjugated polymers is determined by the band gap of the π-π* transition, and the segregation of polymer chains can tune the same. Moreover, the strong stretching forces associated with electrospinning may induce orientation of polymer chains along the long axis of the fiber. It is expected that such aligned nanofibers of conjugated polymers may exhibit unique properties such as high charge-carrier mobility or polarized PL emission. As a result, it is highly desirable to apply electrospinning for the fabrication of nanofibers from this class of functional polymers.

Unfortunately, conjugated polymers cannot be easily electrospun due to their limited solubility, chain rigidity and low molar mass [14]. Because of the limited solubility and relatively poor viscoelastic behavior of conjugated polymers in commonly available solvents, such materials are electrospun as blends or core-shell heterostructures with polymers of better viscoelastic properties and at the same time optical inertness [15]. Albeit, several conjugated polymers are successfully electrospun through various approaches. Through the appropriate selection of solvents, especially uncommon-solvents with a high boiling point and dielectric constant, conjugated polymers are often spinnable [15], *e.g*., pristine and aligned electrospun fibers of MEH-PPV can be fabricated by using a binary solvent during electrospinning. The poor solvent is introduced to increase interchain interactions of MEH-PPV. Moreover, the poor solvent should have low surface tension and high conductivity [16]. Copolymerizing conjugate polymers with monomers of spinnable polymers can also yield defect free fibers. One such example is the fabrication of poly((*2*-(dimethylamino) ethyl methacrylate)-*co*-(stearyl acrylate)-*co*-((*1*-pyrene)methyl *2*-methyl-*2*-propenoate)) (poly(DMAEMA-*co*-SA-*co*-Py) copolymer by electrospinning. These nanofibers have the broad emission band centered at 471 nm originating from pyrene excimer, and it is pH and DNA sensitive [17]. Post-processing of precursor polymer fibers can yield conjugated polymer fibers. The fabrication of luminescent PPV nanofibers by the post-processing of electrospun precursor PPV nanofibers in a nitrogen atmosphere at 120°C [18] and formation of PPV nanofiber by electrospinning the precursor, poly(*p*-xylenetetrahydrothiophenium chloride) with methanol [19] reveals the potential of the above technique. Moreover, by controlling the ratio of precursor to solvent, one can control the morphology of the fibers. Green luminescent PPV nanofibers with disordered, helical, and yarn morphologies (Fig. **4**) are fabricated by electrospinning the cationic precursor poly(xylylene tetrahydro-thiophenium chloride) solution in ethanol through the control of the precursor/ethanol concentration [20].

The pure conjugated polymer fibers can also be obtained by the solvent extraction of a blend or composite nanofibers. Pure poly(*3*-hexylthiophene) (P*3*HT) nanofibers is prepared by the solvent extraction of poly(vinylpyrrolidone) (PVP) from P*3*HT/PVP blend nanofibers [21]. The nanofibers of pure MEH-PPV and MEH-PPV/PHT blend are prepared using coaxial electrospinning of MEH-PPV or MEH-PPV/P*3*HT as core and PVP as shell and the subsequent removal of PVP by ethanol extraction. The emission from MEH-PPV is suppressed in MEH-PPV/P*3*HT blend nanofiber architecture as compared with bulk thin films revealing the efficient energy transfer from MEH-PPV to P*3*HT in a confined environment rather than in thin films, (Fig. **5**) [22]. PVP (core)/MEH-PPV (shell) fibers produce a PL emission maximum of 635 nm when excited by 583 nm source [23].

Addition of conductive salts can improve the spinnability of conjugated polymers. For instance, blue light-emitting nanofibers of, poly[(*9,9*-dioctylfluorenyl-*2,7*-diyl)-co-(*N,N′* diphenyl)-*N,N′*-di(*p*-butyl-oxy-phenyl)-*1,4*-diaminobenzene)] (PFO−PBAB) copolymer obtained using a single good solvent and a small amount of organic salt. The addition of the organic salts like tetrabutylammonium iodide or tetrabutylammonium bromide dramatically improves the resulting fiber morphology and, importantly, leaves almost unaltered PL and spectroscopic properties of the polymer. The process positively affects the waveguiding properties of individual nanofibers as well [24]. In general, the PL emission spectrum of conjugated polymers is broad and shifts to higher energy relative to that of the films. In the case of PFO nanofibers the shift happens due to the presence of higher content of the *β*-phase in nanofibers [25], and its copolymer poly[(*9,9*-dioctylfluorenyl-*2,7*-diyl)-*co*-(*1,4*-benzo-{*2,1′-3*}-thiadiazole)] (F*8*BT) nanofibers with a green emission, when excited by 490 nm, which is blue shifted as compared with the films [14].

2.1.1. Applications of Luminescent Conjugated Polymer Nanofibers

The conjugate nanofibers find suitable for many applications, one of their primary application is the detection of

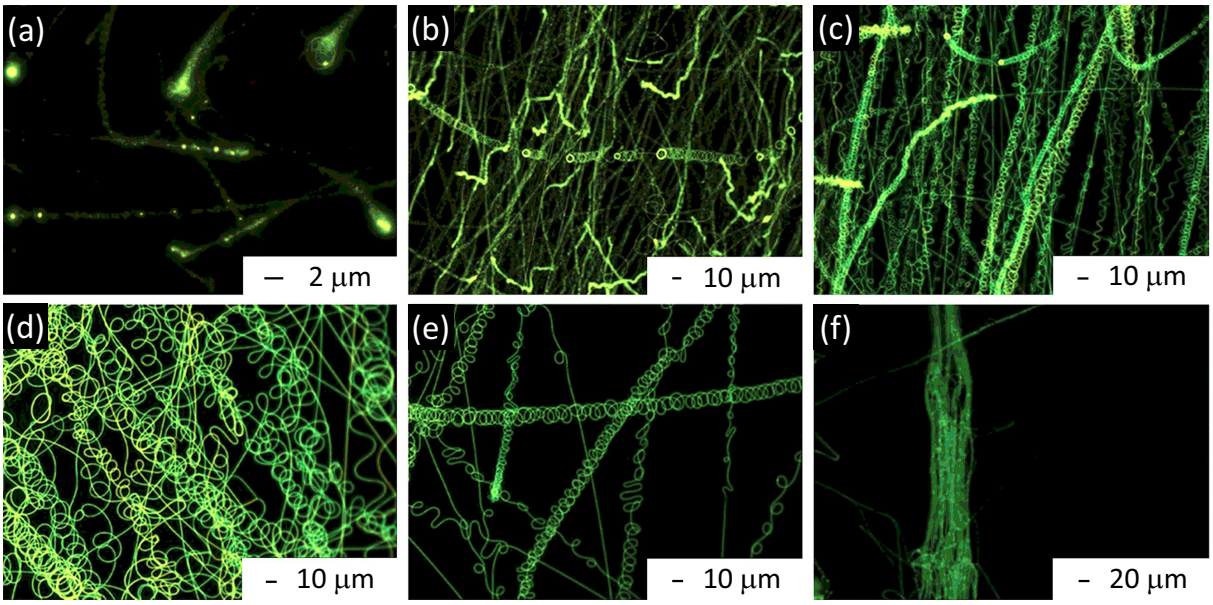

Fig. (4). Fluorescence microscopy images of PPV fibers with different morphologies by controlling precursor concentration in ethanol (**a**) 0.4, (**b**) 0.8, (**c**) 1.2, (**d**) 1.6, and (**e**) 2.0 wt.%, and (**f**) the fiber yarns. From [20], copyright © 2009 by John Wiley Sons, Inc. Reprinted by permission of John Wiley & Sons, Inc.

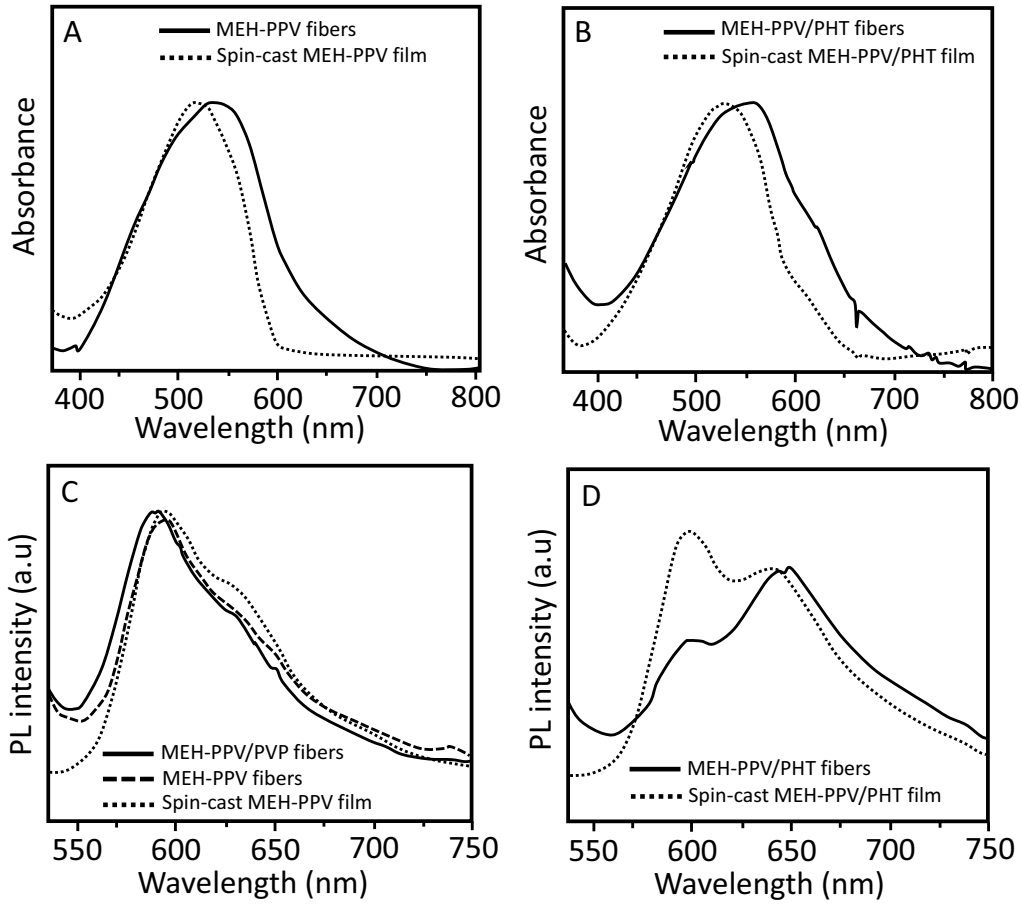

Fig. (5). (**A**) PLE and (**C**) PL spectra of MEH-PPV nanofibers and MEH-PPV thin films, and (**B**) PLE and (**D**) PL spectra of MEH-PPV/PHT blend nanofibers, and MEH-PPV/PHT blend thin films with 30% PHT. From [22], copyright © 2004 by John Wiley Sons, Inc. Reprinted by permission of John Wiley & Sons, Inc.

Fig. (6). Photograph of the fluorescence quenching of FNFM treated with different concentrations of TNT in aqueous phase when viewed under UV (λ_{ex}-254 nm) (**a**) and daylight (**b**), and the corresponding TNT concentrations are also shown in the figure. Adapted with permission from [26]. Copyright (2015) American Chemical Society.

several chemicals, especially warfare stimulants. Nanofibers of *α*-thiophene end-capped styrene copolymers exhibit a broad emission spectrum corresponding to the excimer emissions of pyrene moieties. These nanofibers are successful as a fluorescent probe in tracing Trinitrotoluene (TNT) in aqueous solution as well as vapor phase with the lowest detection limit of 5 nM. The color change in the presence of TNT vapors is identifiable by the naked eye [26], (Fig. **6**). Whereas, nanofibers of zinc porphyrinated polyimide (ZnPPI) polymer fibers with luminescent emission at 646 nm display ON/OFF characteristics in the absence/presence of TNT vapors [27].

Nanofibers of poly{*2*-{*2*-hydroxyl-*4*-[*5*-(acryloxy)-hexyloxy] phenyl}benzoxazole}-*co*-(N-isopropyl-acryl-amide)-*co*-(stearyl acrylate)} (HPBO-*co*-NIPAAm-*co*-SA) exhibit thermoresponsive luminescence in water, and the phenomenon is attributed to the low critical solution temperature of the thermoresponsive NIPAAm moiety [28]. Nanofibers of poly((*2*-(dimethylamino) ethyl methacrylate)-*co*-(stearyl acrylate)-*co*-(*9,9*-dihexyl-*2*-(*4*-vinylpenyl)-*9H*-fluorene) (P4) copolymer also exhibit thermoresponsive luminescence in water due to the structural transformation on the PDMAEMA moiety, from ordered to disordered and *vice versa* as shown in Fig. (**7**) [29]. Polydiarylfluorenes nanofibers exhibit polymorphic behavior, such as amorphous phase, *β*-phase, liquid crystalline, semi-crystalline *α,* and *α* phases, and phase change can occur by thermal annealing, solvent vapor treatment, thermodynamic or mechanical stress and so on and the phase change result in the luminescent behavior [30].

The following luminescent polymers and their copolymers with monomers of spinnable polymers are also successfully electrospun to form defect-free luminescent nanofibers. Nanofibers of Copolyimide derived from pyromellitic dianhydride (PMDA), *4.4'*-oxydianiline (ODA) and 2,6-diaminoanthraquinone (2,6-DAAQ) exhibit a broad emission peaking at 590 nm under excitation of 350 nm and the intensity of the emission increases moderately with an increase in the amount of DAAQ in the polymer chain [31]. Poly

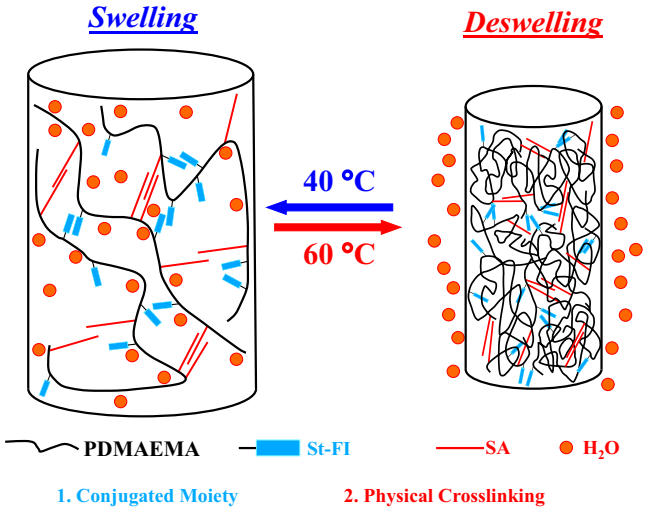

Fig. (7). Schematic illustration of the morphological change for the P4 fibers soaked in water as the temperature heats up and cools down. Adapted with permission from [29]. Copyright (2010) American Chemical Society.

[*2,7*-(*9,9*-dihexyl-fluorene)]-*block*-poly(methyl methacrylate) (PF-*b*- PMMA) emits a blue emission at 437 nm when excited by 380 nm [32]. Polycobaltsilazane (PCSN), formed by Co (II) doping into polysilazane, nanofibers display a series of emission peaks between 490 and 615 nm, greenish fluorescent emission around 490-510 nm under a 340 nm excitation wavelength, while a strong reddish fluorescence emission under a 470 nm [33]. Poly[(*9,9*-dioctyl-fluorenyl-*2,7*-diyl)-*co*-bithiophene] (F*8*T2) nanofibers attain RT photoluminescence in the cyan, yellow, and red wavelength range under ultraviolet, blue, and green light excitation, respectively [34]. Triarylamine-based polyimide nanofibers with high T_g (up to 420°C) and insignificant weight loss up to 550°C, exhibit aggregation induced emission

(AIE) originate from triarylamine moieties. Polyimides (PI) exhibit a maximum UV-vis absorption band at around 258 and 309-412 nm in NMP solution due to the π–π* transitions of the triarylamine chromophores and shows yellowish-green PL emission with the maximum peaks around 468-556 nm [35].

Since the PL of conjugated polymers is dependent of the chain segregation, incorporation of inorganic nanocrystallites into the PPV nanofibers not only improves the spinnability but also strengthened the PL quantum efficiency of the nanofibers [36]. The PL quantum efficiency of PPV–TiO_2 nanofibers is about three times stronger than that of pure PPV nanofibers, though there is no significant difference in the PL emission peak position from pure PPV nanofibers [37]. PPV/ZnS Composite nanofibers exhibit a stronger emission than pure PPV nanofibers. Luminescent emission from conjugated polymers are determined by the band gap of the π–π* transition, which is a function of the structure of PPV and modifications with any specific purpose will affect the band gap and consequently the peak position [38]. The PL spectrum exhibited a blue shift relative to the PPV nanofibers [39].

2.2. Polymer Blend Nanofibers

The traditional polymers with high molecular weight can be easily electrospun to high aspect ratio fiber, but it cannot be applied to conjugated polymers with limited solubility, low molecular weight, and bulky side groups. The most effective way of spinning conjugated polymers is by blending them with conventional polymers or with spinnable luminescent polymers. Under this classification, the electrospun conjugated polymer blends are discussed.

Generally, the luminescent behavior of the conjugated polymers is retained when blended with a non-luminescent polymer, *e.g.*, poly(*4*-vinyl pyridine)/porphyrin (P4-VP/TPPA) nanofiber display an emission as same as that of pure TPPA at about 650 nm [40]. Even though, a slight shift in the emission band is evident as compared to the pure form in the solution/solid state. The chain segregation alters the luminescent behavior of conjugated polymers. Therefore, the color of fluorescence from PPV/poly(vinyl alcohol) (PVA) nanofibers can be tuned by varying the content of PVA in the blend to get the fluorescence from yellow-green to blue. Due to the insulating nature of PVA in the blend fibers, PVA prevents the degree of π–π stacking of PPV [41].

A similar phenomenon is also observed in PPV-poly(ethylene oxide) (PEO) blend nanofibers where the addition of PEO leads to a blue-shift [42]. By the addition of CdS QDs to PVA/PPV blend nanofibers, the fluorescence color of PPV is changed from yellow-green to green and blue accordingly [43]. A nanofiber blend containing a luminescent conjugated polymer, poly(*2*-methoxy-*5*-octoxy)-*1,4*-phenylene vinylene)-*alt*-*1,4*-(phenylene vinylene) (PMO-PPV) and PMMA showed an emission λ_{max} of 549 nm when they were excited with a 466 nm excitation light, the emission maximum is red-shifted compared to 517 nm of the PMO-PPV solution. The redshifts in emission for a solid-state sample of PPV derivatives, when compared to solutions, were due to the increase in the HOMO-LUMO energy gap caused by conformational distortions in solution [44].

A derivative of PPV, MEH-PPV exhibit a near red emission is extensively electrospun by blending with several electrospinnable polymers. Electrospun blend nanofibers of MEH-PPV/PEO blend nanofibers (1:2 ratio) using chloroform as the solvent display an anisotropy in the polarized PL emission. PL polarization ratios parallel/perpendicular to the direction of fibers are higher than 13, and this ratio is further increased up to 25 by stretching the nanofibers, Fig. (**8**) [45]. Addition of $LiCF_3SO_3$ can significantly enhance the emission from MEH-PPV/PEO blend nanofibers [46]. Addition of ZnO in the MEH-PPV/PEO composite nanofibers quenches the intensity of PL emission peak at 587 nm, associated with the relaxation of excited π-electrons in the PPV backbone. In the presence of ZnO, this peak is red shifted until 50% ZnO loading and then blue shifted above 50% loading [47].

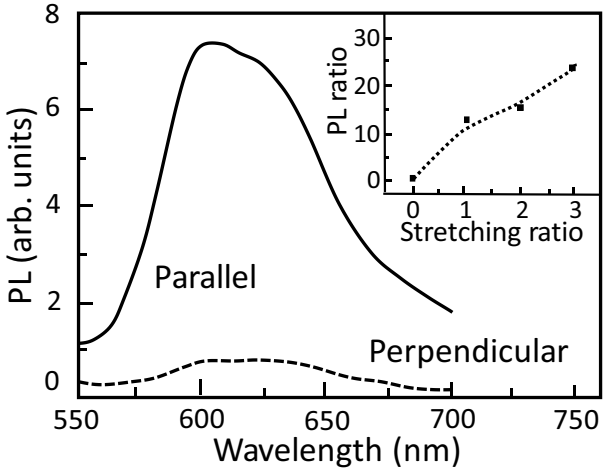

Fig. (8). Polarized PL emission parallel (solid line) and perpendicular (dashed line) to the nanofiber axis for an aligned nonstretched MEH-PPV:PEO. The inset shows the PL ratio as a function of stretching ratio, where 0 and one stand for a random mat and an aligned non-stretched sample, respectively. Reprinted from [45], with the permission of AIP Publishing.

MEH-PPV/PVP blend nanofibers exhibit a higher PL emission than the respective continuous films. The PL spectra are blue-shifted with longer exciton lifetime compared to the films [48]. The miscibility of the conjugated polymers with non-polar polymers such as polystyrene (PS) can be achieved by the addition of a compatibilizer or by adding a minor solvent with a high dielectric constant value, without compromising the emission from the conjugated polymer. For instance, a higher loading of MEH-PPV in PS nanofibers is possible by the addition of pyridinium formate (PF), a volatile salt, resulted in smooth nanofibers. Also, the addition of *1,2*-dichloroethane into chloroform helped to improve the electrospinnability of the resulting solution. Moreover, the PL spectra of the as-spun fibers exhibited a red shift in the emission when compared to similar MEH-PPV solutions [49].

Blending conjugated polymers can yield pure conjugated polymer nanofibers as in the case of MEH-PPV/PHT, and

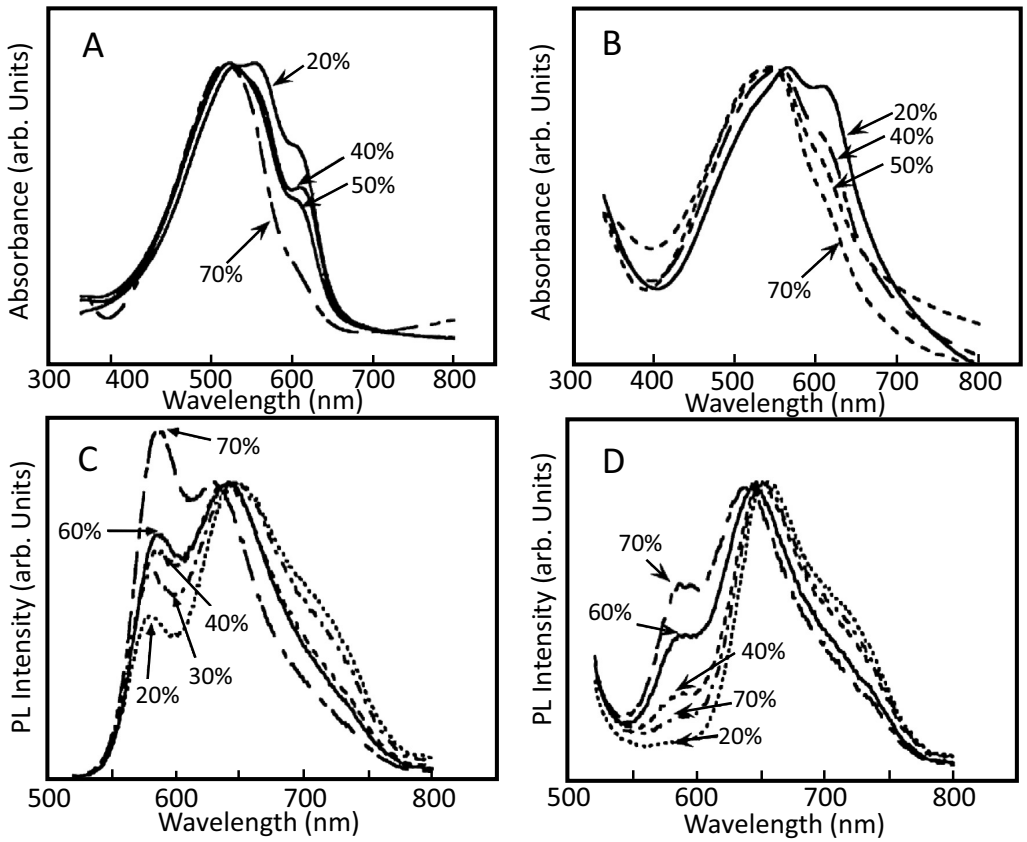

Fig. (9). Optical absorption spectra of (**A**) spin-cast thin films and (**B**) MEH-PPV/PFO blend nanofibers, and PL emission spectra of (**C**) spin-cast thin films and (**D**) MEH-PPV/PFO blend nanofibers. The number on each curve is the wt. % of MEH-PPV with respect to PFO. Adapted with permission from [50]. Copyright (2010) American Chemical Society.

MEH-PPV/PFO blend nanofibers. When comparing the PL emission from MEH-PPV/PHT blend and MEH-PPV/PFO with the respective thin films, the absorption band at 520 nm corresponding to MEH-PPV is red-shifted to 550 nm in the MEH-PPV blend nanofibers and red-shifted by 50 nm from 500 to 550 nm in MEH-PPV/PFO blend fibers, implying more extended chain conformation and better π-electron delocalization of MEH-PPV. Moreover, efficient energy transfer from PHT to MEH-PPV enhanced red emission from PHT in the MEH-PPV/PHT blend nanofibers and the absence of energy transfer in MEH-PPV/PFO blend nanofibers resulted in a broad white light emission contributed by both MEH-PPV and PFO, (Fig. **9**) [50]. In the blend nanofibers of poly(*9*-vinylcarbazole) (PVK)/MEH-PPV, the red emission at 617 nm is consistently blue-shifts with increasing PVK (0 wt.% of PVK) to 531 nm (99.5 wt.% of PVK). The significant blue shift of the MEH-PPV emission band in the blend fibers evidencing that PVK prevents aggregation in the MEH-PPV, suppressing the formation of interchain interactions. The blend nanofibers exhibited a more efficient energy transfer than thin films due to effective interfacial interactions between PVK and MEH-PPV, at low MEH-PPV content [51]. The luminescence characteristics of the MEH-PPV/PVK blend is significantly affected by the applied voltage during the electrospinning process [52]. Addition of SBA-15 to MEH-PPV, not only improve the spinnability of MEH-PPV but also blue-shifts the luminescence as compared to pure MEH-PPV fibers and the film, and red-shifted compared to the solution. Therefore, the π–π stacking between the phenyl rings of PPVs is prevented to some extent during electrospinning and even more in the composite fibers [53].

Polyfluorenes (PF) and its derivatives are another class of conjugate polymer extensively used for various electronic and optoelectronic applications owing to their stability, excellent fluorescence quantum yields and substantial charge-carrier mobility [54]. Nanofibers of PF/polymer blend exhibited enhanced luminescence characteristics in comparison with the spin-coated films and gamut emission through the variation of polyfluorene derivatives. The polyfluorene aggregation in the nanofibers is much smaller than that in the spin-coated films due to the geometrical confinement of the electrospinning process and results in higher luminescence efficiency [55]. PMMA/PF nanofibers are also successfully employed for the sensing of volatile organic compounds (VOCs) including ethanol, toluene, tetrahydrofuran, acetone, dichloromethane, and chloroform. The fluorescence quenching of the nanofibers, when exposed to the VOCs, is attributed to conformational changes from glassy-phase to β-phase of PF [56]. The electrospun ternary blend PFO/MEH-PPV/PMMA nanofibers display tunable emission. The emissions blue, white, yellowish-green, green-

ish-yellow, orange, to yellow, can be achieved by controlling the composition of MEH-PPV [57].

The blend nanofibers of diblock poly[*2,7*-(*9,9*-dihexyl-fluorene)]-*block*-poly(*2*-vinylpyridine)(PF-*b*-P2VP) or tri-block P2VP-*b*-PF-*b*-P2VP (*tri*-PFPVP) with PEO exhibit PL emission in the blue region. The diblock blend has a broad emission peak with a peak maximum at 455 nm, whereas the triblock blend has the emission maximum at 427 nm with the shoulder peaks at 448 and 480 nm, respectively [58]. Nanofibers of a luminescent fluorene-based cationic conjugated polyelectrolyte, poly{*9,9-bis*[*6*'-(*N*, *N*, *N*-trimethylammonium)hexyl] fluorene-*co-1,4*-phenylene} dibromide, blended with cellulose acetate (CA) exhibits an emission spectrum peaking at 420 nm under the excitation of 380 nm source [59]. The PL emission of ternary blend nanofibers of PFO/ poly(*2,3*-dibutoxy-*1,4*-phenylene vinylene) (DB-PPV)/ PMMA emits the only emission correspond to DB-PPV when excited by 380 nm. The PFO emission peaks around 400-450 nm is disappeared, and the emission peak of DB-PPV at around 500-550 nm is significantly enhanced, indicating the Foster energy transfer from PFO to DB-PPV [60].

Polythiophene and their derivatives are also used as luminescent polymer blends in nanofibers. Poly(*3*-buthylthiophene) (P*3*BT)/PEO blend (90/10) nanofibers have a yellow-red emission with a peak wavelength at ~650 nm and a spectral width of ~130 nm [61]. Electrospun conjugated polymers, MEH-PPV or P*3*HT, blended in PEO matrix shows highly anisotropic nature with stronger emission along the nanofiber axis; in contrast, the PL emission of random nanofibers and thin films showed weak emission anisotropy. The aligned electrospun nanofibers have the macromolecular chains oriented preferentially along the nanofiber axes, which led to strong polarized emission. Compared to the aligned nanofibers of MEH-PPV/PEO, the aligned nanofibers of P*3*HT/PEO showed higher luminescence anisotropy due to intrinsic ordering and semi-crystalline nature of P*3*HT in solid states [62]. PEO nanofibrous mat contains a controlled concentration of a single light-emitting hyperbranched conjugated polymer (HCP) exhibit a variety of fluorescence colors depending on HCP concentrations, arises from different degrees of intermolecular energy transfer [63]. The nanofibers of poly(*3*-thiophene)s containing pendant diamidopyridine group (PTDAP) blended with poly1-(*4*-vinylbenzyl uracil) (PVBU) to form physically cross-linked structures of the complementary uracil-diaminopyridine (U-DAP) emits green light under blue excitation [64].

2.2.1. Applications of Luminescent Polymer Blend Nanofibers

Several luminescent blends can be potentially used as fluorescent probes for the detection of oxygen, ammonia, pH, explosives, metal ions, warfare agents, etc. Oxygen-sensitive luminescent probe nanofibers can be successfully fabricated by adding Pt (II) meso-tetra(pentafluoro-phenyl) porphine (PtTFPP) or Pd(II) meso-tetra(pentafluoro-phenyl) porphine (PdTFPP), into poly(ether sulfone) (PES) or polysulfone (PSU) core/polycaprolactone (PCL) nanofibers. The PL emission at 630 nm from the nanofibers is quenched in the presence of oxygen [65]. PtTFPP loaded PS nanofibers also shows sensitivity towards oxygen with an emission maximum at 650 nm under excitation of 505 nm with a rapid response time to oxygen sensitivity realized for opto-chemical sensors [66].

P*3*HT/PMMA blend nanofibers exhibit emission band at 1020 nm in addition to the two bands at 560 nm and 600 nm arising from the chromophore and molecular arrangement (crystallinity) of P*3*HT, respectively. P*3*HT/PMMA fibrous film can effectively detect the lower explosive limit for VOCs, with a detection limit of 500 ppm towards acetone, toluene, and o-xylene [67]. The core-shell structured P*3*HT@PMMA nanofibers can undergo photodegradation followed by forming the charge transfer complex when exposed to air and therefore result in a significant red shift in the PL emission peak (Fig. **10**), reveals the potential of these nanofibers for oxygen sensing [68]. Blending Methacrylic homopolymer functionalized with anthracene moieties through electrospinning emits anthracene PL spectrum peaks, at λ = 419 nm and λ = 444 nm, respectively. The intensity of these PL emission peaks is subsequently reduced with the increase in the ammonia vapor concentration [69].

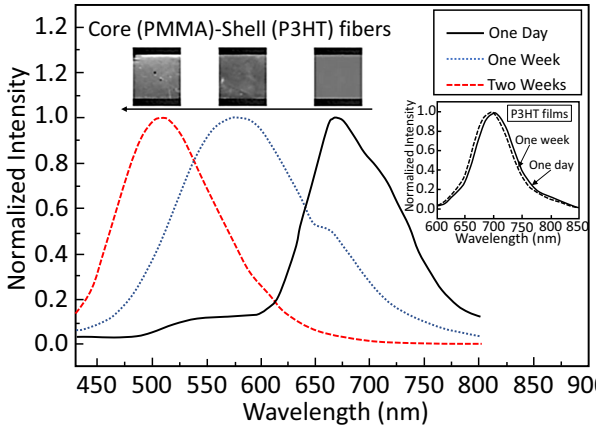

Fig. (10). PL spectra of the core (PMMA)-shell(P*3*HT) ES fibers exposed to air for one day, one week and two weeks, respectively. From [68], copyright © 2009 by John Wiley Sons, Inc. Reprinted by permission of John Wiley & Sons, Inc.

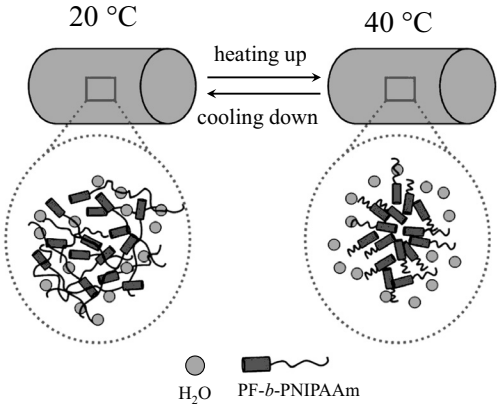

Fig. (11). Schematic illustration of the morphological change of PF-*b*-PNIPAAm in ES nanofibers soaked in water as the temperature heats up and cools down. From [74], copyright © 2010 by John Wiley Sons, Inc. Reprinted by permission of John Wiley & Sons, Inc.

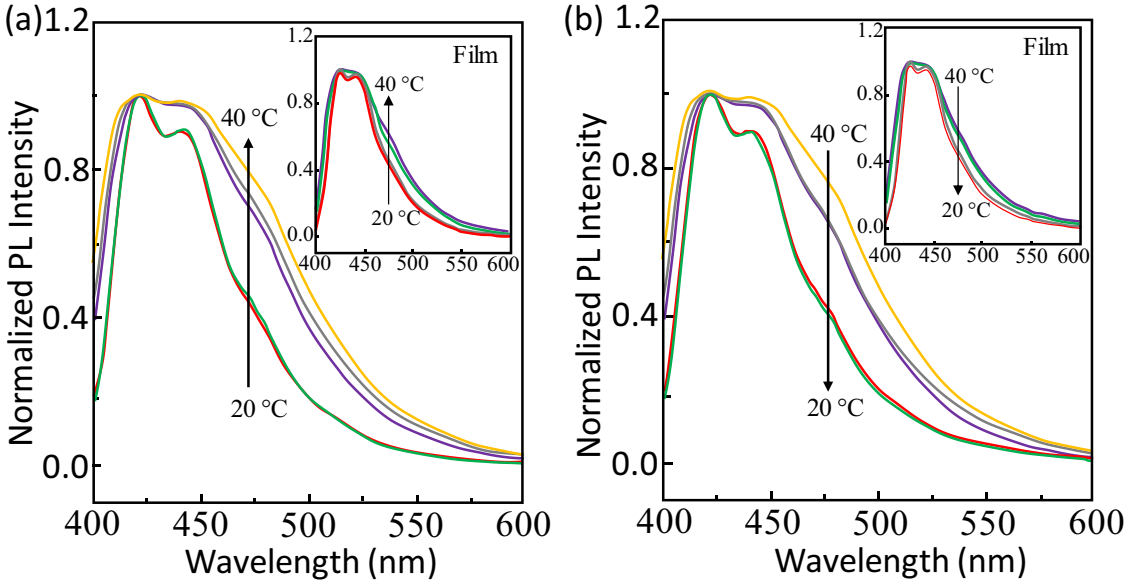

Fig. (12). PL spectra of PF_7-*b*-$PNIPAAm_{516}$/PMMA ES fibers and films as the temperature heats up from 25 to 40°C (**a**) and then cools down to 25°C (**b**). From [74], copyright © 2010 by John Wiley Sons, Inc. Reprinted by permission of John Wiley & Sons, Inc.

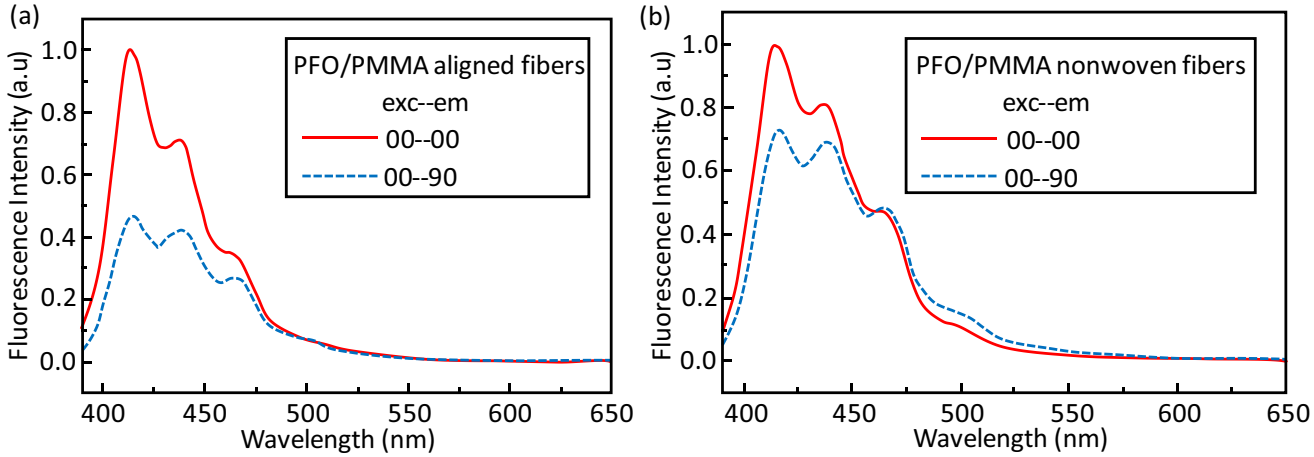

Fig. (13). Polarized steady-state PL emission spectra of the PFO/PMMA blend on the following material structures: (**a**) aligned nanofibers and (**b**) non-woven nanofibers, (Exc 00: excitation parallel to the aligned nanofibers; Em 90: emission perpendicular to the aligned nanofibers). From [54], copyright © 2008 by John Wiley Sons, Inc. Reprinted by permission of John Wiley & Sons, Inc.

The blend nanofibers of poly(*2*-hydroxyethyl methacrylate-*co*-*N*-methylolacrylamide-*co*-nitrobenzoxadia-zolyl derivative) (poly(HEMA-*co*-NMA-*co*-NBD)) and a spirolactam rhodamine derivative (SRhBOH) is fluorescent and featuring high sensitivity towards pH and ferric ions (Fe^{3+}). The fluorescence emission of SRhBOH is highly selective for pH and Fe^{3+}; when SRhBOH is used in acidic media and Fe^{3+}, the spirocyclic form of SRhBOH, which is non-fluorescent, is transformed into the opened cyclic form and exhibited strong fluorescence emission. The emission colors of ES nanofibers in acidic or Fe^{3+} aqueous solutions changed from green to red because of FRET from NBD (donor) to SRhBOH (acceptor) [70]. Poly(phenylquino-line)-*block*-Polystyrene blend nanofibers display pH-tunable PL with the emission maximum varied from 532 to 560 nm [71].

Poly(triphenylamine-alt-biphenylene vinylene) (TPA-PBPV) dip coated on PAN nanofibers is sensitive to TNT vapors. The TNT vapors reduce the luminescence intensity and increase the decay time of the nanofibers. The increase in decay time is more significant in the nanofibers than the thin film counterparts [72]. The derivatives of polydiarylfluorenes, such as, poly [*4*-(hexyloxy)-*9,9*-diphenylfluoren-*2,7*-diyl]-*co*-[*5*-(hexyloxy)-*9,9*-diphenyl fluoren-*2,7*-diyl] (PHDPF), poly [*4*-(octyloxy)-*9,9*- diphenyl fluoren-*2,7*-diyl]-*co*-[*5*-(octyloxy)-*9,9*- diphenylfluoren-*2,7*-diyl] (PODPF) and poly [*4*-(dodecyloxy)-*9,9*-diphenylfluoren-*2,7*-diyl]-*co*-[*5*-(dodecyloxy)-*9,9*-diphenyl-fluoren-*2,7*-diyl] (PNDPF) composites with PVK exhibit fluorescence quenching sensitivity towards *2,4*-dinitrotoluene (DNT) vapor [30]. Pyrene doped polyethersulfone nanofibers are highly sensitive for the detection of explosives, such as a

picric acid (PA), *2,4,6*-trinitrotoluene (TNT), DNT, and 1,3,5-trinitroperhydro-*1,3,5*-triazine (RDX). The fluorescent emission at 470 nm is significantly quenched in the presence of explosives mentioned above [73].

The electrospun luminescent blends also exhibit unique characteristics like temperature sensitivity, upconversion, UV sensitivity, *etc*. The blend nanofibers of poly[*2,7*-(*9, 9*-dihexylfluorene)]-*block*-poly(*N*-isopropylacrylamide)(PF-*b*-P NIPAAm)/PMMA exhibited thermo-reversible luminescence characteristics and are promising for thermo-tunable colorimetric sensor applications. The PL spectra of these nanofibers show two sets of emission peaks around 424-427 nm and 439-442 nm, which are attributed to different vibronic states of the PF excimers. The morphological change of PF-*b*-PNIPAAm in the ES nanofibers soaked in water is exhibited for temperatures above or below the lower critical solution temperature (LCST). When the temperature is below the LCST, the hydrophilic C=O and N-H groups in PNIPAAm forms intermolecular hydrogen bonding with water molecules and intramolecular hydrogen bonding between the C=O and N-H groups above LCST. Which ultimately results in a compact and collapsed conformation of the PNIPAAm chains (Fig. **11**), which makes the PL shoulder peak over 500 nm stronger and vanishing of the same below the LCST (Fig. **12**); when PNIPAAm chains are returned to a more stretched conformation [74]. The crosslinked polyfluorene-*block*-poly(*N*-isopropylacryl amide)-*block*-poly (*N*-methylol-acrylamide) nanofibers show excellent wettability and dimension stability in the aqueous solution and a reversible on/off transition on PL as the temperatures varied for 10°C-40°C [75].

Upconverting luminescence can be achieved in the case of organic nanofibers using UC sensitizer, meso-tetraphenyl-tetrabenzoporphyrin palladium (PdTBP), and emitter, *1,3,5,7*-tetramethyl-*8*-phenyl-*2,6*-diethyl dipyrromethane·BF2 (dye550) loaded to PMMA nanocapsules immobilized to PVA matrix. The nanofibers exhibit bright UC-fluorescence peaking at 550 nm in an ambient atmosphere, under 633 nm excitation [76]. PMMA nanofiber mats containing spironaphthoxazine (SPO)/electron donor-π-acceptor (D-π-A) type fluorescent dye (TCF) shows reversible modulation of fluorescence intensity using alternating irradiation with UV and visible light [77].

It is worthwhile to mention that, the luminescence of electrospun conjugated polymer fibers is critically sensitive to the processing atmosphere and orientation of the fibers. The fibers are smoother and uniform when produced in the nitrogen environment as compared to samples spun in the air. This effect is synergic with the reduced oxygen and moisture incorporation during electrospinning and induces significantly enhanced optical properties and improved waveguiding performances of the resulting light-emitting fibers [78]. Aligning the nanofibers in one direction can improve the polarization ratio among the emission. PFO/PMMA and PF^{+}/PMMA(PF-poly{[*9,9*-di(*3,3′-N,N′*- trimethylammonium) propylfluorenyl-*2,7*-diyl]-*alt*-(*9,9*- dioctylfluorenyl-*2,7*-diyl)} diiodide salt), PFO/PMMA aligned fibers have a polarized steady-state luminescence with a polarization ratio as high as 4, much higher than the non-woven electrospun fibers or spin-coated film, (Fig. **13**). The PF^{+}/PMMA blend aligned electrospun fibers showed an enhanced sensitivity to plasmid DNA [54].

2.3. Polymer Hybrid Nanofibers

2.3.1. Hybrid with Metallic Complexes

The simplest way of synthesizing a luminescent polymeric nanofiber is by dissolving a luminescent metal salt in the electrospinning solution of the polymer. Electrospinning of PVP solution containing $Eu(NO_3)_3$ salt embed Eu^{3+} ions in the polymer matrix, and the resulting fibers exhibit a dominant PL emission in the red region [79]. When used PAN as the matrix for Eu^{3+} ions, due to the interaction between the C≡N groups of PAN and Eu^{3+} ions, the emission centers, the PL emission intensity is continuously increased until the distribution of emission centers in the PAN molecule chains is saturated and after that, the emission intensity is decreased [80]. The PL spectra of Eu^{3+} ions doped PS, Polyvinylidene fluoride (PVDF) [81] PMMA [82] and nanofibers also reveals that the red emission is aroused from hypersensitive $^5D_0 \rightarrow {}^7F_2$ transition and the enhanced intensity ratios of $^5D_0 \rightarrow {}^7F_2$ to $^5D_0 \rightarrow {}^7F_1$ transitions indicate a more polarized chemical environment for the Eu^{3+} ions in the polymer matrix fibers.

Complexes/dyes of several rare earth (RE) elements have good luminescent properties because of the antenna effect of ligands and the *f-f* electron transition of RE^{3+} ions. The poor thermal and mechanical stabilities and processing ability of pure complexes/dyes limits their applications and practical uses. Therefore, incorporating these complexes into organic, inorganic, or organic/inorganic hybrid matrixes, such as zeolites or mesoporous materials improve their prosperity. Embedding rare earth complexes/dyes in the polymer-matrix significantly improve their luminescent properties than the pure form. Loading of the RE complex to polymer matrix nanofibers can significantly improve the luminescent efficiency compared with neat complex due to the enhanced intermolecular interactions between individual complex molecules and the adjacent chain segments of the polymer [83]. The complexes of several rare earth elements such as Eu, Tb, Er, *etc*. or a combination of them with tunable emission with different complexing agents are used as the luminophores in polymer nanofibers.

The PL emission characteristics of the metallic complexes in a particular polymer matrix are dependent on the polymer chains. The interaction of the metal complex molecules and adjacent chain segments of polymer matrix can enhance the electronic dipole-allowed transitions differently in several polymer matrices, and therefore, the increase of polarization degree of RE^{3+} ions than that of pure complex molecules [84] can be different. The PL emission characteristics of europium complex $Eu(TTA)_3(TPPO)_2$ (TTA- thenoyltrifluoroacetone, TPPO- triphenylphosphine oxide) incorporated polymer nanofiber matrices, PMMA, PS, and PVP exhibit a slightly different PL emission characteristics, though the significant emission from all these nanofibers is originated from Eu^{3+} ions. On comparing their luminescence properties to those of the pure complex, in the pure complex, only the $^5D_0$-$^7F_1$ and $^5D_0$-$^7F_2$ lines appear, whereas the $^5D_0$-$^7F_0$ emission is entirely absent. The emission lines from the composite fibers become broader to different degrees based

on the heterogeneous broadening caused by more disordered local environments surrounding the Eu^{3+} ions (Fig. **14**), and the level of disorder on the local environment of Eu^{3+} ions can be different in different polymer matrices. The local symmetry of the coordination sphere for the Eu^{3+} ions is slightly higher in PMMA than PS and PVP matrices [85].

Similarly, when two different Eu^{3+} complex loaded into PMMA nanofibers, $Eu(DBM)_3$/PMMA (DBM = 1,3-diphenyl-propane-1,3-dione) and $Eu(DBM)_3$Phen/PMMA (Phen = *1,10*-phenanthroline) respectively, emits intense red emission characteristic to Eu^{3+} ions. The quantum yield of $Eu(DBM)_3$Phen/PMMA is much higher than $Eu(DBM)_3$/PMMA nanofibers, which can be assigned to the efficient photon absorption of lanthanide organic in the presence of Phen ligand [86]. Green luminescent PL emission is observed from electrospun $Tb(Acac)_3$Phen (Acac-acetylacetone) incorporated PS, PVP, and PMMA nanofibers. The emission intensity for $^5D_4 \rightarrow {}^7F_J$ of Tb^{3+}in the composite fibers considerably increased than the complex alone. Despite the improved photostability of the terbium complex in the composites, the composite fibers have a much better temperature stability of PL over the real complex [87]. $(Eu(BA)_3phen+Tb(BA)_3phen)$/PMMA (BA = benzoic acid) composite nanobelts exhibit tunable fluorescence from red to yellow, yellow-green, and green under the excitation of 290-nm [88]. The luminescence characteristics of Eu (II) complex/polymer blend can be improved further by adding Ag-nanoparticles through surface-enhanced luminescence technique [89].

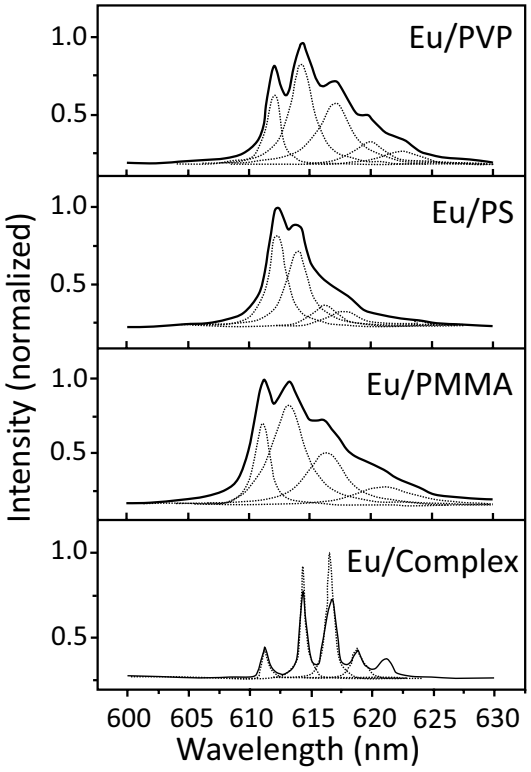

Fig. (14). High-resolution emission spectra of the Eu complex, Eu/PMMA, Eu/PS, and Eu/PVP and five Lorentzian fitting functions. Adapted with permission from [85]. Copyright (2008) American Chemical Society.

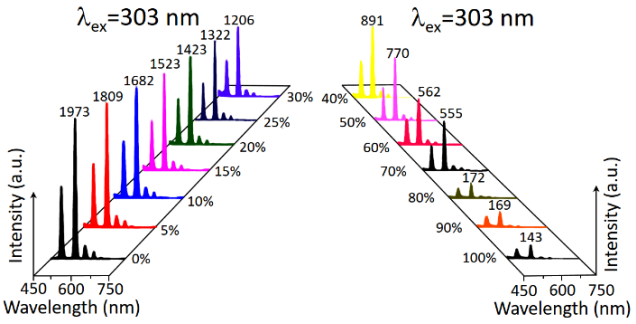

Fig. (15). Fluorescence emission spectra of the PNPLF samples with different oil adsorbing values. Adapted with permission from [93]. Copyright (2008) American Chemical Society.

These RE complex/polymer hybrid nanofibers exhibit unique characteristics. *E.g.*, $Eu(DBM)_3$PIP (PIP = *2*-phenyl-*1H*-imidazo[*4,5*-f][1,10]phenanthroline)/PVP composite fibers exhibit a red emission sensitive to oxygen [90]. $Eu(TTA)_3$(phencarz)/PS (phencarz=*2*-(*N*-ethylcarb-azolyl-*4*) imidazo[*4,5-f*] 1,10-phenanthroline) hybrid nanofibers are also an optical oxygen sensing material [91]. Whereas, the red emission from EuW_{10}/PAN (EuW_{10} = $Na_9[EuW_{10}O_{36}]\cdot 32 H_2O$) nanofibers is quenched by passing gases like H_2S, CO_2, SO_2, *etc*., and it can be recovered by treating them with NH_3, *etc*. The pH-modulated luminescent photoswitching involves two distinct states that can be interconverted between the protonation and deprotonation states of EuW_{10} [92]. Porous electrospun polyethylene terephthalate (PET) nanofibers loaded with *p*-Methylbenzoic acid terbium complex (PATC) using the mixed solvents hexafluoroisopropanol (HFIP) and dichloromethane (DCM) in the ratio 1:3 has good luminescence properties characteristic to terbium ions and fluorescent-indicating function. Despite the good mechanical properties and thermal properties, these nanofibers are excellent oil absorbents with a traceable PL intensity at different oil absorption levels (Fig. **15**), and the reduction in the PL emission intensity is due to the absorption of the excitation energy by the oil [93].

There are a few potential Er (III) complexes those are successfully employed in PVP hybrid nanofibers. They are $Er(HFA)_3$Phen (HFA- *1,1,1,5,5,5*-hexafluoro-2,4-pentanedione), $Er(TTA)_3$Phen and $Er(TTA)_4$CTAB (CTAB-cetyltrimethylammoniumbromide). Among these complexes, $Er(TTA)_3$Phen blended PVP nanofibers exhibit the highest emission [94].

The transition metal complex dyes are also used as luminophores in electrospun hybrid fibers. PEO/$(NH_2)_4$PcCu (Pc = phthalocyanine) hybrid nanofibers show a PL emission at about 450 nm, associated with the energy transition process between the ligands and the metal ion of $(NH_2)_4$PcCu [95]. $[Cu(POP)DPPZ]BF_4$ (POP = bis[*2*-(diphenylphosphino)phenyl]ether; DPPZ = dipyrido[*2,3-a*:3′,2′-*c*]phenazine) complex embedded within PS fibers have the emission band centered at 560 nm when excited by 365 nm source. The luminescence of $[Cu(POP)DPPZ]BF_4$ complex

within the PS nanofibers is rapidly quenched in the presence of oxygen revealing its potential as a food oxygen sensor material [96]. The dinuclear complex of copper $[Cu_2I_2(L1)_2]$ (1) (L1=*3*-((*4*-(pyridin-*2*-yl)-*1H- 1,2,3*-triazol -*1*-yl)methyl) benzonitrile) loaded PMMA nanofibers exhibit strong yellow emission and when blended with PMMA at different weight ratios, a tunable luminescence can be achieved [97].

The blend fibers of PVK/tris-(*8*-hydroxy-quinoline) aluminum (Alq3), an aluminium complex, have the PL emission peaks originated from Alq3. The emission peaks from PVK in the blue range is completely disappeared in the case of blend nanofibers [98]. Alq3/PVP nanofibers exhibit bright green emission [99]. Coaxial fibers of PVK/*4,7*-diphenyl-*1,10*-phenanthroline (Bphen) and PVK/Alq_3 have significantly improved PL green emission from Alq_3 as compared to those produced by simple electrospinning. The enhanced dispersion of the Alq3 allowed a more efficient energy transfer from the PVK to the Alq3 in coaxial fibers [100]. Alq3/P3BT loaded PEO nanofibers can be optimized for white emission by adjusting the Alq3/P3BT ratio when combined with the intrinsic blue emission from the LED [101].

An iridium complex, $Ir(Acac)(F\text{-}BT)_2$ (F-BT = *2*-(*2*-fluorophenyl)benzo[d]thiazole), loaded PVP nanofibers emits a PL spectra peaking at 503 nm under UV illumination [102]. Iridium (III) bis(*2*-phenylbenzothiozolato-*N,C*$^{2'}$) acetylacetonate ($(BT)_2Ir(Acac)$)/PS nanofibers functionalized with the enzyme, glucose oxidases, is a quick and highly sensitive optical biosensor for glucose detection. The fibrous membrane emits yellow luminescence (562 nm) when excited at 405 nm, and it is significantly enhanced in the presence of extremely low concentration glucose, *i.e.*, 1.0×10^{-10} M [103]. Ir (III) complex of $Ir(PD)(PBT)_2$ [PD = pentane-2,4-dione, PBT = 2-phenylbenzo[d]thiazole] doped PVP nanofibers shows yellow emission with a major band at 550 nm and a shoulder band at 589 nm. PL performance of the composite fibers is superior to that of pure $Ir(PD)(PBT)_2$, including blue emission shift, longer excited state lifetime and improved photo-durability [104].

Hydrogels of silica or silicon compounds are another source of luminescent complexes in the polymer nanofibers. Electrospun nanofibers of polymethylhydro-siloxane/PVP blend exhibit a range of visible emission, blue, green and red, and white when excited by different wavelengths, for instance, 267 nm, 385 nm, 488 nm, 561 nm, *etc*. The silica gels exhibit PL emission through the medium of defects, such as carbon-impurities, photo-induced donor-acceptor pairs of nitrogen related species, and oxygen-related defects. This phenomenon vanishes during the calcination process to yield SiO_2 nanofibers [105]. Poly(acrylic acid) (PAA)–silica hydrogel nanofibers mat formed by the colloid-electrospinning of PAA/SiO_2 precursor solution followed by moderate thermal cross-linking of PAA-S nanofiber matrix, and full swelling in water exhibit a high adsorption capacity towards rare earth ions. RE^{3+} ion adsorbed matrix has the characteristic emission from the respective ions, (Fig. **16**) [106].

Metallic ions decorated in the polymer matrix also exhibit strong luminescent characteristics. PMMA–PMAA nanofibers decorated with Ag ions are luminescent with an emission peaking at 576 nm under 490 nm excitation. These nanofibers are antibacterial too [107]. Carboxymethyl

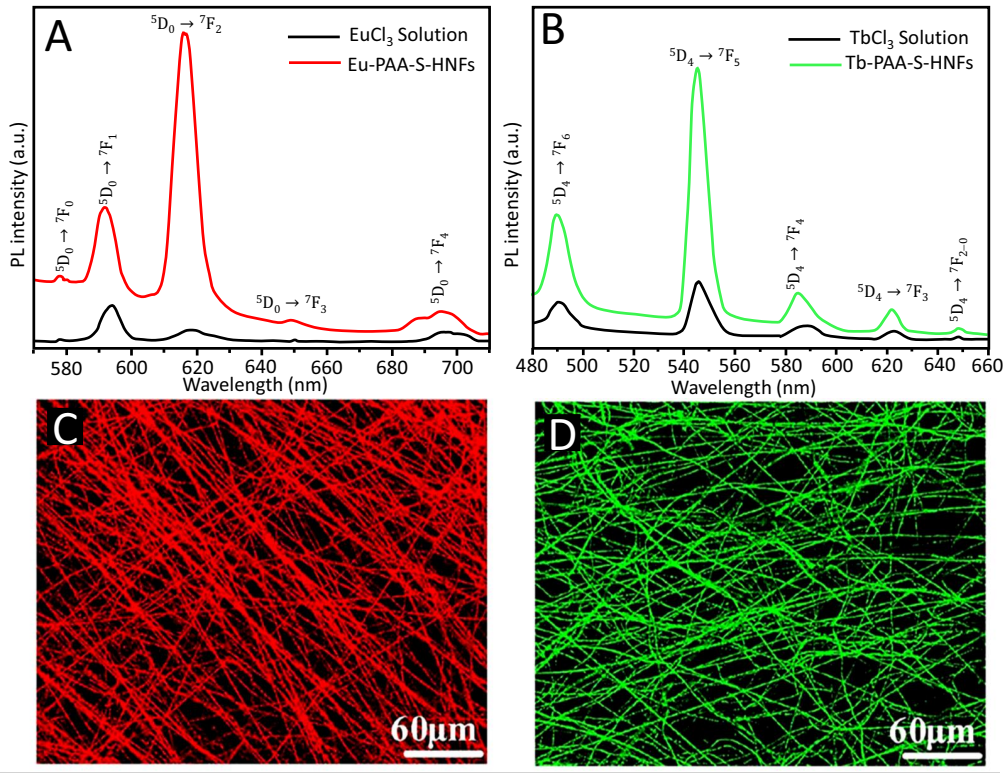

Fig. (16). Emission spectra of (**A**) $EuCl_3$ solution and Eu-PAA-S nanofibers (λ_{ex} = 390 nm) and (**B**) $TbCl_3$ solution and Tb-PAA-S nanofibers (λ_{ex} = 305 nm), and confocal laser scanning microscopy images of (**C**) Eu-PAA-S nanofibers and (**D**) Tb-PAA-S nanofibers. Adapted with permission from [106]. Copyright (2016) American Chemical Society.

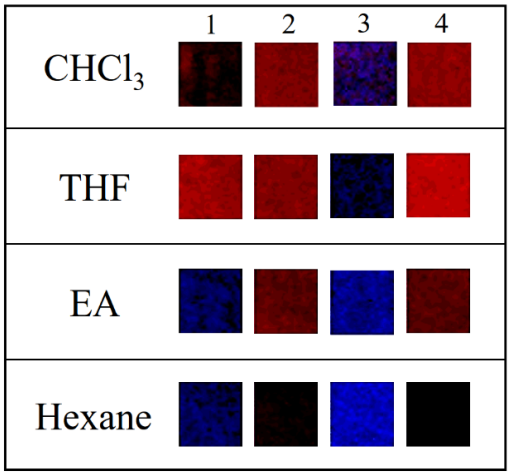

Fig. (17). Photographs of PEO/TEOS fiber mats prepared with diacetylene monomers (1- PCDA, 2- ECDA, 3- PCDA-AP, and 4-HCDA) after exposure to organic solvent. Adapted with permission from [110]. Copyright (2007) American Chemical Society.

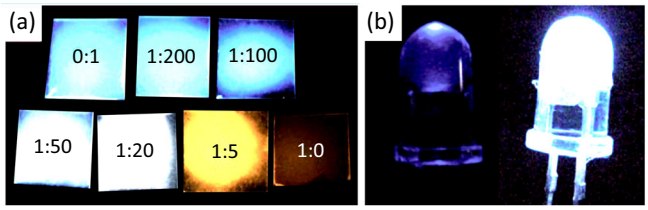

Fig. (18). (**a**) Digital photograph Cm102 loaded DNA–CTMA complex nanofibers illuminated by 365 nm UV lamp. (**b**) 400-nm UV LEDs without (left) and with white-light-emitting DNA nanofiber coating (right). From [115], copyright © 2009 by John Wiley Sons, Inc. Reprinted by permission of John Wiley & Sons, Inc.

cellulose (CMC)/PEO nanofiber mats containing Ag nanoparticles exhibit a PL emission peak at 467 nm when excited at 410 nm. This visible luminescence is due to the excitation of electrons from occupied bands into states above the Fermi level of Ag nanoparticles [108]. At the same time, metallic ions can also quench the PL emission. In the presence of metal ions, the PL emission of 1,10-phenanthroline (F-phen) doped poly(*N*-isopropyl-acrylamide-*co*-*N*-hydroxymethyl-acrylamide) nanofibers are quenched significantly, enabling them as the sensor materials for metal ion detection [109].

Organic fluorophores/chromophores are widely embedded in non-luminescent polymer nanofibers as luminescence source. Example, diacetylene monomers, such as *10,12*-pentaco-sadiynoic acid (PCDA), *5,7*-eicosadiynoic acid (ECDA), N-(pyridin-*3*-yl) pentacosa-*10,12*-diynamide (PCDA-AP), and *8,10*-henicosadiynoic acid (HCDA) embedded in PEO, and tetraethyl orthosilicate (TEOS) matrix can be used as colorimetric sensors for VOCs [110] by visual inspection as in Fig. (**17**). Anionic and cationic fluorescent dendritic molecules AFD-3, AFD-6, CFD-3, and CFD-6 loaded CA- nanofibers show an emission maximum at 445, 475, 480, and 450 nm are yielding unique patterns of fluorescence quenching upon interaction with metal and non-metal containing proteins [111]. Cyanostilbene (CS) derivatives such as *2*-[(E)-*2*-[*4*-[(E)-*2*-(*2*-Cyanophenyl)- ethenyl]-phenyl]-ethenyl]benzonitrile, *1*-(*2*-cyanostyryl)-*4*-(*4*- cyanostyryl) benzene, and *1,4*-bis(*4*-cyanostyryl)benzene loaded PVA matrix exhibit photochromic fluorescence under UV irradiation due to the photoisomerization of CS molecules [112].

2.3.2. Biological Polymer Hybrids

Fluorescent proteins are also blended with non-luminescent polymer nanofibers to use them as fluorescent probes with specific functionalities. For instance, PEO/enhanced green fluorescent proteins (E-GFP) core/PCL shell with green PL emission are used as a model for drug release. The molecules are released from the core at a slower and sustained rate while retaining their functionality both in the core-shell fiber and following release [113]. A hair-based fluorescent keratin loaded PVA nanofibers are entirely transparent after crosslinking the PVA. These biocompatible nanofibers exhibit a white PL emission [114].

Complexing DNA with a cationic surfactant can result in an electro-spinnable polymer with attractive properties for optoelectronic applications. They are soluble in organic solvents and able to form thermally stable and transparent films [115]. Salmon DNA complexed with the cationic surfactant cetyltrimethylammonium chloride (CTMA) along with fluorophores, Coumarin 102 (Cm102) (as a donor) and *4*-[*4*-dimethylamino-styryl]-*1*-docosylpyridinium bromide (Hemi-22) (as acceptor) exhibit emission from blue to orange through pure white controlled by varying the donor-to-acceptor ratio (Fig. **18**). The highly structured mesophasic morphology intrinsic to DNA–CTMA can sequester small molecules in a variety of specific nano-environments within the same matrix allows higher loading of dyes without self-fluorescence quenching [115]. Replacing Coumarin 102 with hemicyanine as chromophore results in the nanofibers with yellow-red emission under 488 nm excitation [116]. Amplified spontaneous emission can be observed when these materials are used as a matrix for laser dyes as a result of both fiber geometry and interactions between the dye and DNA. The fundamental lattice structure isolates individual dye molecules and minimizes the aggregation-induced quenching [115].

2.3.3. Hybrid with Fluorescent Dyes

Various organic dyes are used in the polymer nanofiber matrices to persuade multifunctionality besides the characteristic PL emission. PMMA nanofibers embedded with various dye molecules is considered as an ideal example of such a system (Fig. **19**). These nanofibers exhibit bright luminescence, active optical waveguiding, and laser emission with a linewidth of 0.3 nm and well-behaved input-output characteristics. The lasing performances of these fibers are comparable to state-of-the-art macroscopic polymeric lasers fabricated by soft lithography and imprinting, but with more potential for integration as a coherent light source in biosensors and Microsystems [1]. Several of these properties can be expected from other polymer/dye systems as well.

Nanofibers based on *1',3'*-dihydro-*1',3',3'*-trimethyl-*6*-nitrospiro [*2H-1*-benzopyran-*2,2'*-(*2H*)-indole] (6-NO2-

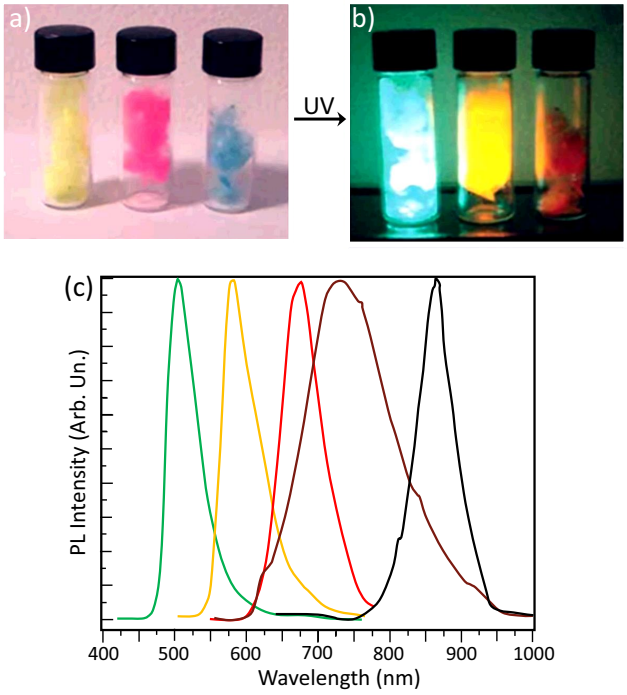

Fig. (19). Photographs of nanofibers embedded with Coumarin 334, R6G, and Nile Blue (From left to right), under (**a**) white and (**b**) UV light; and (**c**) PL spectra of fibers with Coumarin 334, R6G, Nile Blue A Perchlorate, 2-(8-(4-p-Dimetyhlaminophenyl)-2, 4-neopentylene-*1,3,5,7-o*ctatetraenyl)-*3*-methylbenzo-thiazolium Perchlorate, and *5,5'*-dichloro-*11*-diphenylamino- *3,3'*-diethyl-*10, 12*-ethylenethiatri-carbocyanine Perchlorate (From left to right), under 3.05 eV laser light.). From [1], copyright © 2009 by John Wiley Sons, Inc. Reprinted by permission of John Wiley & Sons, Inc.

change in the scattering and propagation of light. Despite the broad scattering bands, the scattering effect in electrospun nanofibers showed considerable wavelength selectivity. Fluorescence enhancement is amplified more in those cases where the scattering bands matched the dye excitation wavelengths [122]. Fluorescent whitening agents, such as, *1,4*-bis(*o*-cyanostyryl) benzene (ER) and *1*-(*o*-cyanostyryl)-*4*-(*p*-cyanostyryl)benzene (EB) incorporated PAN nanofibers exhibit PL emission at 433 nm and 437 nm respectively when excited by 348 nm [123]. Moreover, an organic semiconductor/dye, *5,6,11,12*-tetraphenylnaphthacene (rubrene)/PEO blend nanofibers emit a broad band between 550-580 nm when excited by a 430 nm source [124], as shown in Fig. (**20**).

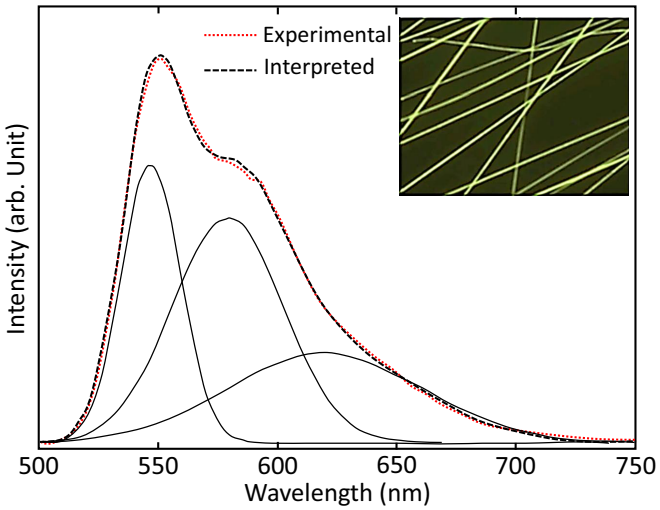

Fig. (20). The deconvoluted PL spectra of rubrene/PEO blend nanofibers, and the epifluorescence image in the inset when excited by 430 nm light. Reprinted from [124], with the permission of AIP Publishing.

BIPS) embedded PMMA nanofibers are photo-switchable. The intensity of emission at 650 nm is deteriorated when these nanofibers are continuously irradiated by a 540 nm source [117]. Adding luminescent polymethine dye, *5,5'*-dichloro-*11*-diphenylamino-*3,3'*-diethyl-*10,12*-ethylenethiatri-carbocyanine perchlorate, dispersed in PMMA nanofibers exhibit NIR fluorescence, when excited by UV light [118]. Fluorescent tracer dyes, such as fluorescein, dibromofluorescein, diidofluorescein, and fluorescein sodium loaded poly(diallyldimethy-lammonium chloride (PDAC) hybrid nanofibers exhibit a PL emission maximum of 516, of 574, 567, and 542 nm, respectively [119]. Poly(lactic acid) (PLA)/poly(glycidyl methacrylate)/fluorescein blend nanofibers are promising for the fingerprint recognition [120]. The electrospun nanofibers of PVK hole-transport and *2*-(*4*-biphenylyl)-*5*-(*4*-tertbutylphenyl)-*1,3,4*-oxadiazole (PBD) an electron-transport polymer blend with an emissive dye Coumarin 6, are promising as submicron fiber LED-waveguides with PL emission from the dye guided in the fibers and with a loss coefficient of 1.2×10^{-3} to 3.9×10^{-3} μm^{-1} at a wavelength of 540 nm [121]. The size difference of the electrospun nanofibers of PMMA/Coumarin 6 exhibit a remarkable

In a donor-acceptor system of dyes, the excitation energy is transferred from the high-energy molecules to the lower ones in order to achieve white emission. Separating the donor-acceptor organic dyes by coaxial electrospinning is an efficient way of tuning the emission from those fibers. The coaxial electrospun fibers *1,8*-naphthalic anhydride (Blue-light-emitting) as the energy-donor (shell), and orange fluorescent perylene mono-anhydride dye as the energy-acceptor (core) using PLA as the polymer matrix can emit white luminescence. The advantage of the coaxial structure is that the spatial separation of the two dyes can effectively impede the energy transfer (ET) of the two dyes and result in the emission of uniform white light [125].

In the presence of ionic liquids, the fluorescent intensity of the dye blended fibers is tremendously enhanced. The PL emission in the green spectral region from cellulose nanofibers are improved by adding a binary mixture of *1*-ethyl-*3*-methylimidazolium acetate and 1-decyl-3-methylimidazolium chloride ionic liquids [126]. However, the addition of anionic hyaluronic acid to PEO nanofibers containing cationic fluorescent dyes pyrene (PyrMA) and porphyrin (TMPyP) improves the energy transfer from pyrene to por-

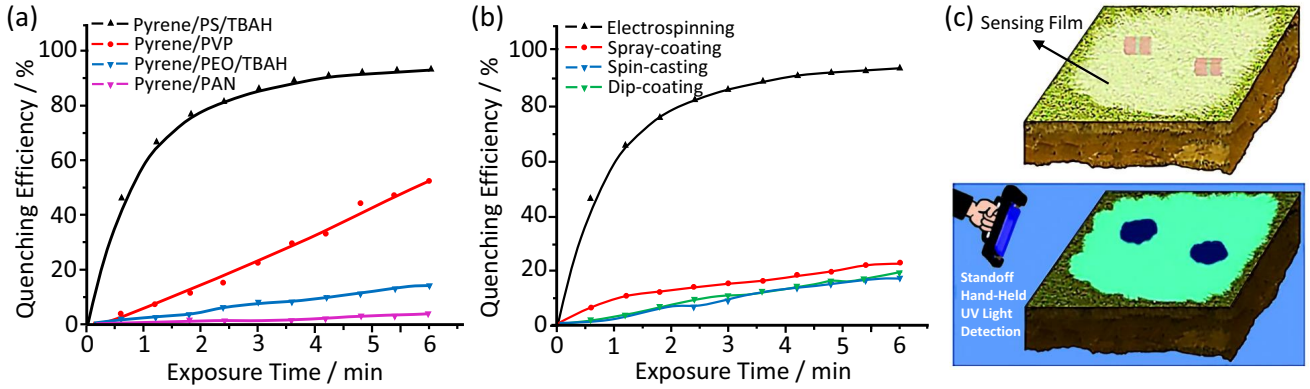

Fig. (21). Time-dependent fluorescence quenching profiles of (**a**) pyrene/PS/TBAH (black), pyrene/PVP (red), pyrene/PEO/TBAH (blue), and pyrene/PAN (magenta) nanofibers and (**b**) comparison of responses of pyrene/PS/TBAH films obtained using different techniques, in the presence of DNT vapor, and (**c**) schematic drawing for mapping buried explosives using the sensing film under a handheld UV light. From [128], copyright © 2012 by John Wiley Sons, Inc. Reprinted by permission of John Wiley & Sons, Inc.

phyrin with high FRET efficiency of 96% upon light excitation at 342 nm. The same resulted in the quenching of pyrene emission from these nanofibers. The energy transfer efficiency of the pre-mixed nanofibers is 27 times higher than post-mixed counterparts [127]. The electrospun nanofibers of pyrene/PS nanofibers in the presence of tetrabutylammonium hexafluorophosphate (TBAH) are smooth and homogeneous. These nanofibers potentially used as a fluorescent probe for nitro explosives, such as TNT, Tetryl, RDX, PETN, and HMX. The potential π–π stacking between pyrene and phenyl pendants of PS in the nanofibers allows the efficient energy migration along the polymer chain and thus significantly amplify the sensing signal in the detection of nitro explosives [128], Fig. (**21**).

The stability of the dyes can be improved by loading them to stable nanostructures before embedding them into polymer fibers. Loading PEO nanofibers with dye-loaded nanosized zeolite L crystals' exhibit a two-step FRET to the dye included in the zeolite channels. The zeolite framework protects the dye against external attacks, such as photo-oxidation, of the organic dye [129, 130].

3. INORGANIC NANOFIBERS

Sol-gel electrospinning followed by the distinct post-processing techniques results in nanofibers of fluorides, sulfides, oxides, nitrides, carbides, and oxy-halides with PL characteristics. In general, the electrospinning of ceramic nanofibers can be divided into three steps; one, preparation of the spinnable sol containing the metal salt with adequate viscosity; two, electrospinning process under appropriate operating conditions and finally, the high-temperature calcination. Electrospun oxide nanofibers are fabricated by direct calcination in air at a high temperature to degrade the volatile part of the precursor composite fiber at a high temperature. The adequate viscosity for the sol is achieved by adding a polymeric binder or by Pechini's method, where the metal salt is complexed by citric acid or ethylene glycol [131]. Altogether, the organic nanofibers are advantageous by its high surface area, porosity, high temperature and chemical resistance, multifunctionality, etc., moreover, they are proven to be ideal hosts for the luminescent rare earth and transition metal ions. The intrinsic luminescence from these nanofibers is due to the various types of defects present in these fibers, which extends from UV-vis to IR region. The energy transfer from the host lattice to the doped luminescent ions allows these nanofibers to emit bright characteristic emissions of the dopants with high photostability. When doped with rare earth ions, these inorganic nanofibers emit sharp luminescent emissions, characteristic to the rare earth ions. One cannot observe such emissions in organic-based luminescent fibers. One of the major disadvantages of the inorganic fibers is its brittleness, as compares with organic fibers, which are flexible in nature.

3.1. Halides and Oxy-Halide Nanofibers

3.1.1. Halides

The halides and oxy-halide nanofibers are fabricated by the two-stage post-processing of electrospun precursor fibers. In the first post-processing stage, the precursor fibers are calcined to yield oxide nanofibers, and these nanofibers are subsequently heated in the presence of respective media, such as ammonia, sulfur, *etc*., to form halide or oxy-halide nanofibers.

The optoelectronic properties of several halides are well established and studied in detail. GaN is one such exotic material most useful in semiconducting LEDs. Nanofibers of GaN can be electrospun using PVP and gallium nitrate as the starting materials. The electrospun PVP/gallium nitrate composite fibers are then successively calcined in air at 500°C to form gallium oxide, followed by treating in an ammonia atmosphere at 850°C. GaN nanofibers exhibit a PL emission peak maximum at ~365 nm. The electrical conductance of GaN nanofibers increases by 830 times under a UV illuminance of 254 nm [132].

ZnS is yet another essential semiconducting material with a band gap of 3.54 eV and a characteristic broad blue emission as in Fig. (**22**), when excited by 325 nm source. The nanofibers of ZnS can be obtained by treating the ZnO nanofibers under H_2S atmosphere [133]. Another derivative of ZnS, ZnS_xSe_{1-x} nanofibers prepared by calcining precursor nanofibers containing polyvinyl butyral (PVB), $ZnCl_2$ and

TOPOS or TOPOSe or TOPOSSe, exhibit a tunable PL emission from ZnS_xSe_{1-x} with various S/Se ratio. As the Se content increases, PL emission is shifted from blue to red, characteristic to ZnS and ZnSe when excited by 442 nm (x=1 and 0.8) and 532 nm (x=0.5, 0.2 and 0) [134].

The excellent properties of fluorides as the luminescent matrices enable them to use as a host lattice for various rare earth ions and transition metals [135, 136]. The preparation of fluoride nanofibers involves a two-stage process, oxidation followed by fluorination. The fabrication of $BaYF_5$ doped with Er^{3+} UC nanofibers is an excellent example of the process. In the fabrication process PVP/[$Ba(CH_3COO)_2$ +$Y(NO_3)_3$ + $Er(NO_3)_3$ composite nanofibers are fabricated first by electrospinning process and then calcined at 600°C to yield mixed oxide nanofibers. These fibers are then placed in a double crucible, with the mixed oxide fibers in the inner crucible and NH_4HF_2 as the fluorinating again in the outer crucible, and the crucible is covered and heated at 280°C first and annealed at 600°C. The schematic of the double crucible method is depicted in Fig. (**23**). These nanofibers emit strong green and weak red upconversion (UC) emissions when excited by 980 nm laser [137].

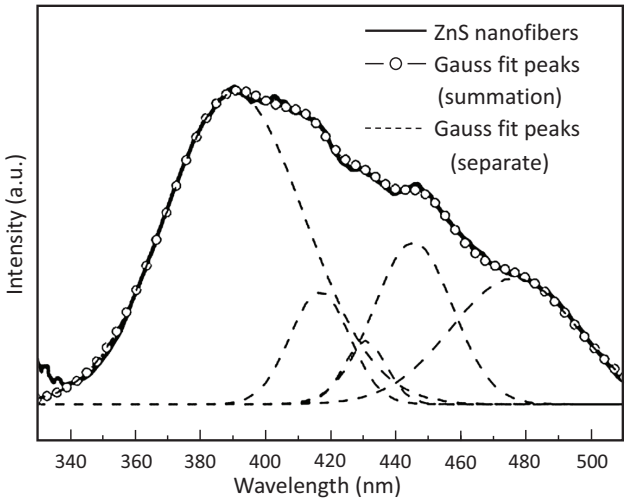

Fig. (22). PL emission from ZnS nanofibers under 325 nm source. From [133], copyright © 2007 by John Wiley Sons, Inc. Reprinted by permission of John Wiley & Sons, Inc.

YF_3 nanofibers codoped with Yb^{3+} and Tm^{3+} [138], YF_3 codoped with Yb^{3+} and Er^{3+} [139] and YF_3 nanofibers doped with Tb^{3+} [140] are also successfully electrospun as nanofibers. $Ba_4Y_3F_{17}:Er^{3+}$ UC nanofibers are another example of the fabrication of luminescent fluoride by electrospinning [141]. Calcining $NaGdF_4:Eu^{3+}$ nanoparticle/PVP composite nanofibers can yield $NaGdF_4:Eu^{3+}$ nanofibers after calcination by sintering, emits red light under 273 nm excitation [142]. The other complex fluorides such as hexafluorosilicates [136], hexafluorogermanate [143], *etc*., can be potentially electrospun as nanofibers with unique luminescent properties.

3.1.2. Oxy-Halides

Lanthanum based oxy-halide nanofibers are extensively studied for their bright luminescence characteristics. LaOCl: Ln^{3+} (Ln = Eu/Sm, Tb, Tm) prepared by aforesaid double crucible method exhibit characteristic PL emissions from the respective rare earth ions, when excited by the host-excitation wavelength of 234 nm. These nanofibers also

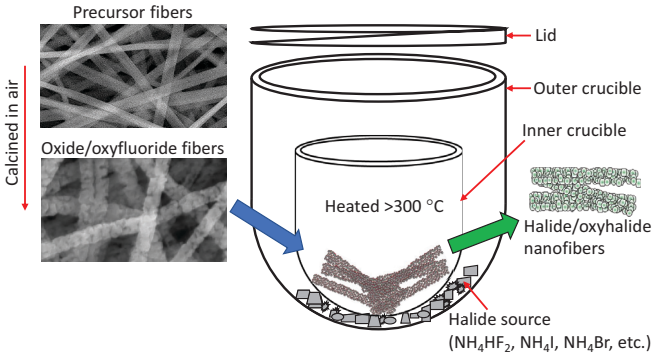

Fig. (23). Double crucible method for the fabrication of halide and oxy-halide fibers.

exhibit CL emissions characteristic to RE ions as shown in Fig. (**24**) [144]. LaOCl: nanofibers doped with Ce^{3+}/Tb^{3+} [145], Eu^{3+} [146], Er^{3+} [147] Yb^{3+}/Er^{3+} [148] are reported as promising phosphors. Green luminescent $LaOI:Tb^{3+}$ nanofibers are prepared by a double crucible method using $La_2O_3:Tb^{3+}$ nanofibers and NH_4I as the precursors [149]. $LaOI:Yb^{3+}/Ho^{3+}$ nanofibers prepared by the same route exhibit up-conversion luminescence emissions centering at 541 nm and 655 nm under 980 nm laser source [150]. Similarly, $LaOBr:Tb^{3+}$ nanofibers with green emissions are also prepared using a double crucible method. The luminescence intensity of hollow $LaOBr:Tb^{3+}$ nanofibers is greater than that of solid nanofiber and nanobelt counterparts under the same measuring conditions [151] $LaOBr:Eu^{3+}$ nanofibers with red emission [152], $LaOBr:Er^{3+}$ and [153] LaOBr: Yb^{3+}/Er^{3+} nanofibers with UC emission [154], and LaOBr: Nd^{3+} nanofibers with IR emission [155] are also fabricated following the same procedure. $La_2O_2CN_2:Eu^{3+}$ nanofibers prepared *via* cyanidation of $La_2O_3:Eu^{3+}$ nanofibers emit the predominant emission peaks at 614 nm, and 622 nm originated from the energy levels transition $^5D_0 \rightarrow {}^7F_2$ of Eu^{3+} ions under the excitation of 284 nm [156]. $La_2O_2CN_2:Tb^{3+}$ nanostructures emit predominantly at 543 nm; this emission originates from the Tb^{3+} ion under 274 nm irradiation [157]. $La_2O_2CN_2:Er^{3+}$ and $La_2O_2CN_2:Er^{3+}/Yb^{3+}$ nanofibers under the excitation of a 980 nm diode laser exhibit a UC emission [158].

Oxyfluorides of rare earth elements can be fabricated using trifluoroacetate salts of rare earths. EuOF and HoOF nanofibers are fabricated using PVP/europium trifluoroacetate ($Eu(CF_3CO_2)_3$) and PVP/holmium trifluoroacetate ($Ho(CF_3CO_2)_3$) composite nanofibers as the precursors for calcination. EuOF exhibit intensity maximum at 609 nm and HoOF at 645 nm when excited by 290 nm [159]. BCNO nanofibers, composed of polycrystalline-BCN and B_2O_3 crystals

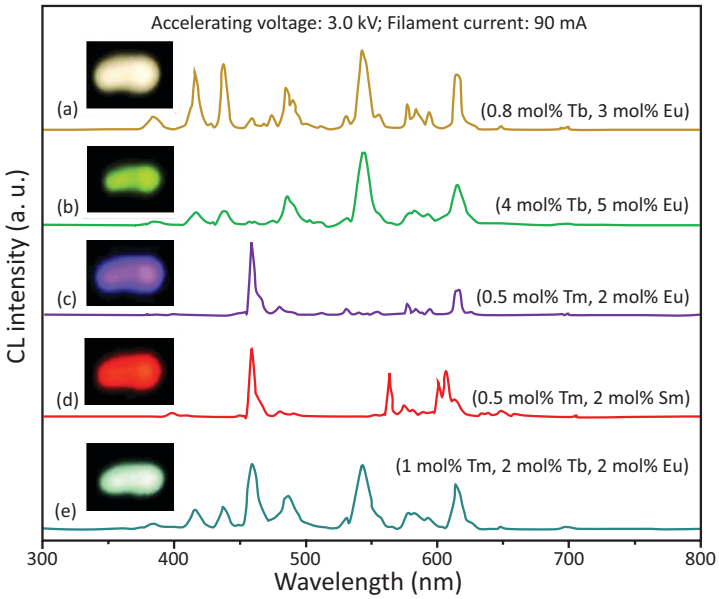

Fig. (24). Typical CL spectra of LaOCl: Ln^{3+} fibers annealed at 900 °C. (**a**) 0.8 mol.% Tb^{3+}, 3 mol.% Eu^{3+}; (**b**) 4 mol.% Tb^{3+}, 5 mol.% Eu^{3+}; (**c**) 0.5 mol.% Tm^{3+}, 2 mol.% Eu^{3+}; (**d**) 0.5 mol.% Tm^{3+}, 2 mol.% Sm^{3+}, and (**e**) LaOCl: 1 mol.% Tm^{3+}, 2 mol.% Tb^{3+}, 2 mol.% Eu^{3+}. The insets show the respective digital photographs. From [144], copyright © 2009 by John Wiley Sons, Inc. Reprinted by permission of John Wiley & Sons, Inc.

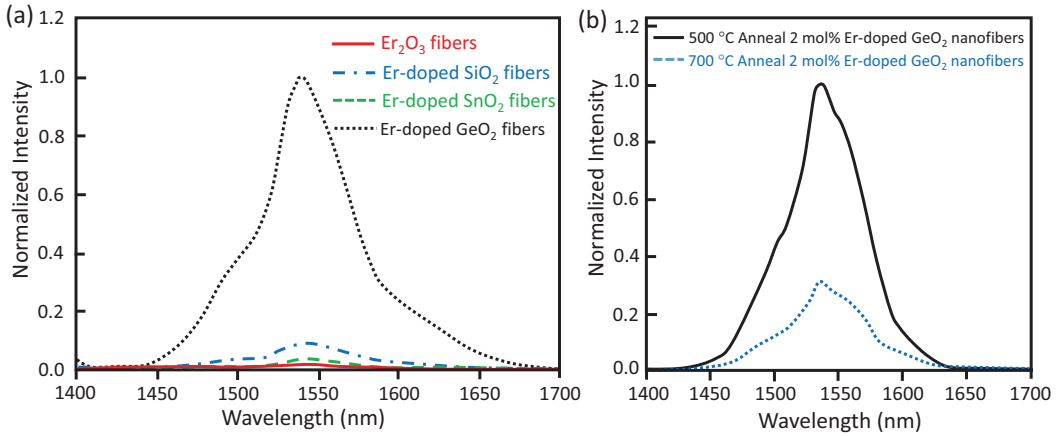

Fig. (25). PL emission of (**a**) i-Er_2O_3, ii-Er-doped SnO_2, iii-Er-doped SiO_2, and iv-Er-doped GeO_2 nanofibers, and (**b**) Er-doped GeO_2 nanofibers annealed at 500 and 700 °C in air for 3 h. Adapted with permission from [177]. Copyright (2007) American Chemical Society.

obtained by calcining PAN/boric acid precursor fibers, show intense green and yellow (528-552 nm) emissions under UV (365 nm) irradiation [160]. $CaSi_2O_2N_2$:Eu by heating the precursor composite fibers in an N_2 atmosphere emits light in a broad band between 500-600 nm when excited by 450 nm [161]. $Ca_{0.68}Si_9Al_3(ON)_{16}$:$Eu^{2+}$ micro-belts prepared by electrospinning and subsequent nitridation exhibits single broadband in the 400 to 700 nm region, with the maximum intensity always being at 580 nm [162].

Electrospun oxy-sulfide nanofibers such as dilutetium dioxide sulfide (Lu_2O_2S) and yttrium dioxide sulfide (Y_2O_2S) are fabricated by heating the respective oxides in the presence of sulfur (sulfurization). Lu_2O_2S doped with Eu^{3+} nanofibers showed strong characteristic red emission of typical Eu^{3+} ($^5D_0$–^7F_J) transitions [163]. Y_2O_2S:Eu^{3+} hollow nanofibers exhibit red emissions [164] and Y_2O_2S:Er^{3+} hollow nanofibers show UC emission spectrum in the significant green and weak red region, originated from $^2H_{11/2}/^4S_{3/2} \rightarrow {}^4I_{15/2}$ and $^4F_{9/2} \rightarrow {}^4I_{I5/2}$ energy levels transition of the Er^{3+} ions [165]. Y_2O_2S:Yb^{3+}, Er^{3+} nanofibers are also upconverting with intense green and red UC emission centering at 526, 548 and 668 nm under 980 nm source [166].

3.2. Transition Oxides/Rare Earth Oxide Nanofibers

Several oxides have been studied extensively as useful host lattices for rare earth ions to produce phosphors emitting a variety of colors with high luminescence quantum yields. The vacancy induced PL emission is predominant in nanosized oxides prepared at high temperature, especially through sol-gel electrospinning, *via* band-gap narrowing.

The energy transfer from the lattice to the dopant ions leads to the PL emission originated from the RE ions in the oxide matrices. Rare earth ions with different emission characteristics can be readily doped to the oxide nanofibers through electrospinning, and ultimately one can achieve a tunable PL emission. Many oxide nanofibers with PL emission are reported in the literature.

The nanofibers of basic oxides such as ZnO, TiO_2, and SiO_2 are broadly studied for their PL characteristics. Most of the oxides in their pure form exhibit a wideband emission corresponding to the vacancies in their lattice structure. ZnO nanofibers fabricated through PVA assisted electrospinning of zinc acetate precursor exhibit PL emissions at UV (3.13 eV) and green (2.21 eV) regions when excited by a 335 nm source [167]. Doping aluminium to the ZnO nanofiber matrix widens the emission in the green region because the extrinsic Al^{3+} impurity increases the free charge carriers in the ZnO matrix [168]. Non-stoichiometry of the dopants strongly influences the PL of ZnO nanofibers. Aluminum well disperses within zincite whereas calcium segregates to a secondary phase forming calcite. The Al^{3+} content controls the relative exciton-to-defect emission band intensity, as well as the frequency of the main ZnO absorption peak [169].

Electrospun TiO_2:RE (RE = Eu^{3+}, Er^{3+}, Ce^{3+}, Pr^{3+}) nanofibers exhibit characteristic emission from the RE ions with a broad excitation band in 300-400 nm region corresponding to the absorption region of TiO_2, which in turn reveals the energy transfer from the TiO_2 matrix to the rare earth ions [170]. Similarly, RE (RE= Eu^{3+}, Er^{3+}) doped TiO_2 nanofibers obtained by calcining at 1,000°C exhibit characteristic cathodoluminescent (CL) emission band of rare earth ions. At a lower calcination temperature of 500°C, a broad green PL emission peak in the visible range peaking at about 550 nm is detected, and it can be attributed to the radiative recombination of self-trapped excitons (STEs) localized within TiO_6 octahedra of TiO_2 structure [171]. Moreover, PL is a very sensitive tool to detect the presence of anatase in rutile phase TiO_2 nanostructures. The weak peaks observed at 467 and 541 nm, respectively are corresponding to the anatase phase of TiO_2 and the PL peak in the IR region at 805 nm is from the rutile phase [172]. The incorporation of Tb^{3+} and Yb^{3+} in TiO_2 nanofibers resulted in delayed anatase to rutile phase transition, accompanied by the formation $Ln_2Ti_2O_7$ (Ln = Tb^{3+}, Yb^{3+}). All samples showed luminescent properties and the relative emission spectra are dominated by the typical Tb^{3+} and Yb^{3+} emission peaks associated with the specific Ln^{3+} *4f*-transitions [173]. SiO_2:Ln^{3+} (Eu^{3+}, Tb^{3+}) hollow nanofibers are characterized by bright emission and are color tunable by adjusting the Eu/Tb doping [174].

GeO_2 nanofibers prepared using poly(vinyl acetate) and germanium dioxide sol by electrospinning shows strong luminescence around 564-580 nm when excited by 325 nm [175]. On a comparison made among the Er_2O_3, Er^{3+} doped SiO_2, GeO_2 and SnO_2 [176] nanofibers with a characteristic emission from Er^{3+} in the IR region (Fig. **25a**), the highest intensity of the characteristic emission observed from Er^{3+} doped GeO_2 nanofibers, moreover, it is entirely dependent on the annealing temperatures used in the calcination process (Fig. **25b**). The several oxygen vacancies at low calcination temperatures act as sensitizers to excite Er^{3+} ions via a carrier-mediated process [177].

Some transition oxide nanofibers in their pure form exhibit luminescence. WO_3 nanofibers exhibit a PL emission peak at 358 and 378 nm, respectively when excited by a 275 nm source [178]. β-Ga_2O_3 nanofibers exhibit PL spectrum under an excitation of 365nm give 470nm, originate from the vacancies of gallium and oxygen and the gallium-oxygen vacancy pairs as well [179]. Undoped SnO_2 nanowires show stable PL with two emission peaks centered at around 470 and 560 nm, which are temperature dependent, originated from the surface oxygen vacancies [180]. In_2O_3 ceramic nanofibers obtained by electrospinning show a strong PL emission in the ultraviolet (UV) region under shorter UV light irradiation. Upon excitation of 238 nm, the In_2O_3 nanofiber emits a strong, broad PL spectrum with a peak maximum at 341 nm originating from the oxygen vacancies generated during the annealing process [181].

Besides using them as dopant ions in various oxide matrices of transition oxides, the oxide nanofibers of lanthanides themselves are used as the active luminescent host matrices. For example, electrospun Ce^{3+} and Tb^{3+}-co-doped La_2O_3 nanofibers emit an intense green emission arising from the energy transfer process from Ce^{3+} to Tb^{3+} as observed in several other instances [182]. Europium oxide (Eu_2O_3) nanobelts obtained electrospinning exhibit a PL spectrum (with peaks ranging from ultraviolet (UV) to near-infrared (NIR) at 727 nm) resulting in a white light emission unlike the bulk powders with traditional red emission (612 nm, due to more excited electronic states in Eu_2O_3 nanobelts [183].

The electrospun non-luminescent oxide nanofibers can be post-processed to functionalize with organic molecules to achieve unique functionalities. Example, porphyrin-functionalized silica fibers exhibit a broad emission with peaks at 655 and 725 nm corresponding to those of the porphyrin dye when excited by 420 nm source. These nanofibers exhibit luminescent quenching in the presence of TNT vapors [184].

3.3. Complex Oxide Nanofibers

Oxides with more than one metallic element in their lattices are also broadly used as luminescent materials or matrices for luminescent ions, and the ligand to activator ion energy transfer allows bright luminescence from these fibers. Perovskite structured, $CaTiO_3$: codoped with Eu^{3+}/Gd^{3+} nanofibers show the characteristic emission of Eu^{3+} under 398 nm excitation, and the luminous intensity increased with the increase of Gd^{3+} concentration, reveals the non-radiative transitions between Gd^{3+} to Eu^{3+} [185]. $CaTiO_3$:*x*Pr^{3+} samples show the red emission at 612 nm, corresponding to the $^1D_2$-$^3H_4$ transition of Pr^{3+} [186] and doping Zn to $CaTiO_3$:Pr^{3+} nanofibers increases the decay time of the bright red emission [187]. Some of these complex oxide fibers are multifunctional, *e.g.*, barium titanate ($BaTiO_3$) perovskite nanofibers are piezoelectric, exhibiting a broad and intense PL emission bands with maximum intensity at 600 nm which is influenced by the calcination temperature [188]. Er^{3+} doped $BaTiO_3$ nanofibers prepared by an electrospinning method are also piezoelectric with UC emission. As the annealing temperature increases, the luminescent properties are improved tremendously due to the site symmetry change of the Er^{3+} ions [189]. The PL spectra of the $ZnTiO_3$:Pb^{2+} sam-

ples under an excitation 488 nm reveal a luminescent phenomenon in blue and green region (516, 524, 532 and 546nm), which can be attributed to the Pb^{2+}-related charge-transfer transitions in $ZnTiO_3$ nanofibers [190].

YVO_4:Ln and Y(V, P)O_4:Ln (Ln = Eu^{3+}, Sm^{3+}, Dy^{3+}) electrospun nanofibers can be tuned for the gamut emission in the visible spectrum by the by partial replacement of VO_4^{3-} by PO_4^{3-} and changing the doping concentrations of Ln. [191], (Fig. **26**). A similar study reveals that the electrospun $CaMoO_4$:Ln^{3+} nanofibers can be tuned from blue-green to green, yellow, and orange-red easily by changing the doping concentrations of Ln^{3+} ions [192], (Fig. **27**). In all the fibers above, the efficient energy transfer from ligands VO_4^{3-}, PO_4^{3-}, MoO_4^{2-} and WO_4^{2-} to the lanthanide ions allow the bright emission favorable for field emission displays and fluorescent lamps. $LaPO_4$ nanofibers are yet another luminescent matrix which exhibits PL emission characteristics. The crystal structure of the $LaPO_4$ nanofibers using PVP as a binder is significantly affected by the ratio of PVP/metal salt. The La_3PO_7 phases appear when PVP/salt ratio is above two, and pure La_3PO_7 phase is obtained when the ratio is six or above. This changes in the phase of the nanofibers from $LaPO_4$ to La_3PO_7 the luminescence intensity of Eu^{3+} is quenched and the lifetime is decreased (Fig. **28**). The quenching of the Eu^{3+} emissions in the La_3PO_7 phase is related to more adsorption of water and the increase of the intensity ratio due to the decreased site symmetry surrounding Eu^{3+} [193]. Electrospun Ce^{3+} and Tb^{3+} doped $LaPO_4$ [194] and $BiPO_4$ [195] nanofibers exhibit a green emission with an energy transfer from Ce^{3+} to Tb^{3+} ions using a 290 nm excitation. Under low-voltage electron beam excitation, micro belt phosphors have a higher CL intensity than the nanofiber phosphors due to lower defect concentration in the former.

Therefore, one can elucidate that, once doped with rare earth elements, most of the oxide fibers emit characteristic emission from those ions. For instance, as a rule of thumb, Eu^{3+} doping results in red emission irrespective of the oxide matrices, though the energy of excitation is dependent on the host lattice. Red emission is observed by Eu^{3+} doping in single element oxides, such as, SiO_2 [196], ZnO [197], TiO_2 [198], CeO_2 [199], ZrO_2 [200], SnO_2 [201], HfO_2 [202], Gd_2O_3 [203], Y_2O_3 [204], Lu_2O_3 [205], β-Ga_2O_3 [206], *etc.*, and in many complex oxides such as YVO_4 [207], $CuAlO_2$ [208], Sr_2SiO_4 [209] $LuBO_3$ [210], $GdBO_3$ [211], Gd_2MoO_6 [212], $Y_3Al_5O_{12}$ (YAG) [213], $CaYAl_3O_7$ [214], Li_2BaSiO_4 [215], $KGdTa_2O_7$ [216], $Tb_2(WO_4)_3$ [217], $Ca_2Gd_8(SiO_4)_6O_2$ [218], YBO_3 [219], $LaBO_3$ [220], $Ca_4Y_6(SiO_4)_6O$ [221], *etc.* Similarly, Tb^{3+} doping cause green emission in several matrices, *e.g.*, SiO_2 [222], Gd_2O_3 [223], ZrO_2 [224], HfO_2 [202], β-Ga_2O_3 [225], La_2O_3 [226], Y_2O_3 [227], $CdWO_4$ [228], $CePO_4$ [229], $LuBO_3$ [210], $GdBO_3$ [211], $LaBO_3$ [220], $Y_3Al_5O_{12}$ [230], $La_{9.33}(SiO_4)_6O_2$ [231], $Gd_2O_2SO_4$ [232], *etc*.

The same holds true when these ions are codoped with a sensitizer ions. For instance, the PL emission of Eu^{3+} doped $La_{1-x}Gd_xVO_4$ nanofibers is characteristic to Eu^{3+} ions, but the introduction of Gd^{3+} in the lattice of Eu:$LaVO_4$ significantly improves the emission bands of Eu^{3+} ions, revealing the possible energy transfer from Gd^{3+} to Eu^{3+} ions. The only difference in the emission by Gd^{3+} codoping is the intensity. The intensity of emission from Eu:$GdVO_4$ nanofibers are also lower than Eu:$La_{1-x}Gd_xVO_4$ nanofibers [233].

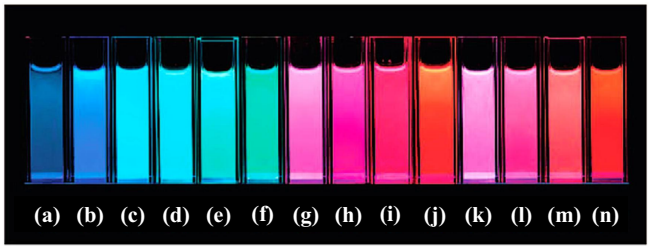

Fig. (26). Luminescence photographs of YVO_4 and $Y_{1-x}P_{0.8}V_{0.2}O_4$:*x*Ln nanofibers dispersed in the ethanol solutions: (**a**) YVO_4; (**b**) $Y(P_{0.8}V_{0.2})O_4$; (**c-f**) $Y_{1-x}P_{0.8}V_{0.2}O_4$:*x*Dy^{3+} (*x* = 0.005, 0.01, 0.02, and 0.05); (**g-j**) $Y_{1-x}P_{0.8}V_{0.2}O_4$:*x*Eu^{3+} (*x* = 0.005, 0.01, 0.02, and 0.05); (**k-n**) $Y_{1-x}P_{0.8}V_{0.2}O_4$:*x*Sm^{3+} (*x* = 0.005, 0.01, 0.02, and 0.05). Adapted with permission from [191]. Copyright (2008) American Chemical Society.

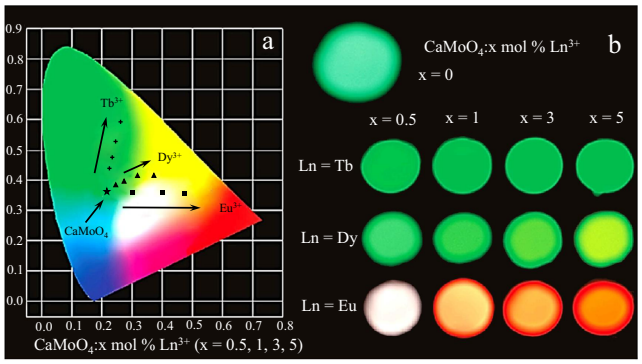

Fig. (27). (**a**) CIE chromaticity diagram and (**b**) luminescent photographs for $CaMoO_4$ and $CaMoO_4$:x mol.% Ln^{3+} under a 254 nm ultraviolet lamp. Adapted with permission from [192]. Copyright (2009) American Chemical Society.

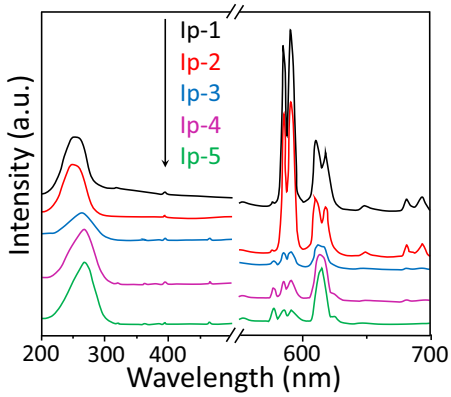

Fig. (28). Room temperature excitation (λ_{em} = 611 nm) and emission (λ_{ex} = 253 nm) spectra for Eu^{3+} ions in samples with different PVP/metal salt ratio. (lp-1) PVP/In = 1.5, (lp-2) PVP/In = 3, (lp-3) PVP/In = 4.5, (lp-4) PVP/In = 6, and (lp-5) PVP/In = 12. Adapted with permission from [193]. Copyright (2009) American Chemical Society.

Ce^{3+} doping in majority of the oxide lattices result in a blue emission as in the case of lutetium pyrosilicate $Lu_2Si_2O_7:Ce^{3+}$ nanofibers emits 386 nm light under 350 nm source, [234] and Ce^{3+}-doped lutetium oxyorthosilicate ($Lu_2SiO_5:Ce^{3+}$) nanofibers exhibit a sharp and robust emission peak located at about 403 nm, corresponding to the Ce^{3+} $5d^1 \rightarrow 4f^1$ transitions [235]. The total emission from the nanofibers need not to be from the dopants alone, the nature of the dopant site in the lattice has an important role or the ligand or the vacancies. In the case of $Ca_{(3-x)}Sr_x(PO_4)_2:Eu^{2+}$ fibers, the emissions are at different peak positions depending on Sr/Ca ratio, and the emission is tunable from blue to green and to green-yellow [236]. Under ultraviolet excitation and low-voltage electron beam excitation, $GdVO_4:Ln^{3+}$ (*Ln*=Eu, Dy, Sm) nanofibers shows the strong characteristic emission from the rare earths due to an efficient energy transfer from vanadate groups to the dopants [237]. YAG is a well-known lasing material, and there are several studies on the nanofibers of garnet group materials. One such study is on Er^{3+} doped YAG fibers. These nanofibers exhibit a series of sharp emission lines from 510 to 580 nm originated from the $^2H_{11/2} \rightarrow {}^4I_{15/2}$, $^4S_{3/2} \rightarrow {}^4I_{15/2}$, and $^2H_{9/2} \rightarrow {}^4I_{13/2}$ transitions. These nanofibers are promising for X-ray scintillation with dominated emission lines at 398 and 467 nm, respectively [238].

Manganese is the major transition metallic element that exhibits a red emission when doped in an inorganic lattice. Electrospun $CaAl_{12}O_{19}:Mn^{4+}$ nanofibers emits red bands owing to the characteristic $^2E \rightarrow {}^4A_2$ transition of Mn^{4+} ions at 655 nm with three satellite peaks. The PL intensity is enhanced by optimizing the morphology and improving the crystallinity and phase purity and are promising for high color rendering in YAG:Ce-based WLEDs [239].

A large number of luminescent oxide nanofibers are reported in the literature, and a few important ones are listed in Table **1**.

4. COMPOSITE NANOFIBERS

4.1. Polymer/Carbon Structure

Carbon nanostructures such as CNTs, fullerenes, graphene, *etc*. are super light absorbing materials as reported in several instances. The absorption these materials fall in the range of UV to IR. Therefore, luminescent quenching is generally observed when loaded them to a luminescent polymer without proper surface modification. PVK is one of the vinyl polymers with aromatic pendant groups have interesting PL properties, with a robust blue-violet emission. Addition of ultrafine fullerene (C60) to PVK composite fibers resulted in luminescent quenching by energy transfer from PVK to C60 [283]. Fluorescent quenching through photoinduced charge transfer from PPV to C60 is also evident in the case of PPV/C60 composite nanofibers [284]. The presence of single-walled carbon nanotubes (SWNT) and phenyl-C_{61}-butyric acid methyl ester (PCBM), fullerene derivative in the P*3*HT composite nanofibers significantly quench the PL emission from P*3*HT [285]. However, aromatic amine-functionalized multiwalled carbon nanotube (MWCNT)/Poly(*L*-lactide) (PLLA) composite nanofibers exhibit broad PL emission peaks at 395 and 443 nm, respectively, due to the conjugation between MWCNT-*g*-PLLAs [286]. Additionally, Eu^{3+} doped P(VDF-HFP)/ graphene composite nanofibers are multifunctional with vibration sensitivity, wearability, red light emission capability and piezoelectric energy harvesting [287].

Fluorescent carbon quantum dots (CQDs) are exceptional from the generalized properties of carbon-based minuscule structures. Recently, fluorescent CQDs have been considered promising alternatives in biomedical applications due to their unique properties, such as high quantum yield of fluorescence emission, excellent biocompatibility, low toxicity, chemical inertness, and abundant and inexpensive precursor materials. CQDs are embedded in several spinnable polymer matrices as substrates, and by doing the same, the non-radiative recombination of electron–holes can be avoided and thereby an enhanced PL performance can be achieved than pristine/colloidal CQDs as in the case of solid-state PVP/CQD nanofibers. The PL quantum yield of these nanofibers is increased to 83.5% from 42.9% of pristine CQDs under the excitation wavelength of 360 nm [288]. The electrospun composite nanofibers of CQD/polymer exhibited multicolor emission under different excitation energies. The PL emission from PAN/PAA/CQDs [289] and CQDs/PAN [290] composite nanofibers are observed at the wavelength of 442 nm, 522 nm and 580 nm corresponding to blue, green and red emissions when excited by the wavelength of 380 nm, 480 nm, and 545 nm, respectively. These emission lines are red-shifted but stronger than the CQDs in the solution.

Room temperature phosphorescence (RTP) and thermally activated delayed fluorescence (TADF) can be achieved simultaneously by incorporating CQDs into PVA by electrospinning process. The triplet states of CQDs are effectively stabilized by the ordered mesoporous structure of the electrospun CQDs/PVA nanofibers. The afterglow of these nanofibers is originated from TADF and RTP, respectively, with a lifetime of 1.61 s with a visually recognizable period of 9 s. The color of the PL can be systematically tailored by adjusting the temperature of measurement with a long average afterglow. These nanofibers are potential in trademark security and fingerprint identification, as the change in PL emission from blue to green is different from rare-earth-containing afterglow materials, always shows the same emitting color after and before the removal of the UV source [291]. CQDs are biocompatible, and the biocompatible composite nanofibers of PVP/CQDs is utilized as a matrix for drug loading and as fluorescence probe to monitor the release of a poorly water-soluble model drug, ketoprofen. These nanofibers exhibit a bright blue-light fluorescence with a PL quantum yield (QY) of 65.7%. During the drug release process, the PL emission intensity of CQDs released from the PVP/CD–KET composite nanofiber is gradually increased, and the emission intensities of the CQDs can be tailored as a function of the released amount of KET, thus facilitating easy monitoring of the drug release process [292]. In another study on CQDs embedded PVA nanofibers, the nanofiber mat is successfully employed as a luminescent test strip for the visual inspection of several antibiotics with high selectivity towards tetracycline hydrochloride (Tc). The high selectivity to Tc is due to the spectral overlap between the CDs and Tc [293]. CQD/polymer composite fibers can be utilized for the sensing of metallic ions too. CQDs encapsulated mesoporous silica immobilized PAN nanofibers

Table 1. A list of the different oxide nanofibers fabricated through electrospinning process and their PL emission/excitation characteristics.

Sr. No.	Oxide Nanofiber	Intense Emission (nm)	Excitation (nm)	Refs.
1	Pr_6O_{11}	521	280	[240]
2	SiO_2	539	488	[241]
3	$TiO_2:Y^{3+}$	595	514.5	[242]
4	$TiO_2:Co^{2+}$	420-450	295	[243]
5	$TiO_2:Er^{3+}$	566	325	[244]
6	$CeO_2:Er^{3+}$, Yb^{3+}	525, 550 and 562	980	[245]
7	$ZrO_2:Er^{3+}$, Yb^{3+}	545 and 565	980	[246]
8	$SnO_2:Er^{3+}$	1540	488	[247]
9	$HfO_2:Eu^{3+}$, Tb^{3+}	616	325	[248]
10	$BaCO_3$	486	325	[249]
11	$BaAl_{12}O_{19}:Mn^{2+}$	516	147	[250]
12	$SrTiO_3:Er^{3+}$	550 and 660	980	[251]
13	$CaTiO_3:Nd^{3+}$	1072	800	[252]
14	YBO_3	591	235	[253]
15	$BiFeO_3$	545	400	[254]
16	$BiFeO_3:Gd^{3+}$	443 and 500	401	[255]
17	$ZnWO_4$	460	280	[256]
18	$MgWO_4$	461	290	[257]
19	$SrWO4:Sm^{3+}$	561, 596 and 643	403	[258]
20	$SrWO_4$	439–441	245	[259]
21	$La_2(WO_4)_3$	415-430	345	[260]
22	InVO4	425	315	[261]
23	$GdVO_4:Bi^{3+}$	550 nm	333	[262]
24	$YVO_4:Bi^{3+}$	550 nm	333	[262]
25	$CuAlO_2:Y^{3+}$	458	365	[263]
26	$ZnAl_2O_4:Ni^{2+}$	1176	576	[264]
27	$ZnAl_2O_4:Nd^{3+}$	905, 1064 and 1335	808	[265]
28	$ZnGa_2O_4:Mn^{2+}$	505	246	[266]
29	$Zn_2SiO_4:Mn^{2+}$	524	268	[267]
30	$SrAl2O4:Eu^{2+}$, Dy^{3+}	515	348	[268]
31	$SrMoO_4:Sm^{3+}$	606	275	[269]
32	$Sr_2MgSi_2O_7:Eu^{2+}$, Dy^{3+}	471	358	[270]
33	$Sr_2MgSi_2O_7:Eu^{2+}$, Dy^{3+}	468	278	[271]
34	$CaAl_2O_4:Eu^{2+}$, Nd^{3+}	445	345	[272]
35	$CaAl_2Si_2O_8:Eu^{2+}$, Dy^{3+}	428	350	[268]

(Table 1) Contd….

Sr. No.	Oxide Nanofiber	Intense Emission (nm)	Excitation (nm)	Refs.
36	$Ca(Sr)Al_2Si_2O_8:Eu^{2+}$	428	330	[273]
37	$Ca_2MgSi_2O_7:Eu^{2+}$	539	355	[274]
38	$Lu_2SiO_5:Ce^{3+}$	403	356	[275]
39	$Y_{3-x}Al_5O_{12}:xCe^{3+}$	530	470	[276]
40	$Y_2Ti_2O_7:Er^{3+}$	420, 470, 485 and 625	700	[277]
41	$Y_2Si_2O_7$: Nd	1061	330	[278]
42	$Y_3Al_5O_{12}:Er^{3+}$, Yb^{3+}	522, 554 and 648	980	[279]
43	$La_{9.33}(SiO_4)_6O_2:Ce^{3+}$	395	315	[231]
44	$Y_2SiO_5:Ce^{3+}$, Tb^{3+}	542	248	[280]
45	Sm_2MoO_6	606 and 648	340	[281]
46	$Gd_2O_2SO_4:Tb^{3+}$	545	230	[232]
47	$PbZr_{0.52}Ti_{0.48}O_3:Er^{3+}$ (PZT:Er^{3+})	660	980	[282]

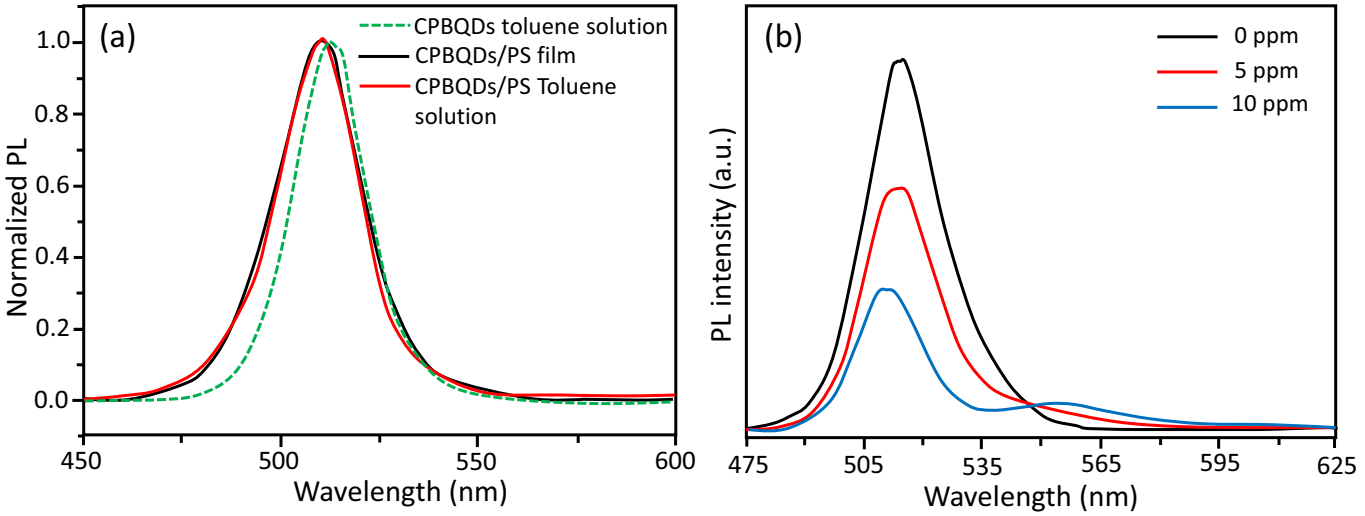

Fig. (29). (**a**) Normalized PL spectra of CPBQD toluene solution, CPBQDs/PS toluene solution, and CPBQDs/PS fibers and (**b**) PL spectra of CPBQDs/PS fibers in R6G aqueous solution with concentrations of 0, 5, 10 ppm. Adapted with permission from [298]. Copyright (2016) American Chemical Society.

have emission at 440 nm when excited by 365 nm source. The intensity of the PL emission is decreased in the presence of Fe (III) ions [294].

Fluorescent graphene quantum dots (GQDs) and carbon nanoparticles are also embedded in polymeric nanofibers to generate luminescent nanofibers. GQDs loaded PVA nanofibers modified by glucose oxidase are dual-purpose fluorescent and electrochemical biosensors for highly sensitive determination of hydrogen peroxide (H_2O_2) and glucose. The GQDs display a series of PL emission under a series of emission from different excitation wavelengths. The composite nanofibers exhibit a series of different emissions under different excitation energies. The fluorescent intensity of the emission at 430 nm under 260 nm excitation from the composite nanofibers are quenched by the presence of glucose and H_2O_2 [295]. The nanofibers of fluorescent carbon nanoparticles grafted with copolymers of styrene and spiropyran (f-CNP-g-poly(St-co-SP)) *via* reversible addition-fragmentation chain transfer polymerization emits blue-green fluorescence at 510 nm when excited by a range of 320-480 nm sources. The fluorescence of the nanofibers is quenched under prolonged exposure to UV or visible light making them photo-switchable [296].

4.2. Polymer/Quantum Dot

Perovskite quantum dots are another class of materials with bright luminescence, which can also be used as emissive fillers in electrospun polymer matrices. Due to the quantum confinement associated full absorption profiles, photochemical stability together with high emission quantum yields, the surface-chemistry-dependent photoluminescent, quantum dots (QDs) is widely gained attention in recent years as luminescent materials. Due to aggregation, the

strong luminescence of QDs is not retained in the solid state. Hence, embedding in polymer nanofibers can successfully retain the characteristics of the individual QDs.

The inorganic halide perovskite, $CsPbBr_3$, QDs (CPBQDs)-PMMA composite fiber membranes possesses comparable optical properties to QDs, with high quantum yields (88%) and a narrow half-peak width (~14 nm). CPBQDs are a potential candidate for fluorescence resonance energy transfer (FRET) based detection of trypsin, Cu^{2+} ions and pH [297]. CPBQDs encapsulated PS matrix exhibit 79.80% fluorescence retention under 365 nm UV-light illuminated for 60 h and are promising for rhodamine 6G (R6G) detection [298], (Fig. **29**). The PL features of the CPBQDs are unaffected on loading them to PS matrix, and a change in their PL intensity observed in the presence of other fluorescent dyes allow them as a platform for the detection of those molecules in aqueous solutions.

Organic halide perovskite, $CH_3NH_3PbBr_3$, QDs are also embedded in polymer matrix nanofibers as the emissive source. By tuning the halide (Cl, Br, and I) composition of perovskite QDs loaded as a core inside PAN nanofiber shell, the color of emission can be tailored. Due to the hydrophobic nature of PAN, these nanofibers are highly stable and water resistance. Moreover, a strong PL emission from the fibers are observed even after immersing the mats for 120 h in water [299]. $CH_3NH_3PbBr_3$ QDs loaded PVDF nanofiber matrix not only shows an intense green light emission but also an improved degree of crystallinity. These nanofibers are suitable for the fabrication of piezoelectric nano-pressure sensor with good piezo-sensitivity (0.1 V/Pa) under different kinds of external mechanical stimulus for application in personal identification, biomedical sector, national security and medical diagnosis [300].

Common inorganic QDs such as CdTe, CdSe, CdS, ZnS, ZnO, etc. are also used as luminescence sources in polymer matrices without compromising on their emission characteristics. As in the case of CdSe/ZnS core-shell, QDs loaded cellulose triacetate (CTA) nanofibers exhibit the emission corresponding to the quantum dot suspensions [301], as shown in Fig. (**30**). The several of these quantum dot loaded nanofibers are summarized below. Cadmium tellurium (CdTe) quantum dots (QDs) incorporated poly(*L*-lactide-*co*-caprolactone) (PLLACL) nanofibers obtained by emulsion electrospinning exhibit a characteristic absorption at about 480 nm and a narrow emission peak at about 600 nm, the same as that of the QDs. The fibrous QD–PLLACL composite showed stable fluorescence over 30 days at room temperature and are promising for the detection of chloramphenicol, an antibiotic drug, through fluorescence quenching caused by resonance energy transfer [302]. CdTe loaded PMMA nanofibers is a successful way of fabricating superhydrophobic luminescent nanofibers [303]. Also, CdTe, CdTeSe quantum dots (QDS) and CdTe/CdS core-shell QDs loaded to PVA nanofibers also exhibit strong luminescent emission characteristic to the QDs [304].

CdSe nanoparticles dispersed in polycarbonate urethane nanofibers have a modified PL emission than pure CdSe suspension due to the formation of the oriented domains in the fibers. Moreover, the PL intensity of the uniaxially aligned fibers is found to be angle dependent [305]. The PL emission and luminescence decay time of Cu-doped ZnS QDs are changed significantly compared with the un-doped sample due to the influence of copper-induced t_2 level [306].

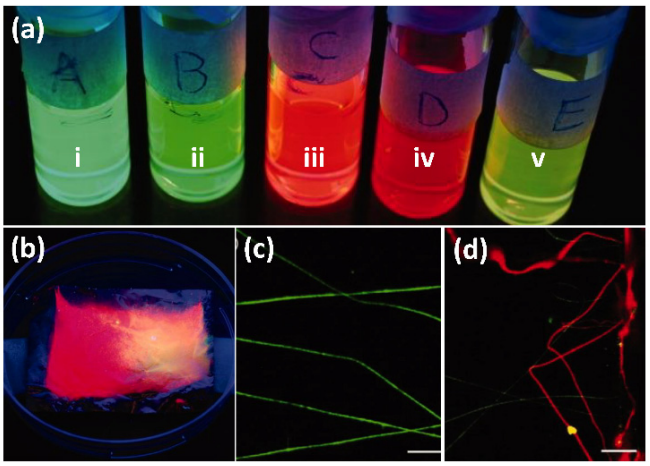

Fig. (30). (**a**) Fluorescent electrospinning solutions containing QDs with fluorescence peaks at (i) 525 nm, (ii) 550 nm, (iii) 590 nm, (iv) 615 nm and (v) 525 and 615 nm, (**b**) macroscopic fluorescence of a mat of CTA fibers containing QDs with fluorescence at 615 nm, and confocal microscopy of fluorescent fibers: (**c**) fibers containing QDs with 525 nm fluorescence and (**d**) fibers containing QDs with either 525 or 615 nm fluorescence. (Scale bars = 20 mm). From [301], copyright © 2009 by John Wiley Sons, Inc. Reprinted by permission of John Wiley & Sons, Inc.

The nanofibers of zein loaded with CdS QDs exhibit a fluorescence emission in bright blue, green and red bands when collected using separate detector channels. The strong fluorescent properties of these nanofibers last over several months. Moreover, zein-CdS nanofibers are highly biocompatible and suitable as a scaffold for attachment, migration, and proliferation of stem cells and fibroblasts [307].

CdSe embedded PVAc nanofibers showed yellow and red fluorescence properties, where the fluorescence emission colors are related to the increase in the size of QDs [308]. Electrospun CdSe/ZnS core-shell QDs loaded PCL nanofibers are light harvesting platform with donor and acceptor QDs in the same nanofibers, which allows the hybridization of the nanofibers with the blue LED to achieve white light. The donor emission lifetime modified from 12.46 ns to 7.45 ns with the change in the ratio of green and red quantum dots in the nanofiber by confining the acceptor QDs in the proximity of donor QDs [309]. The nanofibers of CdSe/ZnS core-shell conjugated with streptavidin Quantum dots loaded to SU8-100, an epoxy-based negative-tone photoresist, can be used as a subwavelength optical waveguide. The PL emission band is characteristic to the PL of QDs with a peak maximum at 605 nm [310]. CdSe/ZnS quantum dots loaded Vistamaxx 6202, a propylene-based elastomer (VM), exhibit an emission peak at 612 nm when excited by 350 nm [311].

Capping the QDs can improve their dispersion and spinnability of the polymer matrices as in the case of CdSe/CdTe quantum dots (QDs) capped with oleic acid (OA) or thiodipropioyic acid (TDPA)-or thioglycollic acid (TGA) [312] or TEMPO-oxidized [313] loaded PVP nanofibers. CdTe QDs-loaded to bacterial cellulose (BC) nanofibers obtained by wet spinning is promising as a fluorescent probe for pH and glucose sensing [314]. The ZnO quantum dot loaded PEO nanofibers exhibit a difference in the PL spectra concerning the applied voltage for electrospinning. This difference is assumed as the degree of passivation of the interface defects by PEO and the subsequent quenching of the visible emission of ZnO quantum dots by the formation of O–Zn bonds with ZnO nanoparticles. As the electrostatic stretch increases with the applied voltage, more ZnO nanoparticles with low aggregation are formed within the fibers. Therefore, the dispersion of the PEO–ZnO clusters is narrower, and the passivation is more effective, resulting in a difference in emission [315]. The same phenomenon is also observed in PVP-ZnO QD composite nanofibers, resulting in an ultraviolet emission [316]. Loading ZnO QDs in the PVA matrix exhibit a white light emission when excited by 325 nm source. The emission in the entire visible spectra from these nanofibers is due to the synergic emission from ZnO QDs and the PVA matrix [317].

4.3. Polymer/Nanoparticle

Nanoparticles loaded into polymer nanofiber matrices to improve the luminescence of conjugated polymers or luminescent nanoparticles are used in the non-luminescent polymer to induce luminescent properties. The incorporation of TiO_2 into the conjugated polymer PPV is an example for the former and TiO_2 strengthens the PL intensity of the PPV nanofibers. Due to the interaction between TiO_2 and PPV, the yellow-green emission of PPV with an emission maximum at 554 nm is modified as two emission peaks at 516 nm and 549 nm in the PL spectrum, which involves the broadening of the band gap and shortening of the conjugated chain length of PPV [318].

Metallic nanoparticles such as gold and silver are extensively used in polymer nanofibers as a luminescent source. Gold nanoparticles–gelatin composite nanofibers exhibit an emission peaking at 619 nm when excited by 520 nm source [319]. The PL emission and lifetime of silica-coated gold nanorods embedded in Eu-polystyrene (PS) nanofibers are changed for different aspect ratio and loading. Which enables these nanofibers to exhibit some unique characteristics such as tunable fluorescence lifetime, good flexibility, superhydrophobicity, and distinct textured patterns, and promising for safer data storage [320]. BSA capped gold nanoclusters incorporated PEO nanofibers exhibit a red luminescence under 488 nm excitation, and the nanofiber mat is a probe for ultra-fast selective visual detection of TNT [321]. Ag nanoparticle loaded PVP nanofibers show a significant PL band between 580 and 640 nm under 325 nm laser excitation which is persistent after several hours of laser excitation [322]. Bovine serum albumin capped gold nanoclusters anchored to PCL nanofibers exhibit a red emission under 488 nm excitation, which is gradually disappeared upon increasing the concentration of Hg^{2+} [323]. Semiconducting germanium nanocrystals (Ge-NCs) generated by laser ablation embedded into PVA nanofibers emit a broad spectrum in the visible range (380-600 nm) when excited by 360 nm with an emission maximum at ca. 417 nm originate from Ge-NCs [324].

Crystals of organo-metallic crystals are also potential fillers in the composite nanofibers, or it can be loaded on the fiber surface by post-processing the electrospun fibers. $Cu(NCS)(py)_2(PPh_3)$ nanocrystals impregnated to different electrospun polymeric mats: PMMA, PS, polyurethane (PU), and PVDF are studied for mechano-optical sensing performance. The triboluminescence characteristics are studied using a drop tower system (Fig. **31a**), and the best triboluminescent characteristics are exhibited by PU nanofiber composite mats [325], (Fig. **31b** & **31c**).

Nanoparticles of various ceramics such as sulfides, selenides, tellurides, fluorides, and oxides with luminescent properties are successfully incorporated to polymer nanofibers which exhibit characteristic luminescence of the nanoparticles. Ag_2S/PVP composite nanofibers is an example of sulfide nanoparticle/polymer composite nanofibers with PL emission; these nanofibers exhibit a blue luminescence [326]. The *in situ* formed CdS nanoparticles in electrospun PMMA nanofibers by heating the as-spun precursor composites nanofibers in H_2S. The nanofibers exhibit a PL emission in the yellow range. The bulk CdS exhibit a PL emission with a peak at 515 nm, whereas the PMMA/CdS composite fibers exhibit an emission peak at 650 nm [327]. When *ex-situ* prepared CdS quantum dot nanowires loaded into PEO fibers, the electrospinning process aligned the quantum dot nanowires parallel to the fiber axis (Fig. **32A** & **32B**). This parallel alignment resulted in a considerable difference in the PL emission parallel to the fiber axis with respect to the perpendicular of the fiber axis [328], reveals the existence of anisotropic physical properties of the quantum wires along different directions, Fig. (**32C**).

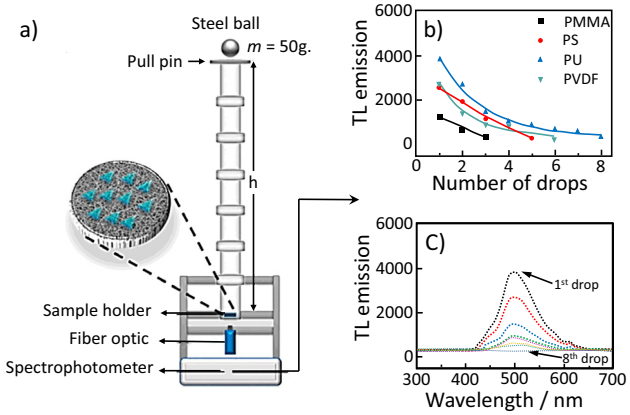

Fig. (31). Drop tower system (**a**); TL emission of the composites prepared by PMMA, PS, PVDF, and PU as a function of a number of drops (**b**); TL response of PU composite (**c**). Adapted with permission from [325]. Copyright (2016) American Chemical Society.

Randomly oriented CdS nanorods are *in-situ* formed in PVP nanofibers after treating PVP/Cadmium acetate precursor fibers under H_2S atmosphere. These nanofibers display

PL emission with a maximum intensity at 684 nm due to the surface states of CdS [329]. The application of CdS loaded polymeric nanofibers are not limited to PL emission alone.

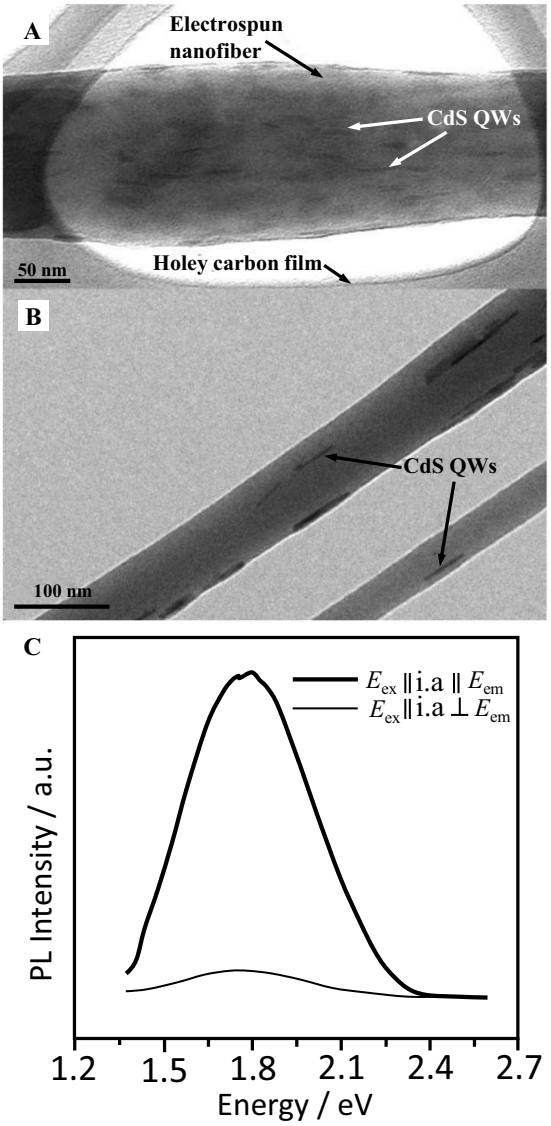

Fig. (32). (**A**, **B**) TEM images of aligned CdS QWs embedded in electrospun PEO polymer nanofibers and (**C**) room-temperature PL spectra of a fibers comprised of separated CdS quantum wires stretched within a nanofiber measured with an electric field component parallel or perpendicular to the quantum wire long axis, as labeled in the figure. From [328], copyright © 2009 by John Wiley Sons, Inc. Reprinted by permission of John Wiley & Sons, Inc.

For instance, the surface modified CdS-OH nanoparticles loaded into Polyacrylonitrile (PAN) matrix exhibit exceptional PL emission and good photocatalytic properties towards hydrogen production [330].

Post-processing of the cadmium salt loaded PAN nanofibers under H_2S, and subsequent carbonization can yield carbon/CdS coaxial nanofibers with PL emission and remarkable conductivity [331]. The blend composite fibers of P3HT/PEO-CdS nanoparticles are porous when CdS concentration is less than 3.8 wt. %. The PL response of P3HT-PEO blend is modified in the presence of CdS, caused by the disordering of P3HT chains in the composite [332]. Luminescent *in situ* formed PbS loaded PVP nanofibers are also successfully synthesized using electrospun PVP/lead acetate composite nanofibers as precursors, followed by treating in H_2S [333]. PbS grafted poly(methyl methacrylate-co-vinylbenzyl chloride) nanofibers exhibit a blue luminescence when excited by 280 nm source [334].

Capping CdS or CdSe nanoparticles with capping agents such as trioctylphosphine oxide (TOPO) or hexadecylamine (HDA) ensures the better dispersion of the particles in PMMA nanofibers. The incorporation of the luminescence nanoparticles also improves the thermal stability of the polymer over the pristine polymer [335]. Composite nanofibers of PVP/SiO_2-coated CdTe exhibit PL emission peaks at 571, 616, and 643 nm, respectively are significantly intense than CdTe/PVP nanofibers due to the passivation effect of inert hybrid silica shell on SiO_2-CdTe particles [336]. PL emission from CdTe nanoparticles loaded to PVA nanofibers is blue shifted from 525 to 426 nm due to the different quantum confinement effects [337]. The addition of CTAB into CdTe/PVP nanocomposite significantly enhances the emission from CdTe nanoparticles [338]. The PL emission intensity of CdTe/PS composite nanofibers is higher than that of CdTe nanoparticles [339]. Adding CdTe nanoparticles to a blend of PPV/PVA can yield a white light emission, as PVA can improve the blue-light emission from PPV significantly by avoiding the π–π stack and increase compatibility between the nanoparticles and the PPV precursor [340].

4.3.1. Polymer/Fluoride Nanoparticle

Fluorides are an excellent substrate for luminescent rare earth ions, and the luminescent fluoride nanostructures are embedded in the polymeric matrices through electrospinning for PL emission characteristics. Composite of *in situ* formed Er^{3+} doped CaF_2 in the PVA matrix are successfully electrospun with upconversion characteristics [341]. Ce^{3+} and Tb^{3+} codoped $NaYF_4$ nanoparticle loaded PVP nanofibers exhibit high-intensity PL luminescence with energy transfer from Ce^{3+} to Tb^{3+}, and the emission intensity is weakened by the addition of $AgNO_3$ in these fibers [342]. Yb^{3+}, Tm^{3+} codoped and Yb^{3+}, Er^{3+}, Tm^{3+} tri-doped $NaYF_4$ nanoparticle loaded/PVP exhibit UC emission under 980-nm excitation. From Yb^{3+}, Er^{3+}, Tm^{3+} tri-doped composite fibers, white light with more stable color balance (blue $^1G_4$-$^3H_6$ of Tm^{3+}, green $^2H_{11/2}$/$^4S_{3/2}$-$^4I_{15/2}$, and red $^4F_{9/2}$-$^4I_{15/2}$ of Er^{3+}) is obtained [343]. $NaYF_4$:Eu^{3+}@ $NaYF_4$: Yb^{3+}, Er^{3+} core-shell nanophosphors in the PVA nanofibers appears white in daylight while emitting strong red ($NaYF_4$:Eu^{3+}) and green ($NaYF_4$:Yb^{3+}, Er^{3+}) colors at excitation wavelengths of 254 nm and 980 nm, respectively, exhibiting both down and upconverting emissions. These nanofibers are promising as nanotaggants for anti-counterfeiting applications [344]. Er^{3+}, Yb^{3+} codoped $NaYF_4$ in PVP [345] and PMMA [346] matrices also exhibit similar UC emission characteristics. Core-shell structured $NaGdF_4$:Yb/Er@ $NaGdF_4$:Yb@mSiO_2-polyethylene glycol nanoparticle incorporated into poly(ε-caprolactone) (PCL) and gelatin loaded with an

antiphlogistic drug, indomethacin (MC), nanofibers exhibit UC emission under 980-nm laser excitation and suitable for orthotopic diagnosis and treatment [347].

4.3.2. Polymer/Oxide Nanoparticle

Luminescent oxide nanoparticles are also successfully loaded to non-luminescent polymer nanofibers. Example, PMMA/Rhodamine B-anchored silica nanoparticle composite nanofibers emit white light when excited by 365 nm source and yellow-orange when excited by 532 nm source [348]. SiO_2:Eu(TTA)$_3$phen spherical nanoparticle loaded PMMA exhibit very intense 614 nm red emission when excited by 344 nm source [349]. Er^{3+}-doped SiO_2/PVA Electrospun Nanofibers produced the highest luminescence intensity at 605 nm when excited with 514 nm source [350]. PVA-SiO_2 nanofibers decorated with conjugated polymer dots obtained by post-processing of PVA−silica nanofibers exhibit absorption at 380 nm and maximum emission at 501 nm. These nanofibers are successfully employed as a fluorescent probe for the rapid and selective detection of chemical warfare agents like diethyl chlorophosphate (DCP), dimethyl methylphosphonate (DMMP), triethylphosphate (TEP), and tributylphosphate (TBP) [351]. BCNO nanoparticle loaded PVP nanofibers exhibit a band emission in the glaucous region, which can be changed by adjusting the C content during the preparation of BCNO phosphor [352].

PVA/Polypyrrole (PPy)–ZnO composite nanofibers exhibit emission in the visible region at circa 526 nm under all the 284, 335, and 498 nm sources. The incorporation of the ZnO–NPs into the polymeric matrix, their characteristic ultraviolet luminescence emission is quenched. PVA/PPy–ZnO nanofibers exhibit a light-sensitive Ohmic behavior [353]. L-Cysteine capped ZnO nanoparticles immobilized in poly(3-hydroxybutyrate-*co*-3-hydroxyhexanoate) [P(*3*HB-*co*-3HHx)] nanofibers exhibit broad blue-green PL emission at 413, 460 and 421 nm of cysteine molecule, which is improved in the presence of ZnO nanoparticles. These nanofibers are photocatalytic towards the degradation of rhodamine B [354].

Polyhydroxy butyrate-co-valerate (PHBV)/ZnO composite nanofibers exhibit strong emission at 380 nm corresponding to ZnO, on the other hand, the visible emission from PHBV is quenched significantly [355]. ZnO nanoparticle loaded PVP nanofibers also exhibit a sharp UV emission around 380 nm [356]. Embedding ceria nanoparticles in crosslinked electrospun PVA nanofibers exhibit a visible emission under a near UV excitation and the intensity of this fluorescent emission is reduced with increasing peroxide concentration through a fluorescence quenching mechanism, revealing the potential of these nanofibers for the sensing of hydrogen peroxide [357].

Luminescent nanoparticles composed of multiple metallic elements are also used as a phosphor in various polymer nanofiber matrices. PL emission at 621 nm can be monitored from electrospun PVA/YVO_4:Eu^{3+} composite nanofibers originated from the charge transfer from O^{2-} to V^{5+}, followed by the energy transfer to Eu^{3+} ions when excited by 314 nm [358]. Similar emission characteristics are observed in PEO/YVO_4:Eu^{3+} nanoparticle composite nanofibers through vanadate to Eu^{3+} energy transfer [359]. $Ba_5Si_8O_{21}$:Eu^{2+}, Nd^{3+} (BSEN) nanoparticles loaded PVP nanofibers possessed broad excitation spectra from 250 nm to 450 nm with an emission maximum at 341 nm and exhibited a fluorescent and phosphorescent emission band from 365 nm to 650 nm with a maximum at around 489 nm with long afterglow up to 240 minutes [360]. La_6MoO_{12}:Eu^{3+}/PVA composite nanofibers exhibits an intense red luminescence corresponding to the electric dipole transition $^5D_0 \rightarrow {}^7F_2$ at 615 nm when excited by 395 nm source [361]. Dy^{3+} doped cobalt niobate ($CoNb_2O_6$) nanoparticle incorporated into Polyamide 6 fibers revealed a dominant yellow emission at 579 nm under an excitation wavelength of 366 nm. The mechanical characteristics of these nanofibrous webs are unaffected by the phosphor particles, but the fiber morphologies and size (diameter) distribution [362]. $Ca_2MgSi_2O_7$:Eu^{2+}, Dy^{3+} nanoparticle/PLA composite fibers exhibit long-persistent luminescence with emission band from 430 nm to 650 nm that peaks at 452 nm and 537 nm, respectively [363]. $SrAl_2O_4$:Eu^{2+}, Dy^{3+} nanophos-phor loaded chitosan (CS)/polycaprolactum (PCL) are biocompatible and are possible material as scaffolds for cell proliferation. The PL emission from the fibers is red-shifted on increasing the nanophosphor loading. The PL emission is at 520-560 nm when excited by 390 nm source [364].

4.4. Polymer Hybrid Composite Nanofibers

The term hybrid composite nanofibers are used to indicate, nanofibers loaded with luminescent complexes and a nanosized structure. Most of the hybrid composite fibers are designed for multi-functionality. For instance, composite nanofibers of europium complex Eu(BA)$_3$phen with Fe_3O_4 [365] and Eu(DBM)$_3$(Bath) (Bath=bathophenanthroline) with Fe_2O_3 [366] nanoparticles in PVP shows a fluorescence emission peaks of Eu^{3+} and magnetic properties of Fe_3O_4/Fe_2O_3. The percentage of Fe_3O_4 can significantly affect the fluorescence intensity of the composite nanofibers. Therefore, the simultaneous optimization of the bifunctionality of these fibers is seldom difficult. In order to overcome this difficulty, nanofibers with different morphologies, *e.g*., coaxial, Janus or bistrand, *etc*. can be fabricated. Fe_3O_4/PVP// Tb(BA)$_3$phen/PVP bifunctional bistrand nanofibers exhibit luminescent emission from Tb^{3+} ions and magnetic behavior [367]. The coaxial bifunctional nanofibers Fe_3O_4/PVP as core and Tb(BA)$_3$phen/PVP as the shell is a green emitting nanofiber. Compared with Tb(BA)$_3$ phen/PVP/Fe_3O_4 composite nanofibers, the luminescent intensity of the Fe_3O_4/PVP@Tb(BA)$_3$phen/PVP coaxial nanofibers is not influenced by non-luminescent Fe_3O_4/PVP core [368]. Fe_3O_4/PVP//Eu(BA)$_3$phen/PVP are bifunctional bistrand nanofibers with red luminescent emission [369] and the core-shell nanofibers with Fe_3O_4/PVP as core and Eu(BA)$_3$ phen/PVP as shell are also red light emitting bifunctional nanofibers [370]. By the appropriate selection of the luminescent part, the emission from the nanofibers can be adjusted. Electrospun [Fe_3O_4/PMMA]@ [$NaYF_4$:Yb^{3+},Er^{3+}/PMMA] coaxial nanoribbons and [Fe_3O_4/PMMA]//[$NaYF_4$:Yb^{3+}, Er^{3+}/PMMA] Janus nano-ribbons are magnetic and UC luminescent [371].

Introduction of polyaniline (PANI) to the bifunctional composite nanofibers makes them trifunctional. Electrospun Janus nanofibers with a coaxial nanocable made of Fe_3O_4/PVP

core and $Eu(BA)_3phen$/PVP shell as one half and (PANI)/PVP nanofiber as the other half exhibit trifunctionality with enhanced PL emission (characteristic to Eu^{3+}), electrical conductivity and superparamagnetism. Janus nanofibers with two independent isolation of $Eu(BA)_3phen$, Fe_3O_4 and PANI have better performance than composite nanofibers without partition [372]. Replacing $Eu(BA)_3phen$ with $Tb(BA)_3phen$ in the nanofibers above exhibit luminescent, magnetic-electrical tri-functionality with characteristic emissions of Tb^{3+} ions [373]. In a similar study, the trifunctional {[$Dy(BA)_3phen$+$Eu(BA)_3phen$]/PMMA}// [PANI/Fe_3O_4/PMMA] composite Janus nanofibers fabricated by electrospinning process exhibit tunable luminescence from yellow-orange-red by adjusting the ratio of rare earth complexes. The anisotropic electrical conductivity can be achieved by modulating the PANI content [374].

Embedding plasmonic nanoparticles like Au and with a fluorophore such as Rhodamine 6G (R6G) in PVP, exhibit PL spectra with peaks at ≈540 and ≈565 nm, respectively, characteristic to R6G. These nanofibers have an enhanced emission than their counterparts without Au nanoparticles. This enhancement in PL emission is due to the complex behavior of fluorophores coupled with Au nanoparticles within polymer nanowires feature localized metal-enhanced fluorescence (MEF) with unique PL characteristics compared to conventional structures. The intensification of PL when the particle is placed in the nanofibers is remarkably higher than that of thin films with comparable thickness [375].

The electrospun PEO/CS nanofibers embedded with CQDs and Fe_3O_4 is another example of multifunctional fibers for a noninvasive fluorescent probe for the removal and detection of Hg(II) ions in water. The nanofibers membrane exhibited a high adsorption efficiency for the mercury ions as the synergistic effects of polymer materials and inorganic nanoparticles. The fluorescence intensity of membranes is decreased linearly with the absorption of mercury and Fe_3O_4 allows the separation of the nonwoven membrane from the solution [376]. There are several nanofibers reported in the literature as bifunctional (Magnetism-luminescence) and trifunctional (Magnetism-luminescence-electrical conductivity) nanofibers with composite, core-shell, and Janus structures [377-393].

4.5. Ceramic Composite Nanofibers

Heterogeneous ceramic nanofibers with two or more functional materials are of great interest because of their unique multifunctional properties. The fabrication of composites of polymer/ceramic and polymer/metal composite nanofibers are already discussed. Different ceramic composite nanofibers with intriguing luminescent emission, structure, composition, and functionalities are also reported in the literature. The composites are formed either by mixing the precursors together or by adding the nanosized fillers to the precursor fibers. Moreover, some composites are formed as coaxial fibers and some others by the post-processing of the calcined fibers. Most of these fibers are obtained by the three-stage sol-gel electrospinning process discussed previously under the section on inorganic fibers.

The ceramic composite fibers of ZnO/SiO_2 hollow fibers have a unique blue luminescence owing to the radiative recombination of a trapped electron from shallow donor levels created by various oxygen vacancies in the valence band of ZnO or by the interface defect of ZnO and SiO_2 [394]. Al_2O_3–SiO_2 composite nanofibers exhibit white light emission contributed by, violet-blue emission from O defects, green emission from ≡Si(Al)–O–C·=O, and red emission from intersystem radiative crossing. White light emission is realized at an Al/(Al–Si) ratio of 40 and 60 mol.% [395]. Incorporation CdO in ZnO matrix alters the luminescent characteristics of pure ZnO. In the case of high CdO content, such as 56.5 wt.% and 72.2%, the PL emission has a single band at 2.75 and 2.64 eV, respectively, whereas for a CdO content of 39.4 wt.%, two peaks are detected at 450 and 575 nm, respectively [396], these nanofibers are useful as visible light photocatalyst for wastewater treatment. La_2O_3–ZrO_2:Eu^{3+} show the characteristic emission of Eu^{3+} corresponding to $^5D_{0,\,1,\,2}$-$^7F_{0,\,1,\,2,\,3,\,4}$ transitions due to an efficient energy transfer from O^{2-} to Eu^{3+} [397]. All these nanofibers are oxide/oxide ceramic composite fibers.

The nanosized luminescent fluoride structures loaded to oxide matrices are a possible light emitting nanostructures for nanophotonics. UC emissive CaF_2:Yb^{3+}, Er^{3+} nanoparticles embedded within SiO_2 nanofibers, prepared using electrospinning can be used for the controlled release of doxorubicin (DOX), an anti-cancerous drug, with the assist of polyacrylic acid (PAA). The optical response to DOX release under the irradiation of NIR (808 nm) laser can be determined by the spectral intensity ratio of green to red emission (I_{550}/I_{660}), and *vice versa* [398]. ZnO nanofibers loaded with $NaYF_4$:Yb^{3+}, Er^{3+} nanoparticles are an example of oxide/fluoride composite nanofibers. The high-intensity UC emission of these nanofibers is sensitive to the temperature changes [399].

Core-shell structured ceramic composite fibers with multiple functionalities are promising for biomedical applications. α-Na(Y/Gd)F_4:Yb^{3+}, Er^{3+}@Hydroxy apatite luminescent core-biocompatible shell nanofibers exhibit multifunctional properties obtained by high-temperature annealing of the hybrid precursor fibers containing α-Na(Y/Gd)F_4:Yb^{3+}, Er^{3+} nanoparticles in the core. In addition to UC luminescent properties, these nanofibers have low cell cytotoxicity making them suitable as carriers for the delivery of drugs; it is also a potential candidate as a fluorescence probe for cell imaging [400]. α-$NaYF_4$:Yb^{3+}, Er^{3+}@ silica nanofibers exhibit UC emission of Er^{3+} under 980 nm NIR laser excitation, and they are promising as drug delivery host carrier [401]. $CaTiO_3$:Yb^{3+}, Er^{3+}@bioactive glass nanofibers are biocompatible with UC emission. These nanofibers can emit green and red light under 980 nm excitation [402]. ZnO/HfO_2:Eu nanocables showed a uniform intact core-shell structure exhibit white light emission. In the PL spectra, the blue and green emissions can be attributed to the zinc vacancy and oxygen vacancy defects in ZnO/HfO_2:Eu nanocables and the yellow-red emissions are derived from Eu^{3+} ions [403]. $CoFe_2O_4$@Y_2O_3:Eu^{3+} coaxial nanofibers are bifunctional exhibiting magnetic and fluorescent properties. Firm fluorescence emission peaks of Eu^{3+} are observed with the absolute emission peak located at 612 nm [404].

Luminescent ceramic composite nanofibers are also formed by the post-processing of the electrospun ceramic

nanofiber mats. For instance, SiC has grown on SiO_2 nanofibers by carbothermal reduction of electrospun SiO_2:Tb^{3+} nanofibers, with Tb as the catalyst. SiC:Tb^{3+} nanorods generate a much stronger fluorescence emission with the characteristic emission of the Tb ions and the emission from the nanorods are stronger than PL emission from the SiC:Tb^{3+} films [405]. TiO_2/CuS fibers obtained by treating electrospun TiO_2/$CuCl_2$ fibers in thioacetamide solution exhibited lower emission intensity than pure TiO_2 fibers, which indicated a lower recombination ratio of photo-induced electrons and holes [406]. SiO_2/ZnO nanocables obtained by electrospinning of SiO_2 followed by vapor transport deposition of ZnO exhibit strong PL emission in the range of 358-406 nm when excited by 325 nm laser [407].

CONCLUSION

Electrospun fluorescent nanofibers are promising materials with a wide array of applications, and the electrospinning process is a matured method to produce these nanofibers at a large scale. The superior fluorescent emissions of the organic nanofibers compared to solution-processed thin films unveil the capability of them as nanoscale light sources, waveguides, LEDs and lasing devices. Unlike organic luminescent nanofibers, the inorganic nanofibers are highly porous and are stable in corrosive environments, high temperature, and radiations, making them suitable as high-end sensors, scintillators, catalysts, *etc*. Also, the novel strategies followed in the fabrication of the nanofibers allow them to exhibit multi-functionalities favorable for photovoltaics, sensing, drug delivery, magnetism, catalysis, *etc*. The potential of these nanofibers can be extended but not limited to smart clothing, tissue engineering, energy harvesting, energy storage, communication, safe data storage, *etc*. and it is anticipated that in the near future, luminescent nanofibers will find many more applications in diverse scientific disciplines.

CONSENT FOR PUBLICATION

Not applicable.

FUNDING

This work was partially supported by the US National Science Foundation HRD 1436120 and DMR 1626376.

CONFLICT OF INTEREST

The authors declare no conflict of interest, financial or otherwise.

ACKNOWLEDGEMENTS

Declared none.

REFERENCES

[1] Camposeo, A.; Di Benedetto, F.; Stabile, R.; Neves, A.A.R.; Cingolani, R.; Pisignano, D. Laser emission from electrospun polymer nanofibers. *Small,* **2009**, *5*(5), 562-566. http://dx.doi.org/10.1002/smll.200801165 PMID: 19189330

[2] Camposeo, A.; Persano, L.; Pisignano, D. Light-emitting electrospun nanofibers for nanophotonics and optoelectronics. *Macromol. Mater. Eng.,* **2013**, *298*, 487-503. http://dx.doi.org/10.1002/mame.201200277

[3] McCann, J.T.; Li, D.; Xia, Y. Electrospinning of nanofibers with core-sheath, hollow, or porous structures. *J. Mater. Chem.,* **2005**, *15*, 735-738. http://dx.doi.org/10.1039/b415094e

[4] Zhao, Y.; Cao, X.; Jiang, L. Bio-mimic multichannel microtubes by a facile method. *J. Am. Chem. Soc.,* **2007**, *129*(4), 764-765. http://dx.doi.org/10.1021/ja068165g PMID: 17243804

[5] Wang, X.; Zhang, K.; Zhu, M.; Yu, H.; Zhou, Z.; Chen, Y.; Hsiao, B.S. Continuous polymer nanofiber yarns prepared by self-bundling electrospinning method. *Polymer (Guildf.),* **2008**, *49*, 2755-2761. http://dx.doi.org/10.1016/j.polymer.2008.04.015

[6] Zhang, D.; Meng, L.; Xu, Q.; Bai, S.; Yang, Z.; Qin, Y. Electrospinning multi-layered nano-solenoid and reticular micro-tubular structure on a microfiber. *Mater. Lett.,* **2013**, *98*, 153-156. http://dx.doi.org/10.1016/j.matlet.2013.02.011

[7] Augustine, R.; Sarry, F.; Kalarikkal, N.; Thomas, S.; Badie, L.; Rouxel, D. Surface acoustic wave device with reduced insertion loss by electrospinning P(VDF–TrFE)/ZnO nanocomposites. *Nano-Micro Lett.,* **2016**, *8*(3), 282-290. http://dx.doi.org/10.1007/s40820-016-0088-2 PMID: 30460288

[8] Sami, S.K.; Siddiqui, S.; Shrivastava, S.; Lee, N-E.; Chung, C-H. The pine-needle-inspired structure of zinc oxide nanorods grown on electrospun nanofibers for high-performance flexible supercapacitors. *Small,* **2017**, *13*(46), 1702142. http://dx.doi.org/10.1002/smll.201702142 PMID: 29045044

[9] Liang, J.; Yuan, C.; Li, H.; Fan, K.; Wei, Z.; Sun, H.; Ma, J. Growth of SnO_2 nanoflowers on n-doped carbon nanofibers as anode for Li- and Na-ion batteries. *Nano-Micro Lett.,* **2018**, *10*(2), 21. http://dx.doi.org/10.1007/s40820-017-0172-2 PMID: 30393670

[10] Lee, J.; Yoon, J.; Kim, J-H.; Lee, T.; Byun, H. Electrospun PAN–GO composite nanofibers as water purification membranes. *J. Appl. Polym. Sci.,* **2018**, *135*, 45858. http://dx.doi.org/10.1002/app.45858

[11] George, G.; Jackson, S.L.; Luo, C.Q.; Fang, D.; Luo, D.; Hu, D.; Wen, J.; Luo, Z. Effect of doping on the performance of high-crystalline $SrMnO_3$ perovskite nanofibers as a supercapacitor electrode. *Ceram. Int.,* **2018**, *44*, 21982-21992. http://dx.doi.org/10.1016/j.ceramint.2018.08.313

[12] George, G.; Elias, L.; Hegde, A.C.; Anandhan, S. Morphological and structural characterisation of sol-gel electrospun Co_3O_4 nanofibres and their electro-catalytic behaviour. *RSC Advances,* **2015**, *5*, 40940-40949. http://dx.doi.org/10.1039/C5RA06368J

[13] Grimsdale, A.C.; Chan, K.L.; Martin, R.E.; Jokisz, P.G.; Holmes, A.B. Synthesis of light-emitting conjugated polymers for applications in electroluminescent devices. *Chem. Rev.,* **2009**, *109*(3), 897-1091. http://dx.doi.org/10.1021/cr000013v PMID: 19228015

[14] Di Camillo, D.; Fasano, V.; Ruggieri, F.; Santucci, S.; Lozzi, L.; Camposeo, A.; Pisignano, D. Near-field electrospinning of light-emitting conjugated polymer nanofibers. *Nanoscale,* **2013**, *5*(23), 11637-11642. http://dx.doi.org/10.1039/c3nr03094f PMID: 24114142

[15] Di Benedetto, F.; Camposeo, A.; Pagliara, S.; Mele, E.; Persano, L.; Stabile, R.; Cingolani, R.; Pisignano, D. Patterning of light-emitting conjugated polymer nanofibres. *Nat. Nanotechnol.,* **2008**, *3*(10), 614-619. http://dx.doi.org/10.1038/nnano.2008.232 PMID: 18839001

[16] Zhong, W.; Li, F.; Chen, L.; Chen, Y.; Wei, Y. A novel approach to electrospinning of pristine and aligned MEH-PPV using binary solvents. *J. Mater. Chem.,* **2012**, *22*, 5523-5530. http://dx.doi.org/10.1039/c2jm15970h

[17] Yeh, C.-T.; Chen, C.-Y. PH-Responsive and pyrene based electrospun nanofibers for DNA adsorption and detection. *RSC Advances,* **2017**, *7*, 6023-6030. http://dx.doi.org/10.1039/C6RA26714A

[18] Zhang, W.; Huang, Z.; Yan, E.; Wang, C.; Xin, Y.; Zhao, Q.; Tong, Y. Preparation of poly(phenylene vinylene) nanofibers by electrospinning. *Mater. Sci. Eng. A,* **2007**, *443*, 292-295. http://dx.doi.org/10.1016/j.msea.2006.05.147

[19] Okuzaki, H.; Takahashi, T.; Miyajima, N.; Suzuki, Y.; Kuwabara, T. Spontaneous formation of poly(*p* -phenylenevinylene) nanofiber

yarns through electrospinning of a precursor. *Macromolecules,* **2006**, *39*, 4276-4278.
http://dx.doi.org/10.1021/ma0608673

[20] Xin, Y.; Huang, Z.; Yang, P.; Jiang, Z.; Wang, C.; Shao, C. Controlling the deposition of light-emitting nanofibers/microfibers by the electrospinning of a poly(p-phenylene vinylene) polyelectrolyte precursor. *J. Appl. Polym. Sci.,* **2009**, *114*, 1864-1869.
http://dx.doi.org/10.1002/app.30686

[21] Chuangchote, S.; Fujita, M.; Sagawa, T.; Yoshikawa, S. Fabrication and characterizations of poly(3-hexylthiophene) nanofibers. *MRS Proceedings, 2010, 1270, 1270-HH14-07,* **2010**.
http://dx.doi.org/10.1557/PROC-1270-HH14-07

[22] Li, D.; Babel, A.; Jenekhe, S.A.; Xia, Y. Nanofibers of conjugated polymers prepared by electrospinning with a two-capillary spinneret. *Adv. Mater.,* **2004**, *16*, 2062-2066.
http://dx.doi.org/10.1002/adma.200400606

[23] Zhao, Q.; Xin, Y.; Huang, Z.; Liu, S.; Yang, C.; Li, Y. Using poly[2-methoxy-5-(2′-ethyl-hexyloxy)-1,4-phenylene vinylene] as shell to fabricate the highly fluorescent nanofibers by coaxial electrospinning. *Polymer (Guildf.),* **2007**, *48*, 4311-4315.
http://dx.doi.org/10.1016/j.polymer.2007.04.068

[24] Fasano, V.; Polini, A.; Morello, G.; Moffa, M.; Camposeo, A.; Pisignano, D. Bright light emission and waveguiding in conjugated polymer nanofibers electrospun from organic salt added solutions. *Macromolecules,* **2013**, *46*(15), 5935-5942.
http://dx.doi.org/10.1021/ma400145a PMID: 23956464

[25] Lee, C-C.; Lai, S-Y.; Su, W-B.; Chen, H-L.; Chung, C-L.; Chen, J-H. Relationship between the microstructure development and the photoluminescence efficiency of electrospun poly(*9,9*-dioctylfluorene-*2,7*-diyl) fibers. *J. Phys. Chem. C,* **2013**, *117*, 20387-20396.
http://dx.doi.org/10.1021/jp4043478

[26] Senthamizhan, A.; Celebioglu, A.; Bayir, S.; Gorur, M.; Doganci, E.; Yilmaz, F.; Uyar, T. Highly fluorescent pyrene-functional polystyrene copolymer nanofibers for enhanced sensing performance of TNT. *ACS Appl. Mater. Interfaces,* **2015**, *7*(38), 21038-21046.
http://dx.doi.org/10.1021/acsami.5b07184 PMID: 26334455

[27] Lv, Y.-Y.; Xu, W.; Lin, F-W.; Wu, J.; Xu, Z.-K. Electrospun nanofibers of porphyrinated polyimide for the ultra-sensitive detection of trace TNT. *Sens. Actuators B Chem.,* **2013**, *184*, 205-211.
http://dx.doi.org/10.1016/j.snb.2013.04.094

[28] Chen, L.-N.; Kuo, C.-C.; Chiu, Y-C.; Chen, W.-C. Ultra metal ions and pH sensing characteristics of thermoresponsive luminescent electrospun nanofibers prepared from poly(HPBO-co-NIPAAm-co-SA). *RSC Advances,* **2014**, *4*, 45345-45353.
http://dx.doi.org/10.1039/C4RA07422J

[29] Chiu, Y.-C.; Kuo, C.-C.; Hsu, J.-C.; Chen, W.-C. Thermoresponsive luminescent electrospun fibers prepared from poly(DMAEMA-co-SA-co-StFl) multifunctional random copolymers. *ACS Appl. Mater. Interfaces,* **2010**, *2*(11), 3340-3347.
http://dx.doi.org/10.1021/am100760a PMID: 20964308

[30] Xue, W.; Lin, J.-Y.; Liu, B.; Shi, N.-E.; Yu, M.-N.; Wu, W.-D.; Zhu, W.-S.; Xie, L.-H.; Wang, L.-H.; Huang, W. Exploring side-chain length effect on *β*-phase of polyfluorene derivatives in electrospinning and their optical behavior. *Polymer (Guildf.),* **2018**, *153*(26), 338-343.
http://dx.doi.org/10.1016/j.polymer.2018.05.025

[31] Wang, Y.; Wang, N.; Yu, Z.; Li, G.; Zhang, X. Novel dye-containing copolyimides: Synthesis, characterization and effect of chain entanglements on developed electrospun nanofiber morphologies. *J. Polym. Res.,* **2015**, *22*, 65.
http://dx.doi.org/10.1007/s10965-015-0713-7

[32] Kuo, C.-C.; Tung, Y.-C.; Lin, C.-H.; Chen, W.-C. Novel luminescent electrospun fibers prepared from conjugated rod-coil block copolymer of poly[*2,7*-(*9,9*-dihexylfluorene)]-block-poly(methyl methacrylate). *Macromol. Rapid Commun.,* **2008**, *29*, 1711-1715.
http://dx.doi.org/10.1002/marc.200800491

[33] Zhang, Q.; Jia, D.; Yang, Z.; Duan, X.; Chen, Q.; Zhou, Y. Synthesis of novel cobalt-containing polysilazane nanofibers with fluorescence by electrospinning. *Polymers (Basel),* **2016**, *8*(10), 350.
http://dx.doi.org/10.3390/polym8100350 PMID: 30974640

[34] Ferreira, I.; Baptista, A.C.; Leitão, J.P.; Soares, J.; Fortunato, E.; Martins, R.; Borges, J.P. Strongly photosensitive and fluorescent F8T2 electrospun fibers. *Macromol. Mater. Eng.,* **2013**, *298*, 174-180.
http://dx.doi.org/10.1002/mame.201200009

[35] Yen, H.-J.; Wu, J.-H.; Wang, W.-C.; Liou, G.-S. High-efficiency photoluminescence wholly aromatic triarylamine-based polyimide nanofiber with aggregation-induced emission enhancement. *Adv. Opt. Mater.,* **2013**, *1*, 668-676.
http://dx.doi.org/10.1002/adom.201300181

[36] Jiang, Z.; Huang, Z.; Yang, P.; Chen, J.; Xin, Y.; Xu, J. High PL-efficiency ZnO nanocrystallites/PPV composite nanofibers. *Compos. Sci. Technol.,* **2008**, *68*, 3240-3244.
http://dx.doi.org/10.1016/j.compscitech.2008.08.010

[37] Xin, Y.; Lin, T.; Li, S.; Ling, Z.; Liu, G.; Huang, Z.; Lin, J. Preparation and photoluminescence of single conjugated polymer-TiO_2 composite nanofibers. *J. Lumin.,* **2012**, *132*, 738-742.
http://dx.doi.org/10.1016/j.jlumin.2011.10.013

[38] Wang, S.; Sun, Z.; Yan, E.; Sun, L.; Huang, N.; Zang, W.; Ni, L. Spectrum-control of poly(p-phenylene vinylene) nanofibers fabricated by electrospinning with highly photoluminescent ZnS quantum dots. *Int. J. Electrochem. Sci.,* **2014**, *9*, 549-569.

[39] Li, W.; Xin, Y.; Jiang, Z.; Huang, Z.; Wang, C. Preparation and characterization of *in situ* electrospun ZnS nanoparticles/PPV nanofibers. *Pigm. Resin Technol.,* **2015**, *44*, 74-78.
http://dx.doi.org/10.1108/PRT-09-2013-0084

[40] Song, Y.; Zhan, N.; Yu, M.; Yang, Q.; Zhang, C.; Wang, H.; Li, Y. Fabrication of poly(*4*-vinylpyridine) nanofiber and fluorescent poly(*4*-vinylpyridine)/porphyrin nanofiber by electrospinning. *Chem. Res. Chin. Univ.,* **2008**, *24*, 722-725.

[41] Zhang, W.; Yan, E.; Huang, Z.; Wang, C.; Xin, Y.; Zhao, Q.; Tong, Y. Preparation and study of PPV/PVA nanofibers *via* electrospinning PPV precursor alcohol solution. *Eur. Polym. J.,* **2007**, *43*, 802-807.
http://dx.doi.org/10.1016/j.eurpolymj.2006.11.015

[42] Xin, Y.; Huang, Z.; Jiang, Z.; Che, L.; Sun, M.; Wang, C.; Liu, S. Fluorescent poly(*p*-phenylene vinylene)/poly(ethylene oxide) nanofibers obtained by electrospinning. *J. Polym. Res.,* **2011**, *18*, 477-482.
http://dx.doi.org/10.1007/s10965-010-9439-8

[43] Wang, C.; Yan, E.; Li, G.; Sun, Z.; Wang, S.; Tong, Y.; Li, W.; Xin, Y.; Huang, Z.; Yan, P. Tunable photoluminescence of poly(phenylene vinylene) nanofibers by doping of semiconductor quantum dots and polymer. *Synth. Met.,* **2010**, *160*, 1382-1386.
http://dx.doi.org/10.1016/j.synthmet.2010.01.039

[44] Tan, S.; Feng, X.; Zhao, B.; Zou, Y.; Huang, X. Preparation and photoluminescence properties of electrospun nanofibers containing PMO-PPV and $Eu(ODBM)_3$phen. *Mater. Lett.,* **2008**, *62*, 2419-2421.
http://dx.doi.org/10.1016/j.matlet.2007.12.036

[45] Campoy-Quiles, M.; Ishii, Y.; Sakai, H.; Murata, H. Highly polarized luminescence from aligned conjugated polymer electrospun nanofibers. *Appl. Phys. Lett.,* **2008**, *92*, 213305.
http://dx.doi.org/10.1063/1.2936998

[46] Ishii, Y.; Murata, H. True photoluminescence spectra revealed in electrospun light-emitting single nanofibers. *J. Mater. Chem.,* **2012**, *22*, 4695-4703.
http://dx.doi.org/10.1039/c2jm14831e

[47] Cho, M.Y.; Cho, K.; Kim, S. Luminescence shift of electrospun ZnO/MEH-PPV/PEO composite nanofibers. *J. Lumin.,* **2013**, *134*, 79-82.
http://dx.doi.org/10.1016/j.jlumin.2012.09.009

[48] Zhou, R.; Chen, W.; Jiang, X.; Wang, S.; Gong, Q. Enhanced exciton migration in electrospun poly[*2*-methoxy-*5*- (*2′*-ethylhexyloxy)-*1,4*- phenylenevinylene]/poly(vinyl pyrrolidone) nanofibers. *Appl. Phys. Lett.,* **2010**, *96*, 133309.
http://dx.doi.org/10.1063/1.3374336

[49] Wutticharoenmongkol, P.; Supaphol, P.; Srikhirin, T.; Kerdcharoen, T.; Osotchan, T. Electrospinning of polystyrene/poly(*2*-methoxy-*5*-(*2′*-ethylhexyloxy)-*1,4*-phenylene vinylene) blends. *J. Polym. Sci., B, Polym. Phys.,* **2005**, *43*, 1881-1891.
http://dx.doi.org/10.1002/polb.20478

[50] Babel, A.; Li, D.; Xia, Y.; Jenekhe, S.A. Electrospun nanofibers of blends of conjugated polymers: Morphology, optical properties, and field-effect transistors. *Macromolecules,* **2005**, *38*, 4705-4711.
http://dx.doi.org/10.1021/ma047529r

[51] Balderas, U.; Falcony, C.; Moggio, I.; Arias, E.; Mondragón, M. A photoluminescence study of electrospun fibers of conjugated poly[*2*-methoxy-*5*-(*2'*-ethylhexyloxy)-*1,4*-phenylenevinylene] blended with poly(*9*-vinylcarbazole). *Polymer (Guildf.),* **2013**, *54*, 2062-2066. http://dx.doi.org/10.1016/j.polymer.2013.02.015

[52] Mondragón, M.; Balderas, J.U.; Jiménez, G.L.; Sánchez-Espíndola, M.E.; Falcony, C. Energy transfer and compatibility analysis of PVK/MEH-PPV blends processed *via* electrospraying and electrospinning. *Org. Electron.,* **2014**, *15*, 2993-2999. http://dx.doi.org/10.1016/j.orgel.2014.08.040

[53] Madhugiri, S.; Dalton, A.; Gutierrez, J.; Ferraris, J.P.; Balkus, K.J., Jr. Electrospun MEH-PPV/SBA-15 composite nanofibers using a dual syringe method. *J. Am. Chem. Soc.,* **2003**, *125*(47), 14531-14538. http://dx.doi.org/10.1021/ja030326i PMID: 14624602

[54] Kuo, C.-C.; Wang, C.-T.; Chen, W.-C. Highly-aligned electrospun luminescent nanofibers prepared from polyfluorene/PMMA blends: Fabrication, morphology, photophysical properties and sensory applications. *Macromol. Mater. Eng.,* **2008**, *293*, 999-1008. http://dx.doi.org/10.1002/mame.200800224

[55] Kuo, C.-C.; Lin, C.-H.; Chen, W.-C. Morphology and photophysical properties of light-emitting electrospun nanofibers prepared from poly(fluorene) derivative/PMMA blends. *Macromolecules,* **2007**, *40*, 6959-6966. http://dx.doi.org/10.1021/ma0711821

[56] Terra, I.A.A.; Sanfelice, R.C.; Valente, G.T.; Correa, D.S. Optical sensor based on fluorescent PMMA/PFO electrospun nanofibers for monitoring volatile organic compounds. *J. Appl. Polym. Sci.,* **2018**, *135*, 46128. http://dx.doi.org/10.1002/app.46128

[57] Chen, H-C.; Wang, C-T.; Liu, C-L.; Liu, Y-C.; Chen, W-C. Full color light-emitting electrospun nanofibers prepared from PFO/MEH-PPV/PMMA ternary blends. *J. Polym. Sci., B Polym. Phys.,* **2009**, *47*, 463-470. http://dx.doi.org/10.1002/polb.21651

[58] Kuo, C.-C.; Lin, C.-H.; Tzeng, P.; Chen, W.-C. Morphology and photophysical properties of luminescent electrospun fibers prepared from diblock and triblock polyfluorene-*block*-poly(*2*-vinylpyridine)/PEO blends. *J. Polym. Res.,* **2011**, *18*, 1091-1100. http://dx.doi.org/10.1007/s10965-010-9511-4

[59] Vázquez-Guilló, R.; Calero, A.; Valente, A.J.M.; Burrows, H.D.; Mateo, C.R.; Mallavia, R. Novel electrospun luminescent nanofibers from cationic polyfluorene/cellulose acetate blend. *Cellulose,* **2013**, *20*, 169-177. http://dx.doi.org/10.1007/s10570-012-9809-y

[60] Wang, C.-T.; Kuo, C.-C.; Chen, H.-C.; Chen, W.-C. Non-woven and aligned electrospun multicomponent luminescent polymer nanofibers: effects of aggregated morphology on the photophysical properties. *Nanotechnology,* **2009**, *20*(37), 375604. http://dx.doi.org/10.1088/0957-4484/20/37/375604 PMID: 19706951

[61] Park, S.K.; Dhakal, K.P.; Kim, J.; Kim, J.H.; Rho, H. Fabrication and optical characterization of electrospun poly(3-buthylthiophene) nanofibers. *Synth. Met.,* **2011**, *161*, 1088-1091. http://dx.doi.org/10.1016/j.synthmet.2011.03.020

[62] Yin, K.; Zhang, L.; Lai, C.; Zhong, L.; Smith, S.; Fong, H.; Zhu, Z. Photoluminescence anisotropy of uni-axially aligned electrospun conjugated polymer nanofibers of MEH-PPV and P3HT. *J. Mater. Chem.,* **2010**, *21*, 444-448. http://dx.doi.org/10.1039/C0JM02713H

[63] Kim, J.; Lee, T.S. Full-color emissive poly(ethylene oxide) electrospun nanofibers containing a single hyperbranched conjugated polymer for large-scale, flexible light-emitting sheets. *Macromol. Rapid Commun.,* **2016**, *37*(4), 303-310. http://dx.doi.org/10.1002/marc.201500532 PMID: 26641028

[64] Cheng, C.-C.; Wang, Y.-S.; Chang, F.-C.; Lee, D.-J.; Yang, L.-C.; Chen, J.-K. Supramolecular assembly-induced enhanced emission of electrospun nanofibers. *Chem. Commun. (Camb.),* **2015**, *51*(4), 672-675. http://dx.doi.org/10.1039/C4CC07971J PMID: 25415758

[65] Xue, R.; Ge, C.; Richardson, K.; Palmer, A.; Viapiano, M.; Lannutti, J.J. Microscale sensing of oxygen *via* encapsulated porphyrin nanofibers: effect of indicator and polymer "core" permeability. *ACS Appl. Mater. Interfaces,* **2015**, *7*(16), 8606-8614. http://dx.doi.org/10.1021/acsami.5b00403 PMID: 25850567

[66] Wolf, C.; Tscherner, M.; Köstler, S. Ultra-fast opto-chemical sensors by using electrospun nanofibers as sensing layers. *Sens. Actuators B Chem.,* **2015**, *209*, 1064-1069. http://dx.doi.org/10.1016/j.snb.2014.11.070

[67] Wu, M.-C.; Chan, S.-H.; Lin, T.-F.; Lu, C.-F.; Su, W.-F. Detection of volatile organic compounds using electrospun P3HT/PMMA fibrous film. *J. Taiwan Inst. Chem. Eng.,* **2017**, *78*, 552-560. http://dx.doi.org/10.1016/j.jtice.2017.06.036

[68] Kuo, C.-C.; Wang, C.-T.; Chen, W.-C. Poly(*3*-hexylthiophene)/poly(methyl methacrylate) core-shell electrospun fibers for sensory applications. *Macromol. Symp.,* **2009**, *279*, 41-47. http://dx.doi.org/10.1002/masy.200950506

[69] Petropoulou, A.; Christodoulou, K.; Polydorou, C.; Krasia-Christoforou, T.; Riziotis, C. Cost-effective polymethacrylate-based electrospun fluorescent fibers toward ammonia sensing. *Macromol. Mater. Eng.,* **2017**, *302*, 1600453. http://dx.doi.org/10.1002/mame.201600453

[70] Chen, B.-Y.; Kuo, C.-C.; Huang, Y.-S.; Lu, S.-T.; Liang, F.-C.; Jiang, D.-H. Novel highly selective and reversible chemosensors based on dual-ratiometric fluorescent electrospun nanofibers with pH- and $Fe^{(3+)}$-modulated multicolor fluorescence emission. *ACS Appl. Mater. Interfaces,* **2015**, *7*(4), 2797-2808. http://dx.doi.org/10.1021/am508029x PMID: 25585636

[71] Kuo, C.-C.; Tung, Y.-C.; Chen, W.-C. Morphology and pH sensing characteristics of new luminescent electrospun fibers prepared from poly(phenylquinoline)-block-polystyrene/polystyrene blends. *Macromol. Rapid Commun.,* **2010**, *31*(1), 65-70. http://dx.doi.org/10.1002/marc.200900566 PMID: 21590838

[72] Deng, C.; Gong, P.; He, Q.; Cheng, J.; He, C.; Shi, L.; Zhu, D.; Lin, T. Highly fluorescent TPA-PBPV nanofibers with amplified sensory response to TNT. *Chem. Phys. Lett.,* **2009**, *483*, 219-223. http://dx.doi.org/10.1016/j.cplett.2009.10.060

[73] Sun, X.; Liu, Y.; Shaw, G.; Carrier, A.; Dey, S.; Zhao, J.; Lei, Y. Fundamental study of electrospun pyrene–polyethersulfone nanofibers using mixed solvents for sensitive and selective explosives detection in aqueous solution. *ACS Appl. Mater. Interfaces,* **2015**, *7*(24), 13189-13197. http://dx.doi.org/10.1021/acsami.5b03655 PMID: 26030223

[74] Tzeng, P.; Kuo, C.-C.; Lin, S.-T.; Chiu, Y.-C.; Chen, W.-C. New thermoresponsive luminescent electrospun nanofibers prepared from poly[*2,7*-(*9,9*-dihexylfluorene)]-*block*-poly(*n*-isopropylacrylamide)/PMMA blends. *Macromol. Chem. Phys.,* **2010**, *211*, 1408-1416. http://dx.doi.org/10.1002/macp.201000088

[75] Chiu, Y.-C.; Chen, Y.; Kuo, C.-C.; Tung, S.-H.; Kakuchi, T.; Chen, W.-C. Synthesis, morphology, and sensory applications of multifunctional rod-coil-coil triblock copolymers and their electrospun nanofibers. *ACS Appl. Mater. Interfaces,* **2012**, *4*(7), 3387-3395. http://dx.doi.org/10.1021/am300315v PMID: 22712723

[76] Wohnhaas, C.; Friedemann, K.; Busko, D.; Landfester, K.; Baluschev, S.; Crespy, D.; Turshatov, A. All organic nanofibers as ultralight versatile support for triplet–triplet annihilation upconversion. *ACS Macro Lett.,* **2013**, *2*, 446-450. http://dx.doi.org/10.1021/mz400100j

[77] Lee, E.-M.; Gwon, S.-Y.; Son, Y.-A.; Kim, S.-H. Modulation of a fluorescence switch of nanofiber mats containing photochromic spironaphthoxazine and D-π-A charge transfer dye. *J. Lumin.,* **2012**, *132*, 1427-1431. http://dx.doi.org/10.1016/j.jlumin.2012.01.034

[78] Fasano, V.; Moffa, M.; Camposeo, A.; Persano, L.; Pisignano, D. Controlled atmosphere electrospinning of organic nanofibers with improved light emission and waveguiding properties. *Macromolecules,* **2015**, *48*(21), 7803-7809. http://dx.doi.org/10.1021/acs.macromol.5b01377 PMID: 26617419

[79] Tang, S.S.; Shao, C.L.; Li, S.Z. Electrospun nanofibers of poly(vinyl pyrrolidone)/Eu^{3+} and its photoluminescence properties. *Chin. Chem. Lett.,* **2007**, *18*, 465-468. http://dx.doi.org/10.1016/j.cclet.2007.01.040

[80] Tang, S.; Shao, C.; Liu, Y.; Mu, R. Electrospun nanofibers of poly(acrylonitrile)/Eu^{3+} and their photoluminescence properties. *J. Phys. Chem. Solids,* **2010**, *71*, 273-278. http://dx.doi.org/10.1016/j.jpcs.2009.12.076

[81] Itankar, S.G.; Dandekar, M.P.; Kondawar, S.B.; Bahirwar, B.M. Eu^{3+} -doped polystyrene and polyvinylidene fluoride nanofibers made by electrospinning for photoluminescent fabric designing. *Luminescence,* **2017**, *32*(8), 1535-1540. http://dx.doi.org/10.1002/bio.3356 PMID: 28634993

[82] Li, M.; Zhang, Z.; Cao, T.; Sun, Y.; Liang, P.; Shao, C.; Liu, Y. Electrospinning preparation and photoluminescence properties of poly (methyl methacrylate)/Eu^{3+} ions composite nanofibers and nanoribbons. *Mater. Res. Bull.,* **2012**, *47*, 321-327. http://dx.doi.org/10.1016/j.materresbull.2011.11.029

[83] Zhang, X.; Wen, S.; Hu, S.; Chen, Q.; Fong, H.; Zhang, L.; Liu, L. Luminescence properties of Eu(III) complex/polyvinylpyrrolidone electrospun composite nanofibers. *J. Phys. Chem. C,* **2010**, *114*, 3898-3903. http://dx.doi.org/10.1021/jp9119843

[84] Bai, J.; Gu, H.; Hou, Y.; Wang, S. Luminescence properties and molecular mechanics calculation of bis-*β*-diketonate Eu^{3+} complex/polymer hybrid fibers. *Opt. Mater.,* **2018**, *79*, 310-316. http://dx.doi.org/10.1016/j.optmat.2018.03.029

[85] Zhang, H.; Song, H.; Dong, B.; Han, L.; Pan, G.; Bai, X.; Fan, L.; Lu, S.; Zhao, H.; Wang, F. Electrospinning preparation and luminescence properties of europium complex/polymer composite fibers. *J. Phys. Chem. C,* **2008**, *112*, 9155-9162. http://dx.doi.org/10.1021/jp7115005

[86] Yu, H.; Li, T.; Chen, B.; Wu, Y.; Li, Y. Preparation of aligned $Eu(DBM)_3phen$/PS fibers by electrospinning and their luminescence properties. *J. Colloid Interface Sci.,* **2013**, *400*, 175-180. http://dx.doi.org/10.1016/j.jcis.2013.03.017 PMID: 23578517

[87] Zhang, H.; Song, H.; Han, L.; Dong, B.; Pan, G.; Zhao, H.; Dai, Q.; Qin, R.; Qu, X.; Lu, S. Electrospinning preparation of uniaxially aligned ternary terbium complex/polymer composite fibers and considerably improved photostability. *J. Nanosci. Nanotechnol.,* **2010**, *10*(3), 2070-2076. http://dx.doi.org/10.1166/jnn.2010.2068 PMID: 20355629

[88] Tian, J.; Ma, Q.; Dong, X.; Yang, M.; Yang, Y.; Wang, J.; Yu, W.; Liu, G. Flexible composite nanobelts: Facile electrospinning construction, structure and color-tunable photoluminescence. *J. Mater. Sci. Mater. Electron.,* **2015**, *26*, 8413-8420. http://dx.doi.org/10.1007/s10854-015-3509-y

[89] Kim, J.-M.; Jeong, Y.-K.; Sohn, Y.; Kang, J.-G. Synthesis and photophysical properties of an Eu(II)-complex/PS blend: role of Ag nanoparticles in surface-enhanced luminescence. *Langmuir,* **2012**, *28*(25), 9842-9848. http://dx.doi.org/10.1021/la301547z PMID: 22656326

[90] Li, S.; Zhao, X. Oxygen sensing nanofibers doped with red-emitting Eu(III) complex: Synthesis, characterization, mechanism, and sensing performance. *Synth. Met.,* **2011**, *161*, 737-742. http://dx.doi.org/10.1016/j.synthmet.2011.01.023

[91] Wang, Y.; Li, B.; Zhang, L.; Zuo, Q.; Li, P.; Zhang, J.; Su, Z. High-performance oxygen sensors based on Eu(III) complex/polystyrene composite nanofibrous membranes prepared by electrospinning. *ChemPhysChem,* **2011**, *12*(2), 349-355. http://dx.doi.org/10.1002/cphc.201000884 PMID: 21275027

[92] Wang, X.; Wang, J.; Tsunashima, R.; Pan, K.; Cao, B.; Song, Y.-F. Electrospun self-supporting nanocomposite films of $Na_9[EuW_{10}O_{36}]\cdot 32H_2O$/PAN as pH-modulated luminescent switch. *Ind. Eng. Chem. Res.,* **2013**, *52*, 2598-2603. http://dx.doi.org/10.1021/ie302712s

[93] Shu, D.; Xi, P.; Li, S.; Li, C.; Wang, X.; Cheng, B. Morphologies and properties of PET nano porous luminescence fiber: Oil absorption and fluorescence-indicating functions. *ACS Appl. Mater. Interfaces,* **2018**, *10*(3), 2828-2836. http://dx.doi.org/10.1021/acsami.7b16655 PMID: 29294290

[94] Sun, X.; Li, B.; Song, L.; Gong, J.; Zhang, L. Electrospinning preparation and photophysical properties of one-dimensional (1D) composite nanofibers doped with erbium(III) complexes. *J. Lumin.,* **2010**, *130*, 1343-1348. http://dx.doi.org/10.1016/j.jlumin.2010.02.024

[95] Tang, S.; Shao, C.; Liu, Y.; Li, S.; Mu, R. Electrospun nanofibers of poly(ethylene oxide)/teraamino-phthalocyanine copper(II) hybrids and its photoluminescence properties. *J. Phys. Chem. Solids,* **2007**, *68*, 2337-2340. http://dx.doi.org/10.1016/j.jpcs.2007.07.014

[96] Zhang, H.; Lei, B.; Dong, H.; Liu, Y. Oxygen sensing properties of Cu(I) complex/polystyrene composite nanofibers prepared by electrospinning. *J. Nanosci. Nanotechnol.,* **2011**, *11*(11), 9840-9845. http://dx.doi.org/10.1166/jnn.2011.5241 PMID: 22413306

[97] Bai, S.-Q.; Kai, D.; Ke, K.L.; Lin, M.; Jiang, L.; Jiang, Y.; Young, D.J.; Loh, X.J.; Li, X.; Hor, T.S.A. A triazolyl-pyridine-supported cui dimer: Tunable luminescence and fabrication of composite fibers. *ChemPlusChem,* **2015**, *80*(8), 1235-1240. http://dx.doi.org/10.1002/cplu.201500202 PMID: 31973300

[98] Jiménez, G.L.; Balderas, J.U.; Falcony, C.; Caro, R.; Salmerón-Quiroz, B.B.; Mondragón, M. Morphology and photoluminescence properties of electrospun microfibers of poly(*9*-vinylcarbazole)/tris-(*8*-hydroxyquinoline)aluminum and poly(*9*-vinylcarbazole)/*4,7*-diphenyl-*1,10*-phenanthroline blends. *Opt. Mater.,* **2015**, *42*, 462-467. http://dx.doi.org/10.1016/j.optmat.2015.01.042

[99] Yan, E.; Huang, Z.; Xin, Y.; Zhao, Q.; Zhang, W. Polyvinylpyrrolidone/Tris(*8*-Quinolinolato) aluminum hybrid polymer fibers by electrospinning. *Mater. Lett.,* **2006**, *60*, 2969-2973. http://dx.doi.org/10.1016/j.matlet.2006.02.045

[100] Mondragón, M.; Garzón, A.-S.; Caro, R. Improving photoluminescence of poly(*9*-vinylcarbazole)/*4,7*-diphenyl-*1,10*-phenanthroline/tris-(*8*-hydroxyquinoline) aluminum fibers *via* coaxial electrospinning. *J. Appl. Polym. Sci.,* **2016**, *133*, 44019. http://dx.doi.org/10.1002/app.44019

[101] Dhakal, K.P.; Lee, H.; Kim, J. White light-emitting LED using electrospun Alq3/P3BT composite microfibers. *Synth. Met.,* **2014**, *190*, 44-47. http://dx.doi.org/10.1016/j.synthmet.2014.02.002

[102] Zhang, J.; Li, Y.; Hui, C.; Zhu, J. Nanofibers doped with a phosphorescent iridium complex: Synthesis, characterization, and photophysical property study. *Synth. Met.,* **2011**, *161*, 1166-1171. http://dx.doi.org/10.1016/j.synthmet.2011.03.025

[103] Zhou, C.; Shi, Y.; Ding, X.; Li, M.; Luo, J.; Lu, Z.; Xiao, D. Development of a fast and sensitive glucose biosensor using iridium complex-doped electrospun optical fibrous membrane. *Anal. Chem.,* **2013**, *85*(2), 1171-1176. http://dx.doi.org/10.1021/ac303107d PMID: 23215003

[104] Chang, T.; Han, G.; Zhang, Y. Improved photoluminescence performance from polymer nanofibers doped with phosphorescent Ir(III) complex. *Opt. Mater.,* **2014**, *37*, 147-154. http://dx.doi.org/10.1016/j.optmat.2014.05.014

[105] Mitra, J.; Ghosh, M.; Bordia, R.K.; Sharma, A. Photoluminescent electrospun submicron fibers of hybrid organosiloxane and derived silica. *RSC Advances,* **2013**, *3*, 7591-7600. http://dx.doi.org/10.1039/c3ra23408h

[106] Wang, M.; Li, X.; Hua, W.; Shen, L.; Yu, X.; Wang, X. Electrospun poly(acrylic acid)/silica hydrogel nanofibers scaffold for highly efficient adsorption of lanthanide ions and its photoluminescence performance. *ACS Appl. Mater. Interfaces,* **2016**, *8*(36), 23995-24007. http://dx.doi.org/10.1021/acsami.6b08294 PMID: 27537710

[107] Gao, W.; Wang, X.; Xu, W.; Xu, S. Luminescent composite polymer fibers: *in situ* synthesis of silver nanoclusters in electrospun polymer fibers and application. *Mater. Sci. Eng. C,* **2014**, *42*, 333-340. http://dx.doi.org/10.1016/j.msec.2014.05.020 PMID: 25063126

[108] Wang, F.; Shi, D.; Lan, T.; Zhang, Y.; Shao, Z. One-step preparation of carboxymethyl cellulose/polyoxyethylene nanofiber mats containing silver nanoparticles. *Integr. Ferroelectr.,* **2016**, *169*, 50-57. http://dx.doi.org/10.1080/10584587.2016.1162613

[109] Lin, H.-J.; Chen, C.-Y. Thermo-responsive electrospun nanofibers doped with 1,10-phenanthroline-based fluorescent sensor for metal ion detection. *J. Mater. Sci.,* **2016**, *51*, 1620-1631. http://dx.doi.org/10.1007/s10853-015-9485-z

[110] Yoon, J.; Chae, S.K.; Kim, J.-M. Colorimetric sensors for volatile organic compounds (VOCs) based on conjugated polymer-embedded electrospun fibers. *J. Am. Chem. Soc.,* **2007**, *129*(11), 3038-3039. http://dx.doi.org/10.1021/ja067856+ PMID: 17315999

[111] Davis, B.W.; Niamnont, N.; Dillon, R.; Bardeen, C.J.; Sukwattanasinitt, M.; Cheng, Q. FRET detection of proteins using fluorescently doped electrospun nanofibers and pattern recognition. *Langmuir,* **2011**, *27*(10), 6401-6408. http://dx.doi.org/10.1021/la2006925 PMID: 21491867

[112] Gao, R.; Cao, D.; Guan, Y.; Yan, D. Flexible self-supporting nanofibers thin films showing reversible photochromic fluorescence. *ACS Appl. Mater. Interfaces,* **2015**, *7*(18), 9904-9910. http://dx.doi.org/10.1021/acsami.5b01996 PMID: 25897557

[113] Romano, L.; Camposeo, A.; Manco, R.; Moffa, M.; Pisignano, D. Core-shell electrospun fibers encapsulating chromophores or luminescent proteins for microscopically controlled molecular release. *Mol. Pharm.,* **2016**, *13*(3), 729-736. http://dx.doi.org/10.1021/acs.molpharmaceut.5b00560 PMID: 26870885

[114] Park, M.; Lee, K.S.; Shim, J.; Liu, Y.; Lee, C.; Cho, H.; Kim, M.J.; Park, S.-J.; Yun, Y.J.; Kim, H.Y.; Son, D.I. Environment friendly, transparent nanofiber textiles consolidated with high efficiency PLEDs for wearable electronics. *Org. Electron.,* **2016**, *36*, 89-96. http://dx.doi.org/10.1016/j.orgel.2016.05.030

[115] Ner, Y.; Grote, J.G.; Stuart, J.A.; Sotzing, G.A. White luminescence from multiple-dye-doped electrospun DNA nanofibers by fluorescence resonance energy transfer. *Angew. Chem. Int. Ed. Engl.,* **2009**, *48*(28), 5134-5138. http://dx.doi.org/10.1002/anie.200900885 PMID: 19504507

[116] Ner, Y.; Grote, J.G.; Stuart, J.A.; Sotzing, G.A. Enhanced fluorescence in electrospun dye-doped DNA nanofibers. *Soft Matter,* **2008**, *4*, 1448-1453. http://dx.doi.org/10.1039/b717581g

[117] Di Benedetto, F.; Mele, E.; Camposeo, A.; Athanassiou, A.; Cingolani, R.; Pisignano, D. Photoswitchable organic nanofibers. *Adv. Mater.,* **2008**, *20*, 314-318. http://dx.doi.org/10.1002/adma.200700980

[118] Camposeo, A.; Di Benedetto, F.; Stabile, R.; Cingolani, R.; Pisignano, D. Electrospun dye-doped polymer nanofibers emitting in the near infrared. *Appl. Phys. Lett.,* **2007**, *90*, 143115. http://dx.doi.org/10.1063/1.2720262

[119] Liang, X.; Li, Y.; Peng, W.; Bai, J.; Zhang, C.; Yang, Q. Efficient method for fabrication of fluorescein derivative/PDAC composite nanofibers and characteristics of their photoluminescent properties. *Eur. Polym. J.,* **2008**, *44*, 3156-3162. http://dx.doi.org/10.1016/j.eurpolymj.2008.07.016

[120] Wei, J.; Yang, S.; Wang, L.; Wang, C.-F.; Chen, L.; Chen, S. Electrospun fluorescein-embedded nanofibers towards fingerprint recognition and luminescent patterns. *RSC Advances,* **2013**, *3*, 19403-19408. http://dx.doi.org/10.1039/c3ra42328j

[121] Ishii, Y.; Omori, K.; Satozono, S.; Fukuda, M. Dye-doped submicron fiber waveguides composed of hole- and electron-transport materials. *Org. Electron.,* **2017**, *41*, 215-220. http://dx.doi.org/10.1016/j.orgel.2016.11.007

[122] Chang, C.-C.; Huang, C.-M.; Chang, Y.-H.; Kuo, C. Enhancement of light scattering and photoluminescence in electrospun polymer nanofibers. *Opt. Express,* **2010**, *18*(Suppl. 2), A174-A184. http://dx.doi.org/10.1364/OE.18.00A174 PMID: 20588586

[123] Wang, S.; Yang, Q.; Du, J.; Bai, J.; Li, Y. Variety of photoluminescence intensity of fluorescent whitening agents introduced into polyacrylonitrile nanofibers. *J. Appl. Polym. Sci.,* **2007**, *103*, 2382-2386. http://dx.doi.org/10.1002/app.25342

[124] Dhakal, K.P.; Lee, H.; Woo Lee, J.; Joo, J.; Guthold, M.; Kim, J. Electrospinning and optical characterization of organic rubrene nanofibers. *J. Appl. Phys.,* **2012**, *111*, 123504. http://dx.doi.org/10.1063/1.4729537

[125] Qin, Z.; Zhang, P.; Wu, Z.; Yin, M.; Geng, Y.; Pan, K. Coaxial electrospinning for flexible uniform white-light-emitting porous fibrous membrane. *Mater. Des.,* **2018**, *147*, 175-181. http://dx.doi.org/10.1016/j.matdes.2018.03.040

[126] Freire, M.G.; Teles, A.R.R.; Ferreira, R.A.S.; Carlos, L.D.; Lopes-da-Silva, J.A.; Coutinho, J.A.P. Electrospun nanosized cellulose fibers using ionic liquids at room temperature. *Green Chem.,* **2011**, *13*, 3173-3180. http://dx.doi.org/10.1039/c1gc15930e

[127] Kaerkitcha, N.; Sagawa, T. Amplified polarization properties of electrospun nanofibers containing fluorescent dyes and helical polymer. *Photochem. Photobiol. Sci.,* **2018**, *17*(3), 342-351. http://dx.doi.org/10.1039/C7PP00413C PMID: 29445786

[128] Wang, Y.; La, A.; Ding, Y.; Liu, Y.; Lei, Y. Novel signal-amplifying fluorescent nanofibers for naked-eye-based ultrasensitive detection of buried explosives and explosive vapors. *Adv. Funct. Mater.,* **2012**, *22*, 3547-3555. http://dx.doi.org/10.1002/adfm.201200047

[129] Vohra, V.; Calzaferri, G.; Destri, S.; Pasini, M.; Porzio, W.; Botta, C. Toward white light emission through efficient two-step energy transfer in hybrid nanofibers. *ACS Nano,* **2010**, *4*(3), 1409-1416. http://dx.doi.org/10.1021/nn9017922 PMID: 20131877

[130] Vohra, V.; Devaux, A.; Dieu, L.-Q.; Scavia, G.; Catellani, M.; Calzaferri, G.; Botta, C. Energy transfer in fluorescent nanofibers embedding dye-loaded zeolite L crystals. *Adv. Mater.,* **2009**, *21*, 1146-1150. http://dx.doi.org/10.1002/adma.200801693

[131] Danks, E.A.; Hall, S.R.; Schnepp, Z. The evolution of 'sol-gel' chemistry as a technique for materials synthesis. *Mater. Horiz.,* **2016**, *3*, 91-112. http://dx.doi.org/10.1039/C5MH00260E

[132] Wu, H.; Sun, Y.; Lin, D.; Zhang, R.; Zhang, C.; Pan, W. GaN nanofibers based on electrospinning: facile synthesis, controlled assembly, precise doping, and application as high performance UV photodetector. *Adv. Mater.,* **2009**, *21*, 227-231. http://dx.doi.org/10.1002/adma.200800529

[133] Lin, D.; Wu, H.; Zhang, R.; Pan, W. Preparation of ZnS nanofibers *via* electrospinning. *J. Am. Ceram. Soc.,* **2007**, *90*, 3664-3666. http://dx.doi.org/10.1111/j.1551-2916.2007.01942.x

[134] Chen, L.-J.; Lee, C.-R.; Chuang, Y.-J.; Wu, Z.-H.; Chen, C. Compositionally controlled band gap and photoluminescence of ZnSSe nanofibers by electrospinning. *CrystEngComm,* **2015**, *17*, 4434-4438. http://dx.doi.org/10.1039/C5CE00477B

[135] Luo, Z.; Moch, J.G.; Johnson, S.S.; Chen, C.C. A review on X-ray detection using nanomaterials. *Curr. Nanosci.,* **2017**, *13*, 364-372. http://dx.doi.org/10.2174/1573413713666170329164615

[136] George, G.; Jackson, S.L.; Mobley, Z.R.; Gautam, B.R.; Fang, D.; Peng, J.; Luo, D.; Wen, J.; Davis, J.E.; Ila, D.; Luo, Z. Fast luminescence from rare-earth-codoped $BaSiF_6$ nanowires with high aspect ratios. *J. Mater. Chem. C Mater. Opt. Electron. Devices,* **2018**, *6*, 7285-7294. http://dx.doi.org/10.1039/C8TC01651H

[137] Liu, Y.; Li, D.; Ma, Q.; Dong, X.; Xi, X.; Yu, W.; Wang, X.; Wang, J.; Liu, G. Er^{3+} doped $BaYF_5$ nanofibers: Facile construction technique, structure and upconversion luminescence. *J. Mater. Sci. Mater. Electron.,* **2016**, *27*, 5277-5283. http://dx.doi.org/10.1007/s10854-016-4425-5

[138] Yang, R.; Song, W.; Liu, S.; Qin, W. Electrospinning preparation and upconversion luminescence of yttrium fluoride nanofibers. *CrystEngComm,* **2012**, *14*, 7895-7897. http://dx.doi.org/10.1039/c2ce26160j

[139] Li, D.; Dong, X.; Yu, W.; Wang, J.; Liu, G. Synthesis and upconversion luminescence properties of YF_3:Yb^{3+}/Er^{3+} hollow nanofibers derived from Y_2O_3:Yb^{3+}/Er^{3+} hollow nanofibers. *J. Nanopart. Res.,* **2013**, *15*, 1704. http://dx.doi.org/10.1007/s11051-013-1704-4

[140] Li, D.; Dong, X.; Yu, W.; Wang, J.; Liu, G. Fabrication and luminescence of YF_3:Tb^{3+} hollow nanofibers. *J. Mater. Sci. Mater. Electron.,* **2013**, *24*, 3041-3048. http://dx.doi.org/10.1007/s10854-013-1209-z

[141] Liu, Y.; Li, D.; Ma, Q.; Yu, W.; Xi, X.; Dong, X.; Wang, J.; Liu, G. Fabrication of novel $Ba_4Y_3F_{17}$:Er^{3+} nanofibers with upconversion fluorescence *via* combination of electrospinning with fluorination. *J. Mater. Sci. Mater. Electron.,* **2016**, *27*, 11666-11673. http://dx.doi.org/10.1007/s10854-016-5302-y

[142] Dali, L.; Guolei, W.; Biao, D.; Xue, B.; Yu, W.; Hongwei, S.; Lin, X. Electrospinning preparation and properties of $NaGdF_4$:Eu^{3+} nanowires. *Solid State Sci.,* **2010**, *12*, 1837-1842. http://dx.doi.org/10.1016/j.solidstatesciences.2010.08.011

[143] George, G.; Simpson, M.D.; Gautam, B.R.; Fang, D.; Peng, J.; Wen, J.; Davis, J.E.; Ila, D.; Luo, Z. Luminescence characteristics of rare-earth-doped barium hexafluorogermanate $BaGeF_6$ nanowi-

res: Fast subnanosecond decay time and high sensitivity in H_2O_2 detection. *RSC Advances,* **2018**, *8*, 39296-39306.
http://dx.doi.org/10.1039/C8RA07806H

[144] Li, G.; Hou, Z.; Peng, C.; Wang, W.; Cheng, Z.; Li, C.; Lian, H.; Lin, J. Electrospinning derived one-dimensional LaOCl:Ln^{3+} (Ln = Eu/Sm, Tb, Tm) nanofibers, nanotubes and microbelts with multi-color-tunable emission properties. *Adv. Funct. Mater.,* **2010**, *20*, 3446-3456.
http://dx.doi.org/10.1002/adfm.201001114

[145] Yu, H.; Yu, A.; Li, Y.; Song, Y.; Wu, Y.; Sheng, C.; Chen, B. Energy transfer processes in electrospun LaOCl:Ce/Tb nanofibres. *J. Alloys Compd.,* **2016**, *683*, 256-262.
http://dx.doi.org/10.1016/j.jallcom.2016.05.048

[146] Kong, Q.; Wang, J.; Dong, X.; Yu, W.; Liu, G. Synthesis and luminescence properties of LaOCl:Eu^{3+} nanostructures *via* the combination of electrospinning with chlorination technique. *J. Mater. Sci. Mater. Electron.,* **2013**, *24*, 4745-4756.
http://dx.doi.org/10.1007/s10854-013-1469-7

[147] Kong, Q.; Wang, J.; Dong, X.; Yu, W.; Liu, G. Synthesis and luminescence properties of LaOCl:Nd^{3+} nanostructures *via* combination of electrospinning with chlorination technique. *Mater. Express,* **2014**, *4*, 13-22.
http://dx.doi.org/10.1166/mex.2014.1147

[148] Kong, Q.; Wang, J.; Dong, X.; Yu, W.; Liu, G. Synthesis and luminescence properties of Yb^{3+}–Er^{3+} co-doped LaOCl nanostructures. *J. Mater. Sci.,* **2014**, *49*, 2919-2931.
http://dx.doi.org/10.1007/s10853-013-8003-4

[149] Wu, S.; Dong, X.; Wang, J.; Kong, Q.; Yu, W.; Liu, G. Facile electrospinning fabrication and photoluminescence of LaOI:Tb^{3+} one-dimensional nanomaterials. *J. Mater. Sci. Mater. Electron.,* **2014**, *25*, 1053-1062.
http://dx.doi.org/10.1007/s10854-013-1686-0

[150] Wu, S.; Yu, W.; Dong, X.; Wang, J.; Liu, G. A feasible strategy to synthesize LaOI:Yb^{3+}/Ho^{3+} upconversion luminescence nanostructures *via* succeeding to the morphologies of precursors. *Chem. Eng. J.,* **2015**, *266*, 189-198.
http://dx.doi.org/10.1016/j.cej.2014.12.070

[151] Ma, W.; Dong, X.; Wang, J.; Yu, W.; Liu, G. Electrospinning preparation of LaOBr:Tb^{3+} nanostructures and their photoluminescence properties. *J. Mater. Sci.,* **2013**, *48*, 2557-2565.
http://dx.doi.org/10.1007/s10853-012-7046-2

[152] Yu, W.S.; Zhu, C.S.; Ma, Q.L.; Ma, W.W.; Wang, J.X.; Dong, X.T. Fabrication and characterization of LaOBr:Eu^{3+} luminescent nanofibers. *Adv. Mat. Res.,* **2015**, *1118*, 92-96.

[153] Ma, W.; Yu, W.; Dong, X.; Wang, J.; Liu, G. Electrospinning preparation and up-conversion luminescence properties of LaOBr:Er^{3+} nanofibers and nanoribbons. *Chem. Eng. J.,* **2014**, *244*, 531-539.
http://dx.doi.org/10.1016/j.cej.2014.02.005

[154] Ma, W.; Yu, W.; Dong, X.; Wang, J.; Liu, G. Preparation and up-conversion luminescence properties of LaOBr:Yb^{3+}/Er^{3+} nanofibers *via* electrospinning. *Luminescence,* **2014**, *29*(7), 908-913.
http://dx.doi.org/10.1002/bio.2640 PMID: 24523144

[155] Ma, W.; Dong, X.; Wang, J.; Yu, W.; Liu, G. Controlled synthesis and near-infrared luminescence of LaOBr:Nd^{3+} nanofibers and nanobelts. *J. Nanosci. Nanotechnol.,* **2014**, *14*(8), 6196-6201.
http://dx.doi.org/10.1166/jnn.2014.8865 PMID: 25936086

[156] Guo, X.; Wang, J.; Dong, X.; Yu, W.; Liu, G. New strategy to achieve $La_2O_2CN_2$:Eu^{3+} novel luminescent one-dimensional nanostructures. *CrystEngComm,* **2014**, *16*, 5409-5417.
http://dx.doi.org/10.1039/C4CE00223G

[157] Guo, X.; Yu, W.; Dong, X.; Wang, J.; Ma, Q.; Liu, G.; Yang, M. A technique to fabricate $La_2O_2CN_2$:Tb^{3+} nanofibers and nanoribbons with the same morphologies as the precursors. *Eur. J. Inorg. Chem.,* **2015**, *2015*, 389-396.
http://dx.doi.org/10.1002/ejic.201402860

[158] Guo, X.; Yu, W.; Dong, X.; Wang, J.; Ma, Q.; Liu, G.; Yang, M. Fabrication and upconversion luminescent properties of Er^{3+}-doped and Er^{3+}/Yb^{3+} codoped $La_2O_2CN_2$ nanofibers. *J. Am. Ceram. Soc.,* **2015**, *98*, 1215-1222.
http://dx.doi.org/10.1111/jace.13466

[159] Wang, H.Y.; Yang, Y.; Wang, Y.; Zhao, Y.Y.; Li, X.; Wang, C. Luminescent properties of rare-earth oxyfluoride nanofibers prepared *via* electrospinning. *J. Nanosci. Nanotechnol.,* **2009**, *9*(2), 1522-1525.
http://dx.doi.org/10.1166/jnn.2009.C193 PMID: 19441561

[160] Suryamas, A.B.; Munir, M.M.; Ogi, T. Khairurrijal; Okuyama, K. Intense green and yellow emissions from electrospun BCNO phosphor nanofibers. *J. Mater. Chem.,* **2011**, *21*, 12629-12631.
http://dx.doi.org/10.1039/c1jm12654g

[161] Gu, Y.; Zhang, Q.; Wang, H.; Li, Y. $CaSi_2O_2N_2$:Eu nanofiber mat based on electrospinning: Facile synthesis, uniform arrangement, and application in white LEDs. *J. Mater. Chem.,* **2011**, *21*, 17790-17797.
http://dx.doi.org/10.1039/c1jm13351a

[162] Zhao, H.; Cui, B.; Wang, H.; Zhang, Q.; Li, Y. Facile synthesis of $Ca_{0.68}Si_9Al_3(ON)_{16}$:$Eu^{2+}$ microbelts mat with the enhanced fluorescence and mechanical performance. *J. Solid State Chem.,* **2016**, *233*, 374-380.
http://dx.doi.org/10.1016/j.jssc.2015.10.044

[163] Zhang, B.; Zou, H.; Song, Y.; Guan, H.; Zhou, X.; Shi, Z.; Sheng, Y. Electrospinning fabrication and luminescence properties of Lu_2O_2S:Eu^{3+} fibers. *CrystEngComm,* **2017**, *19*, 699-707.
http://dx.doi.org/10.1039/C6CE02391F

[164] Han, L.; Pan, M.; Lv, Y.; Gu, Y.; Wang, X.; Li, D.; Kong, Q.; Dong, X. Fabrication of Y_2O_2S:Eu^{3+} hollow nanofibers by sulfurization of Y_2O_3:Eu^{3+} hollow nanofibers. *J. Mater. Sci. Mater. Electron.,* **2015**, *26*, 677-684.
http://dx.doi.org/10.1007/s10854-014-2449-2

[165] Han, L.; Pan, M.; Hu, Y.; Xie, Y.; Liu, Y.; Li, D.; Dong, X. A novel scheme to obtain Y_2O_2S:Er^{3+} upconversion luminescent hollow nanofibers *via* precursor templating. *J. Am. Ceram. Soc.,* **2015**, *98*, 2817-2822.
http://dx.doi.org/10.1111/jace.13696

[166] Lu, X.; Yang, M.; Yang, L.; Ma, Q.; Dong, X.; Tian, J.Y. $_2O_2S$:Yb^{3+}, Er^{3+} nanofibers: Novel fabrication technique, structure and up-conversion luminescent characteristics. *J. Mater. Sci. Mater. Electron.,* **2015**, *26*, 4078-4084.
http://dx.doi.org/10.1007/s10854-015-2947-x

[167] Viswanathamurthi, P.; Bhattarai, N.; Kim, H.Y.; Lee, D.R. The photoluminescence properties of zinc oxide nanofibres prepared by electrospinning. *Nanotechnology,* **2004**, *15*, 320.
http://dx.doi.org/10.1088/0957-4484/15/3/015

[168] Lee, D.Y.; Cho, J.-E.; Cho, N.-I.; Lee, M.-H.; Lee, S.-J.; Kim, B.-Y. characterization of electrospun aluminum-doped zinc oxide nanofibers. *Thin Solid Films,* **2008**, *517*, 1262-1267.
http://dx.doi.org/10.1016/j.tsf.2008.05.027

[169] Santangelo, S.; Patanè, S.; Frontera, P.; Pantò, F.; Triolo, C.; Stelitano, S.; Antonucci, P. Effect of calcium- and/or aluminum-incorporation on morphological, structural and photoluminescence properties of electro-spun zinc oxide fibers. *Mater. Res. Bull.,* **2017**, *92*, 9-18.
http://dx.doi.org/10.1016/j.materresbull.2017.03.062

[170] Wang, H.; Wang, Y.; Yang, Y.; Li, X.; Wang, C. Photoluminescence properties of the rare-earth ions in the TiO_2 host nanofibers prepared *via* electrospinning. *Mater. Res. Bull.,* **2009**, *44*, 408-414.
http://dx.doi.org/10.1016/j.materresbull.2008.05.001

[171] Cacciotti, I.; Bianco, A.; Pezzotti, G.; Gusmano, G. Synthesis, thermal behaviour and luminescence properties of rare earth-doped titania nanofibers. *Chem. Eng. J.,* **2011**, *166*, 751-764.
http://dx.doi.org/10.1016/j.cej.2010.07.008

[172] Nasr, M.; Abou Chaaya, A.; Abboud, N.; Bechelany, M.; Viter, R.; Eid, C.; Khoury, A.; Miele, P. Photoluminescence: A very sensitive tool to detect the presence of anatase in rutile phase electrospun TiO_2 nanofibers. *Superlattices Microstruct.,* **2015**, *77*, 18-24.
http://dx.doi.org/10.1016/j.spmi.2014.10.034

[173] Cacciotti, I.; Bianco, A.; Pezzotti, G.; Gusmano, G. Terbium and ytterbium-doped titania luminescent nanofibers by means of electrospinning technique. *Mater. Chem. Phys.,* **2011**, *126*, 532-541.
http://dx.doi.org/10.1016/j.matchemphys.2011.01.034

[174] Chen, J.; Song, Y.; Sheng, Y.; Chang, M.; Xie, X.; Abualrejal, M.M.A.; Guan, H.; Shi, Z.; Zou, H. Luminescence properties and Judd–Ofelt analysis of SiO_2:Ln^{3+} (Eu, Tb) hollow nanofibers fabricated by co-axial electrospinning method. *J. Alloys Compd.,* **2017**, *716*, 144-155.
http://dx.doi.org/10.1016/j.jallcom.2017.05.070

[175] Viswanathamurthi, P.; Bhattarai, N.; Kim, H.Y.; Khil, M.S.; Lee, D.R.; Suh, E.-K. GeO_2 fibers: preparation, morphology and photoluminescence property. *J. Chem. Phys.,* **2004**, *121*(1), 441-445. http://dx.doi.org/10.1063/1.1755666 PMID: 15260565

[176] Wu, J.; Coffer, J.L. Strongly emissive erbium-doped tin oxide nanofibers derived from sol gel/electrospinning methods. *J. Phys. Chem. C,* **2007**, *111*, 16088-16091. http://dx.doi.org/10.1021/jp076338y

[177] Wu, J.; Coffer, J.L. Emissive erbium-doped silicon and germanium oxide nanofibers derived from an electrospinning process. *Chem. Mater.,* **2007**, *19*, 6266-6276. http://dx.doi.org/10.1021/cm702226x

[178] Lu, X.; Liu, X.; Zhang, W.; Wang, C.; Wei, Y. Large-scale synthesis of tungsten oxide nanofibers by electrospinning. *J. Colloid Interface Sci.,* **2006**, *298*(2), 996-999. http://dx.doi.org/10.1016/j.jcis.2006.01.032 PMID: 16457838

[179] Sun, C.; Deng, J.; Kong, L.; Chen, L.; Shen, Z.; Cao, Y.; Zhang, H.; Wang, X. Structure and photoluminescence properties of β-Ga_2O_3 nanofibres synthesized *via* electrospinning method. *IOP Conf. Ser. Mater. Sci. Eng.*, **2017**, *275*, 012046. http://dx.doi.org/10.1088/1757-899X/275/1/012046

[180] Luo, S.; Fan, J.; Liu, W.; Zhang, M.; Song, Z.; Lin, C.; Wu, X.; Chu, P.K. Synthesis and low-temperature photoluminescence properties of SnO_2 nanowires and nanobelts. *Nanotechnology,* **2006**, *17*(6), 1695-1699. http://dx.doi.org/10.1088/0957-4484/17/6/025 PMID: 26558579

[181] Zhang, Y.; Li, J.; Li, Q.; Zhu, L.; Liu, X.; Zhong, X.; Meng, J.; Cao, X. Preparation of In_2O_3 ceramic nanofibers by electrospinning and their optical properties. *Scr. Mater.,* **2007**, *56*, 409-412. http://dx.doi.org/10.1016/j.scriptamat.2006.10.032

[182] Yu, H.; Li, Y.; Lan, X.; Liang, Z. Electrospinning preparation and luminescence properties of La_2O_3:Ce^{3+}/Tb^{3+} nanofibers. *J. Mater. Sci. Mater. Electron.,* **2017**, *28*, 8832-8836. http://dx.doi.org/10.1007/s10854-017-6611-5

[183] Li, J.-M.; Zeng, X.-L.; Dong, Y.-H.; Xu, Z.-A. White-light emission and weak antiferromagnetism from cubic rare-earth oxide Eu_2O_3 electrospun nanostructures. *CrystEngComm,* **2013**, *15*, 2372-2377. http://dx.doi.org/10.1039/c3ce26770a

[184] Tao, S.; Li, G.; Yin, J. Fluorescent nanofibrous membranes for trace detection of TNT vapor. *J. Mater. Chem.,* **2007**, *17*, 2730-2736. http://dx.doi.org/10.1039/b618122h

[185] Li, Q.; Yan, R.; Dong, L.M.; Zhang, Y.F. Electrospinning preparation and luminescene properties of $CaTiO_3$: RE (Eu^{3+}/Gd^{3+}) nanofibers. *Dig. J. Nanomater. Biostruct.,* **2017**, *12*, 59-65.

[186] Peng, C.; Hou, Z.; Zhang, C.; Li, G.; Lian, H.; Cheng, Z.; Lin, J. Synthesis and luminescent properties of $CaTiO_3$: Pr^{3+} microfibers prepared by electrospinning method. *Opt. Express,* **2010**, *18*(7), 7543-7553. http://dx.doi.org/10.1364/OE.18.007543 PMID: 20389776

[187] Haranath, D.; Khan, A.F.; Chander, H. Bright red luminescence and energy transfer of Pr^{3+} -doped (Ca,Zn)TiO_3 phosphor for long decay applications. *J. Phys. D Appl. Phys.,* **2006**, *39*, 4956. http://dx.doi.org/10.1088/0022-3727/39/23/009

[188] Li, H.; Huang, S.; Zhang, W.; Pan, W. Visible photoluminescence from amorphous barium titanate nanofibers. *J. Alloys Compd.,* **2013**, *551*, 131-135. http://dx.doi.org/10.1016/j.jallcom.2012.10.046

[189] Chen, X.; Wang, Q.; Wu, X.; Wang, T.; Tang, Y.; Duan, Z.; Sun, D.; Zhao, X.; Wang, F.; Shi, W. Piezoelectric/photoluminescence effect in one-dimensional lead-free nanofibers. *Scr. Mater.,* **2018**, *145*, 81-84. http://dx.doi.org/10.1016/j.scriptamat.2017.10.018

[190] Sang, R.L.; Chen, Y.; Zhang, Q.J.; Wang, L. Structural and photoluminescence characteristics of $ZnTiO_3$:Pb^{2+} nanofibers produced by electrospinning. *Key Eng. Mater.,* **2013**, *562-565*, 908-913. http://dx.doi.org/10.4028/www.scientific.net/KEM.562-565.908

[191] Hou, Z.; Yang, P.; Li, C.; Wang, L.; Lian, H.; Quan, Z.; Lin, J. Preparation and luminescence properties of YVO_4:Ln and Y(V, P)O_4:Ln (Ln = Eu^{3+}, Sm^{3+}, Dy^{3+}) nanofibers and microbelts by sol-gel/electrospinning process. *Chem. Mater.,* **2008**, *20*, 6686-6696. http://dx.doi.org/10.1021/cm801538t

[192] Hou, Z.; Chai, R.; Zhang, M.; Zhang, C.; Chong, P.; Xu, Z.; Li, G.; Lin, J. Fabrication and luminescence properties of one-dimensional $CaMoO_{(4)}$: $Ln^{(3+)}$ (Ln = Eu, Tb, Dy) nanofibers *via* electrospinning process. *Langmuir,* **2009**, *25*(20), 12340-12348. http://dx.doi.org/10.1021/la9016189 PMID: 19583182

[193] Xu, L.; Song, H.; Dong, B.; Wang, Y.; Bai, X.; Wang, G.; Liu, Q. Electrospinning preparation and photoluminescence properties of lanthanum phosphate nanowires and nanotubes. *J. Phys. Chem. C,* **2009**, *113*, 9609-9615. http://dx.doi.org/10.1021/jp900916j

[194] Hou, Z.; Wang, L.; Lian, H.; Chai, R.; Zhang, C.; Cheng, Z.; Lin, J. Preparation and luminescence properties of Ce^{3+} and/or Tb^{3+} doped $LaPO_4$ nanofibers and microbelts by electrospinning. *J. Solid State Chem.,* **2009**, *182*, 698-708. http://dx.doi.org/10.1016/j.jssc.2008.12.021

[195] Yang, Y.; Liu, B.; Zhang, Y.; Lv, X.; Wei, L.; Wang, X. Fabrication and luminescence of $BiPO_4$:Tb^{3+}/Ce^{3+} nanofibers by electrospinning. *Superlattices Microstruct.,* **2016**, *90*, 227-235. http://dx.doi.org/10.1016/j.spmi.2015.12.020

[196] Chen, J.; Sheng, Y.; Zhou, X.A.; Abualrejal, M.M.; Chang, M.; Shi, Z.; Zou, H. Dendrimer-based preparation and luminescence studies of SiO_2 fibers doping Eu^{3+} activator in interstitial sites. *RSC Advances,* **2016**, *6*, 16452-16460. http://dx.doi.org/10.1039/C5RA25859F

[197] Zhang, Y.; Liu, Y.; Li, X.; Wang, Q.J.; Xie, E. Room temperature enhanced red emission from novel $Eu^{(3+)}$ doped ZnO nanocrystals uniformly dispersed in nanofibers. *Nanotechnology,* **2011**, *22*(41), 415702. http://dx.doi.org/10.1088/0957-4484/22/41/415702 PMID: 21914938

[198] Chang, M.; Sheng, Y.; Song, Y.; Zheng, K.; Zhou, X.; Zou, H. Luminescence properties and Judd–Ofelt analysis of TiO_2:Eu^{3+} nanofibers *via* polymer-based electrospinning method. *RSC Advances,* **2016**, *6*, 52113-52121. http://dx.doi.org/10.1039/C6RA07509F

[199] Fang, D.; Zhang, M.; Luo, Z.; Cao, T.; Wang, Q.; Zhou, Z.; Jiang, M.; Xiong, C. Photoluminescent properties of Eu^{3+} doped electrospun CeO_2 nanofibers. *Opt. Mater.,* **2014**, *38*, 1-5. http://dx.doi.org/10.1016/j.optmat.2014.08.006

[200] Suryamas, A.B.; Munir, M.M.; Ogi, T.; Christopher, J. Hogan, J.; Okuyama, K. Photoluminescent ZrO_2:Eu^{3+} nanofibers prepared *via* electrospinning. *Jpn. J. Appl. Phys.,* **2010**, *49*, 115003. http://dx.doi.org/10.1143/JJAP.49.115003

[201] Gu, Y.; Shen, H.; Li, L.; Liu, W.; Wang, W.; Xu, D. Electrospinning synthesis and photoluminescence properties of SnO_2:*x*Eu^{3+}. *Chem. Res. Chin. Univ.,* **2014**, *30*, 879-884. http://dx.doi.org/10.1007/s40242-014-4252-2

[202] Liu, L.X.; Ma, Z.W.; Xie, Y.Z.; Su, Y.R.; Zhao, H.T.; Zhou, M.; Zhou, J.Y.; Li, J.; Xie, E.Q. Photoluminescence of rare earth^{3+} doped uniaxially aligned HfO_2 nanotubes prepared by sputtering with electrospun polyvinylpyrolidone nanofibers as templates. *J. Appl. Phys.,* **2010**, *107*, 024309. http://dx.doi.org/10.1063/1.3290974

[203] Yu, H.; Li, Y.; Song, Y.; Wu, Y.; Chen, B.; Li, P. Preparation and luminescent properties of Gd_2O_3:Eu^{3+} nanofibres made by electrospinning. *Ceram. Int.,* **2016**, *42*, 1307-1313. http://dx.doi.org/10.1016/j.ceramint.2015.09.066

[204] Dong, G.; Chi, Y.; Xiao, X.; Liu, X.; Qian, B.; Ma, Z.; Wu, E.; Zeng, H.; Chen, D.; Qiu, J. Fabrication and optical properties of Y_2O_3: Eu^{3+} nanofibers prepared by electrospinning. *Opt. Express,* **2009**, *17*(25), 22514-22519. http://dx.doi.org/10.1364/OE.17.022514 PMID: 20052176

[205] Zhang, H.; Chen, J.; Guo, H. Electrospinning Synthesis and luminescent properties of Lu_2O_3:Eu^{3+} nanofibers. *J. Rare Earths,* **2010**, *28*, 232-235. http://dx.doi.org/10.1016/S1002-0721(10)60331-6

[206] Zhao, J.; Zhang, W.; Xie, E.; Ma, Z.; Zhao, A.; Liu, Z. Structure and photoluminescence of β-Ga_2O_3:Eu^{3+} nanofibers prepared by electrospinning. *Appl. Surf. Sci.,* **2011**, *257*, 4968-4972. http://dx.doi.org/10.1016/j.apsusc.2010.12.157

[207] Yu, H.; Song, H.; Pan, G.; Qin, R.; Fan, L.; Zhang, H.; Bai, X.; Li, S.; Zhao, H.; Lu, S. Preparation and luminescent properties of YVO_4:Eu^{3+} nanofibers by electrospinning. *J. Nanosci. Nanotechnol.,* **2008**, *8*(3), 1432-1436.

http://dx.doi.org/10.1166/jnn.2008.361 PMID: 18468169

[208] Liu, Y.; Gong, Y.; Mellott, N.P.; Wang, B.; Ye, H.; Wu, Y. Luminescence of delafossite-type $CuAlO_2$ fibers with Eu substitution for Al cations. *Sci. Technol. Adv. Mater.,* **2016**, *17*(1), 200-209. http://dx.doi.org/10.1080/14686996.2016.1172024 PMID: 27877870

[209] Dong, G.; Xiao, X.; Liu, X.; Qian, B.; Zhang, Q.; Lin, G.; Ma, Z.; Chen, D.; Qiu, J. Intense red and yellow emissions from $Sr_2SiO_4:Eu^{3+}$ (Eu^{2+}) electrospun nanofibers. *J. Electrochem. Soc.,* **2009**, *156*, J347-J350. http://dx.doi.org/10.1149/1.3223667

[210] Shen, H.; Liu, R.; Yang, M.; Zhou, J.; Gu, Y.; Yang, H.; Wang, W.; Xu, D. Electrospinning synthesis and photoluminescence properties of one-dimensional $LuBO_3:Ln^{3+}$ (Ln = Tb, Eu) nanofibers. *Phys. Status Solidi. A Appl. Mater. Sci.,* **2013**, *210*, 1839-1845. http://dx.doi.org/10.1002/pssa.201329139

[211] Shen, H.; Feng, S.; Wang, Y.; Gu, Y.; Zhou, J.; Yang, H.; Feng, G.; Li, L.; Wang, W.; Liu, X.; Xu, D. Synthesis and photoluminescence properties of $GdBO_3:Ln^{3+}$ (Ln=Eu, Tb) nanofibers by electrospinning. *J. Alloys Compd.,* **2013**, *550*, 531-535. http://dx.doi.org/10.1016/j.jallcom.2012.10.156

[212] Hou, Z.; Lian, H.; Zhang, M.; Wang, L.; Lü, M.; Zhang, C.; Lin, J. Preparation and luminescence properties of $Gd_2MoO_6:Eu^{3+}$ nanofibers and nanobelts by electrospinning. *J. Electrochem. Soc.,* **2009**, *156*, J209-J214. http://dx.doi.org/10.1149/1.3138702

[213] Bi, F.; Dong, X.; Wang, J.; Liu, G.; Bi, F.; Dong, X.; Wang, J.; Liu, G. Electrospinning preparation and photoluminescence properties of $Y_3Al_5O_{12}:Eu^{3+}$ nanobelts. *Mater. Res.,* **2015**, *18*, 411-416. http://dx.doi.org/10.1590/1516-1439.351314

[214] Yim, C.J.; Unithrattil, S.; Chung, W.J.; Im, W.B. Comparative study of optical and structural properties of electrospun 1-dimensional $CaYAl_3O_7:Eu^{3+}$ nanofibers and bulk phosphor. *Mater. Charact.,* **2014**, *95*, 27-35. http://dx.doi.org/10.1016/j.matchar.2014.06.002

[215] Xie, M.; Luo, C. Synthesis and luminescence properties of $Li_2BaSiO_4:Eu^{3+}$ phosphors. *Phys. Status Solidi Rapid Res. Lett.,* **2012**, *6*, 412-414. http://dx.doi.org/10.1002/pssr.201206316

[216] Yim, C.J.; Unithrattil, S.; Chung, W.J.; Im, W.B. Preparation of electrospun pyrochlore-structure $KGdTa_2O_7:Eu^{3+}$ phosphor: the optical and structural properties for white light emitting diode applications. *J. Nanosci. Nanotechnol.,* **2013**, *13*(12), 7850-7854. http://dx.doi.org/10.1166/jnn.2013.8113 PMID: 24266151

[217] Hou, Z.; Cheng, Z.; Li, G.; Wang, W.; Peng, C.; Li, C.; Ma, P.; Yang, D.; Kang, X.; Lin, J. Electrospinning-derived $Tb_2(WO_4)_3:Eu(^{3+})$ nanowires: energy transfer and tunable luminescence properties. *Nanoscale,* **2011**, *3*(4), 1568-1574. http://dx.doi.org/10.1039/c0nr00774a PMID: 21327213

[218] Peng, C.; Li, G.; Hou, Z.; Shang, M.; Lin, J. Electrospinning synthesis and luminescent properties of one-dimensional $Ca_2Gd_8(SiO_4)_6O_2:Eu^{3+}$ microfibers and microbelts. *Mater. Chem. Phys.,* **2012**, *136*, 1008-1014. http://dx.doi.org/10.1016/j.matchemphys.2012.08.040

[219] Song, H.; Yu, H.; Pan, G.; Bai, X.; Dong, B.; Zhang, X.; Hark, S.K. Electrospinning preparation, structure, and photoluminescence properties of $YBO_3:Eu^{3+}$ nanotubes and nanowires. *Chem. Mater.,* **2008**, *20*, 4762-4767. http://dx.doi.org/10.1021/cm8007864

[220] Qin, C.; Qin, L.; Chen, G.; Lin, T. One-dimensional Eu^{3+} and Tb^{3+} doped $LaBO_3$ nanofibers: Fabrication and improved luminescence performances. *Mater. Lett.,* **2013**, *106*, 436-438. http://dx.doi.org/10.1016/j.matlet.2013.05.105

[221] Peng, C.; Li, G.; Kang, X.; Li, C.; Lin, J. The fabrication of one-dimensional $Ca_4Y_6(SiO_4)_6O$: Ln^{3+} (Ln=Eu, Tb) phosphors by electrospinning method and their luminescence properties. *J. Colloid Interface Sci.,* **2011**, *355*(1), 89-95. http://dx.doi.org/10.1016/j.jcis.2010.11.082 PMID: 21186034

[222] Abualrejal, M.M.A.; Zou, H.; Chen, J.; Song, Y.; Sheng, Y. Electrospinning synthesis and photoluminescence properties of one-dimensional $SiO_2:Tb^{3+}$ nanofibers and nanobelts. *Adv. Nanopart.,* **2017**, *6*, 33-47. http://dx.doi.org/10.4236/anp.2017.62004

[223] Du, P.; Song, L.; Xiong, J.; Xi, Z.; Jin, D.; Wang, L. Preparation and the luminescent properties of Tb^{3+}-doped Gd_2O_3 fluorescent nanofibers *via* electrospinning. *Nanotechnology,* **2011**, *22*(3), 035602. http://dx.doi.org/10.1088/0957-4484/22/3/035602 PMID: 21149966

[224] Xie, Y.; Ma, Z.; Liu, L.; Su, Y.; Zhao, H.; Liu, Y.; Zhang, Z.; Duan, H.; Li, J.; Xie, E. Oxygen defects-modulated green photoluminescence of Tb-doped ZrO_2 nanofibers. *Appl. Phys. Lett.,* **2010**, *97*, 141916. http://dx.doi.org/10.1063/1.3496471

[225] Zhao, J.; Zhang, W.; Xie, E.; Liu, Z.; Feng, J.; Liu, Z. Photoluminescence properties of β-$Ga_2O_3:Tb^{3+}$ nanofibers prepared by electrospinning. *Mater. Sci. Eng. B,* **2011**, *176*, 932-936. http://dx.doi.org/10.1016/j.mseb.2011.05.004

[226] Song, L.; Du, P.; Xiong, J.; Fan, X.; Jiao, Y. Preparation and luminescence properties of terbium-doped lanthanum oxide nanofibers by electrospinning. *J. Lumin.,* **2012**, *132*, 171-174. http://dx.doi.org/10.1016/j.jlumin.2011.08.007

[227] Li, X.; Chen, Y.; Qian, Q.; Liu, X.; Xiao, L.; Chen, Q. Preparation and photoluminescence characteristics of Tb-, Sm- and Dy-doped Y_2O_3 nanofibers by electrospinning. *J. Lumin.,* **2012**, *132*, 81-85. http://dx.doi.org/10.1016/j.jlumin.2011.07.003

[228] Li, B.; Zhang, H.; Lan, A.; Tang, H. One-dimensional $CdWO_4:Tb^{3+}$ nanofibers: Electrospinning fabrication and luminescence. *Chem. Phys. Lett.,* **2015**, *636*, 22-25. http://dx.doi.org/10.1016/j.cplett.2015.07.010

[229] Li, Q.; Liu, Z.P.; Dong, L.M.; Zhang, Y.F. Facile synthesis and luminescene properties of $CePO_4:Tb^{3+}$ by electrospinning. *Dig. J. Nanomater. Biostruct.,* **2016**, *11*, 1311-1317.

[230] Bi, F.; Dong, X.; Wang, J.; Liu, G. Electrospinning preparation and photoluminescence properties of $Y_3Al_5O_{12}:Tb^{3+}$ nanostructures. *Luminescence,* **2015**, *30*(6), 751-759. http://dx.doi.org/10.1002/bio.2816 PMID: 25428033

[231] Peng, C.; Shang, M.; Li, G.; Hou, Z.; Geng, D.; Lin, J. Electrospinning synthesis and luminescence properties of one-dimensional $La_{(9.33)}(SiO_4)_6O_2$: Ln^{3+} (Ln = Ce, Eu, Tb) microfibers. *Dalton Trans.,* **2012**, *41*(16), 4780-4788. http://dx.doi.org/10.1039/c2dt12220k PMID: 22382636

[232] Song, L.; Du, P.; Jiang, Q.; Cao, H.; Xiong, J. Synthesis and luminescence of high-brightness $Gd_2O_2SO_4:Tb^{3+}$ nanopieces and the enhanced luminescence by alkali metal ions co-doping. *J. Lumin.,* **2014**, *150*, 50-54. http://dx.doi.org/10.1016/j.jlumin.2014.01.043

[233] Huang, Z.; Huang, S.; Ou, G.; Pan, W. Systhesis, phase transformation and photoluminescence properties of Eu:$La_{(1-x)}Gd_{(x)}VO_4$ nanofibers by electrospinning method. *Nanoscale,* **2012**, *4*(16), 5065-5070. http://dx.doi.org/10.1039/c2nr31135f PMID: 22772795

[234] Lu, Q.; Liu, Q.; Zhuang, J.; Liu, G.; Wei, Q. Ce^{3+}-doped $Lu_2Si_2O_7$ luminescent fibers derived from electrospinning: Facile preparation and flexible fiber molding. *J. Mater. Sci.,* **2013**, *48*, 8471-8482. http://dx.doi.org/10.1007/s10853-013-7664-3

[235] Lu, Q.; Liu, Q.; Wei, Q.; Liu, G.; Zhuang, J. Preparation and characterization of $Lu_2SiO_5:Ce^{3+}$ luminescent ceramic fibers *via* electrospinning. *Ceram. Int.,* **2013**, *39*, 8159-8164. http://dx.doi.org/10.1016/j.ceramint.2013.03.090

[236] Li, B.; Zhang, H.; Lan, A.; Tang, H. $Ca_{(3-x)}Sr_x(PO_4)_2:Eu^{2+}$ nanofibers: Electrospinning fabrication and tunable luminescence. *Superlattices Microstruct.,* **2015**, *86*, 425-429. http://dx.doi.org/10.1016/j.spmi.2015.08.014

[237] Li, X.; Yu, M.; Hou, Z.; Li, G.; Ma, P.; Wang, W.; Cheng, Z.; Lin, J. One-dimensional $GdVO_4:Ln^{3+}$ (Ln=Eu, Dy, Sm) nanofibers: Electrospinning preparation and luminescence properties. *J. Solid State Chem.,* **2011**, *184*, 141-148. http://dx.doi.org/10.1016/j.jssc.2010.11.019

[238] Chen, Z.; Trofimov, A.A.; Jacobsohn, L.G.; Xiao, H.; Kornev, K.G.; Xu, D.; Peng, F. Permeation and optical properties of YAG:Er^{3+} fiber membrane scintillators prepared by novel sol-gel/electrospinning method. *J. Sol-Gel Sci. Technol.,* **2017**, *83*, 35-43. http://dx.doi.org/10.1007/s10971-017-4387-y

[239] Liu, Z.; Yuwen, M.; Liu, J.; Yu, C.; Xuan, T.; Li, H. Electrospinning, optical properties and white led applications of one-

dimensional $CaAl_{12}O_{19}:Mn^{4+}$ nanofiber phosphors. *Ceram. Int.,* **2017**, *43*, 5674-5679.
http://dx.doi.org/10.1016/j.ceramint.2017.01.105

[240] Hassan, M.S.; Kang, Y.-S.; Kim, B.-S.; Kim, I.-S.; Kim, H.-Y.; Khil, M.-S. Synthesis of praseodymium oxide nanofiber by electrospinning. *Superlattices Microstruct.,* **2011**, *50*, 139-144.
http://dx.doi.org/10.1016/j.spmi.2011.05.010

[241] Hou, Z.; Zhang, C.; Li, C.; Xu, Z.; Cheng, Z.; Li, G.; Wang, W.; Peng, C.; Lin, J. Luminescent porous silica fibers as drug carriers. *Chemistry,* **2010**, *16*(48), 14513-14519.
http://dx.doi.org/10.1002/chem.201000900 PMID: 21077051

[242] Kumar, K.S.; Song, C.-G.; Bak, G.M.; Heo, G.; Seong, M.-J.; Yoon, J.-W. Phase control of yttrium (Y)-doped TiO_2 nanofibers and intensive visible photoluminescence. *J. Alloys Compd.,* **2014**, *617*, 683-687.
http://dx.doi.org/10.1016/j.jallcom.2014.08.067

[243] Das, K.; Sharma, S.N.; Kumar, M.; De, S.K. Morphology dependent luminescence properties of co doped TiO_2 nanostructures. *J. Phys. Chem. C,* **2009**, *113*, 14783-14792.
http://dx.doi.org/10.1021/jp9048956

[244] Jia, C.W.; Zhao, J.G.; Duan, H.G.; Xie, E.Q. Visible photoluminescence from Er^{3+}-doped TiO_2 nanofibres by electrospinning. *Mater. Lett.,* **2007**, *61*, 4389-4392.
http://dx.doi.org/10.1016/j.matlet.2007.02.010

[245] Bai, J.; Zhao, R.; Han, G.; Li, Z.; Diao, G. Synthesis of 1D upconversion CeO_2:Er, Yb nanofibers *via* electrospinning and their performance in dye-sensitized solar cells. *RSC Advances,* **2015**, *5*, 43328-43333.
http://dx.doi.org/10.1039/C5RA06917C

[246] Zhang, X.; Xu, D.; Zhou, G.; Wang, X.; Liu, H.; Yu, Z.; Zhang, G.; Zhu, L. Color tunable up-conversion emission from $ZrO_2:Er^{3+}$, Yb^{3+} textile fibers. *RSC Advances,* **2016**, *6*, 103973-103980.
http://dx.doi.org/10.1039/C6RA20388D

[247] Wu, J.; Coffer, J.L.; Wang, Y.; Schulze, R. Oxidized germanium as a broad-band sensitizer for Er-doped SnO_2 nanofibers. *J. Phys. Chem. C,* **2009**, *113*, 12-16.
http://dx.doi.org/10.1021/jp8080996

[248] Liu, L.; Wang, Y.; Su, Y.; Ma, Z.; Xie, Y.; Zhao, H.; Chen, C.; Zhang, Z.; Xie, E. Synthesis and white light emission of rare earth-doped HfO_2 nanotubes. *J. Am. Ceram. Soc.,* **2011**, *94*, 2141-2145.
http://dx.doi.org/10.1111/j.1551-2916.2010.04375.x

[249] Li, J.-M.; Wei, D.-P.; Hu, Y.-B. Jie-Fang; Xu, Z.-A. Synthesis of ultrafine green-emitting $BaCO_3$ nanowires with 18.5 nm-diameter by CO_2 vapor-assisted electrospinning. *CrystEngComm,* **2014**, *16*, 964-968.
http://dx.doi.org/10.1039/c3ce41988f

[250] Dong, Q.Z.; He, L.; Li, W.S.; Sun, W.M. The fabrication of one-dimensional $BaAl_{12}O_{19}:Mn^{2+}$ phosphors by electrospinning method. *Mater. Sci.,* **2016**, *852*, 565-572.

[251] Fu, Y.; Li, X.; Sun, C.; Ren, Z.; Weng, W.; Mao, C.; Han, G. pH-triggered $SrTiO_3$:Er nanofibers with optically monitored and controlled drug delivery functionality. *ACS Appl. Mater. Interfaces,* **2015**, *7*(45), 25514-25521.
http://dx.doi.org/10.1021/acsami.5b08953 PMID: 26544158

[252] Li, X.; Zhang, Q.; Ahmad, Z.; Huang, J.; Ren, Z.; Weng, W.; Han, G.; Mao, C. Near-infrared luminescent $CaTiO_3:Nd^{3+}$ nanofibers with tunable and trackable drug release kinetics. *J. Mater. Chem. B Mater. Biol. Med.,* **2015**, *3*(37), 7449-7456.
http://dx.doi.org/10.1039/C5TB01158B PMID: 27398215

[253] Yu, H.; Wang, S.; Zhou, L.; Wang, W.; Wang, M. Fabrication and luminescent properties of Eu^{3+} doped lanthanide oxide nanowires and nanotubes by electrospinning. *Proceedings of the 2009 Asia-Pacific Power and Energy Engineering Conference,* **2009**, pp. 1-4.

[254] Miriyala, N.; Prashanthi, K.; Thundat, T. Oxygen vacancy dominant strong visible photoluminescence from $BiFeO_3$ nanotubes. *Phys. Status Solidi Rapid Res. Lett.,* **2013**, *7*, 668-671.
http://dx.doi.org/10.1002/pssr.201308069

[255] Philip, G.G.; Senthamizhan, A.; Natarajan, T.S.; Chandrasekaran, G.; Therese, H.A. The effect of gadolinium doping on the structural, magnetic and photoluminescence properties of electrospun bismuth ferrite nanofibers. *Ceram. Int.,* **2015**, *41*, 13361-13365.
http://dx.doi.org/10.1016/j.ceramint.2015.07.122

[256] Keereeta, Y.; Thongtem, T.; Thongtem, S. Fabrication of $ZnWO_4$ nanofibers by a high direct voltage electrospinning process. *J. Alloys Compd.,* **2011**, *509*, 6689-6695.
http://dx.doi.org/10.1016/j.jallcom.2011.03.140

[257] Wannapop, S.; Thongtem, T.; Thongtem, S. Photoemission and energy gap of $MgWO_4$ particles connecting as nanofibers synthesized by electrospinning-calcination combinations. *Appl. Surf. Sci.,* **2012**, *258*, 4971-4976.
http://dx.doi.org/10.1016/j.apsusc.2012.01.133

[258] Xu, X.; Zhao, S.; Liang, K.; Zeng, J. Electrospinning preparation and luminescence properties of one-dimensional $SrWO_4:Sm^{3+}$ nanofibers. *J. Mater. Sci. Mater. Electron.,* **2014**, *25*, 3324-3331.
http://dx.doi.org/10.1007/s10854-014-2021-0

[259] Wannapop, S.; Thongtem, T.; Thongtem, S. Characterization of $SrWO_4$–PVA and $SrWO_4$ spiders' webs synthesized by electrospinning. *Ceram. Int.,* **2011**, *37*, 3499-3507.
http://dx.doi.org/10.1016/j.ceramint.2011.06.005

[260] Keereeta, Y.; Thongtem, T.; Thongtem, S. Synthesis of lanthanum tungstate interconnecting nanoparticles by high voltage electrospinning. *Appl. Surf. Sci.,* **2015**, *351*, 1075-1080.
http://dx.doi.org/10.1016/j.apsusc.2015.05.194

[261] Song, L.; Liu, S.; Lu, Q.; Zhao, G. Fabrication and characterization of electrospun orthorhombic $InVO_4$ nanofibers. *Appl. Surf. Sci.,* **2012**, *258*, 3789-3794.
http://dx.doi.org/10.1016/j.apsusc.2011.12.029

[262] Rambabu, U.; Han, S.-D. Synthesis and luminescence properties of broad band greenish-yellow emitting $LnVO_4:Bi^{3+}$ and (Ln1, Ln2)$VO_4:Bi^{3+}$ (Ln=La, Gd and Y) as down conversion phosphors. *Ceram. Int.,* **2013**, *39*, 701-708.
http://dx.doi.org/10.1016/j.ceramint.2012.06.081

[263] Liu, Y.; Huang, Y.; Seo, H.J.; Wu, Y. Blueshift in near-band-edge emission in Y^{3+}-doped $CuAlO_2$ nanofibers. *Opt. Mater. Express,* **2014**, *4*, 2602-2607.
http://dx.doi.org/10.1364/OME.4.002602

[264] Dong, G.; Liang, M.; Qin, H.; Chai, G.; Zhang, X.; Ma, Z.; Peng, M.; Qiu, J. Controllable fabrication and broadband near-infrared luminescence of various Ni^{2+}-activated $ZnAl_2O_4$ nanostructures by a single-nozzle electrospinning technique. *Phys. Chem. Chem. Phys.,* **2012**, *14*(39), 13594-13600.
http://dx.doi.org/10.1039/c2cp42235b PMID: 22962668

[265] Yang, D.; Zhao, G.; Pan, Q.; Liang, M.; Ma, Z.; Dong, G.; Chen, D.; Qiu, J. Electrospun Nd^{3+}-doped spinel nanoparticles/nanofibers with both excitation and emission wavelengths in the optical window of cells and tissues. *Mater. Express,* **2013**, *3*, 210-216.
http://dx.doi.org/10.1166/mex.2013.1119

[266] Wang, L.; Hou, Z.; Quan, Z.; Lian, H.; Yang, P.; Lin, J. Preparation and luminescence properties of Mn^{2+}-doped $ZnGa_2O_4$ nanofibers *via* electrospinning process. *Mater. Res. Bull.,* **2009**, *44*, 1978-1983.
http://dx.doi.org/10.1016/j.materresbull.2009.06.008

[267] Wang, L.; Liu, X.; Hou, Z.; Li, C.; Yang, P.; Cheng, Z.; Lian, H.; Lin, J. Electrospinning synthesis and luminescence properties of one-dimensional $Zn_2SiO_4:Mn^{2+}$ microfibers and microbelts. *J. Phys. Chem. C,* **2008**, *112*, 18882-18888.
http://dx.doi.org/10.1021/jp806392a

[268] Dong, G.; Xiao, X.; Zhang, L.; Ma, Z.; Bao, X.; Peng, M.; Zhang, Q.; Qiu, J. Preparation and optical properties of red, green and blue afterglow electrospun nanofibers. *J. Mater. Chem.,* **2011**, *21*, 2194-2203.
http://dx.doi.org/10.1039/C0JM02851G

[269] Du, P.; Song, L.; Xiong, J.; Cao, H.; Xi, Z.; Guo, S.; Wang, N.; Chen, J. Electrospinning fabrication and luminescent properties of $SrMoO_4:Sm^{3+}$ nanofibers. *J. Alloys Compd.,* **2012**, *540*, 179-183.
http://dx.doi.org/10.1016/j.jallcom.2012.06.025

[270] He, L.; Jia, B.; Che, L.; Li, W.; Sun, W. Preparation and optical properties of afterglow $Sr_2MgSi_2O_7:Eu^{2+}$, Dy^{3+} electrospun nanofibers. *J. Lumin.,* **2016**, *172*, 317-322.
http://dx.doi.org/10.1016/j.jlumin.2015.12.012

[271] Zhu, Y.; Chen, Z.; Ge, M. Preparation of $Sr_2MgSi_2O_7:Eu^{2+}$, Dy^{3+} nanofiber by electrospinning assisted solid-state reaction. *J. Mater. Sci. Mater. Electron.,* **2014**, *25*, 2857-2862.
http://dx.doi.org/10.1007/s10854-014-1952-9

[272] Xin, S.; Wang, Y.; Dong, P.; Zeng, W.; Zhang, J. Preparation, characterization, and luminescent properties of $CaAl_2O_4:Eu^{2+}$, Nd^{3+}

nanofibers using core-sheath $CaAl_2O_4$:Eu^{2+}, Nd^{3+}/carbon nanofibers as templates. *J. Mater. Chem. C Mater. Opt. Electron. Devices,* **2013**, *1*, 8156-8160.
http://dx.doi.org/10.1039/c3tc31356e

[273] Dong, G.; Xiao, X.; Liu, X.; Qian, B.; Ma, Z.; Chen, D.; Qiu, J. Preparation and optical properties of long afterglow europium-doped Ca(Sr)$Al_2Si_2O_8$ electrospun nanofibers. *J. Electrochem. Soc.,* **2009**, *156*, J356-J360.
http://dx.doi.org/10.1149/1.3223986

[274] Xu, C.; Guo, J.; Li, Y.; Seo, H.J. Enhanced luminescence of $Ca_2MgSi_2O_7$:Eu^{2+} fibers by sol-gel assisted electrospinning. *Opt. Mater.,* **2013**, *35*, 893-897.
http://dx.doi.org/10.1016/j.optmat.2012.10.048

[275] Esfahani, H.; Jose, R.; Ramakrishna, S. Electrospun ceramic nanofiber mats today: Synthesis, properties, and applications. *Materials (Basel),* **2017**, *10*(11), 1238.
http://dx.doi.org/10.3390/ma10111238 PMID: 29077074

[276] Suryamas, A.B.; Munir, M.M.; Iskandar, F.; Okuyama, K. Photoluminescent and crystalline properties of $Y_{3-x}Al_5O_{12}$:Ce_x^{3+} phosphor nanofibers prepared by electrospinning. *J. Appl. Phys.,* **2009**, *105*, 064311.
http://dx.doi.org/10.1063/1.3095483

[277] Mondal, K.; Hartman, K.; Dasgupta, D.; Trifon, G.; Dasari, M. Synthesis and characterization of $Y_2Ti_2O_7$ and $Er_xY_{2-x}Ti_2O_7$ nanofibers. *J. Sol-Gel Sci. Technol.,* **2015**, *73*, 265-269.
http://dx.doi.org/10.1007/s10971-014-3574-3

[278] Liu, Y.; Olson, T.L.; Wu, Y. Luminescence and microstructure of Nd doped $Y_2Si_2O_7$ electrospun fibers. *J. Am. Ceram. Soc.,* **2014**, *97*, 2390-2393.
http://dx.doi.org/10.1111/jace.13070

[279] Bi, F.; Dong, X.; Wang, J.; Liu, G. Facile electrospinning preparation and up-conversion luminescence performance of $Y_3Al_5O_{12}$:Er^{3+}, Yb^{3+} nanobelts. *J. Inorg. Organomet. Polym. Mater.,* **2014**, *24*, 407-415.
http://dx.doi.org/10.1007/s10904-013-9999-2

[280] Wang, L.; Hou, Z.; Quan, Z.; Li, C.; Yang, J.; Lian, H.; Yang, P.; Lin, J. One-dimensional Ce^{3+}- and/or Tb^{3+}-doped X_1-Y_2SiO_5 nanofibers and microbelts: electrospinning preparation and luminescent properties. *Inorg. Chem.,* **2009**, *48*(14), 6731-6739.
http://dx.doi.org/10.1021/ic9006789 PMID: 19522469

[281] Mani, K.P.; George, V.; Ramakrishnan, B.P.; Joseph, C.; Viswambharan, U.N.; Abraham, I.M. Synthesis and photoluminescence studies of one dimensional Sm_2MoO_6 nanofibers derived from electrospinning process. *J. Mater. Res. Technol.,* **2015**, *4*, 224-227.
http://dx.doi.org/10.1016/j.jmrt.2015.01.005

[282] Fu, Y.; Gong, S.; Liu, X.; Xu, G.; Ren, Z.; Li, X.; Han, G. Crystallization and concentration modulated tunable upconversion luminescence of Er^{3+} doped PZT nanofibers. *J. Mater. Chem. C Mater. Opt. Electron. Devices,* **2014**, *3*, 382-389.
http://dx.doi.org/10.1039/C4TC01784F

[283] Gao, L.; Li, C. Preparation and photoluminescence properties of electrospun nanofibers of C60/PVK. *J. Lumin.,* **2010**, *130*, 236-239.
http://dx.doi.org/10.1016/j.jlumin.2009.08.015

[284] Yang, P.; Zhan, S.; Huang, Z.; Zhai, J.; Wang, D.; Xin, Y.; Zhang, L.; Sun, M.; Shao, C. The fabrication of PPV/C60 composite nanofibers with highly optoelectric response by optimization solvents and electrospinning technology. *Mater. Lett.,* **2011**, *65*, 537-539.
http://dx.doi.org/10.1016/j.matlet.2010.10.038

[285] Bounioux, C.; Itzhak, R.; Avrahami, R.; Zussman, E.; Frey, J.; Katz, E.A.; Yerushalmi-Rozen, R. Electrospun fibers of functional nanocomposites composed of single-walled carbon nanotubes, fullerene derivatives, and poly(*3*-hexylthiophene). *J. Polym. Sci. B Polym. Phys.,* **2011**, *49*, 1263-1268.
http://dx.doi.org/10.1002/polb.22281

[286] Amirian, M.; Chakoli, A.N.; Sui, J.H.; Cai, W. Enhanced mechanical and photoluminescence effect of poly(l-lactide) reinforced with functionalized multiwalled carbon nanotubes. *Polym. Bull.,* **2012**, *68*, 1747-1763.
http://dx.doi.org/10.1007/s00289-012-0700-7

[287] Adhikary, P.; Biswas, A.; Mandal, D. Improved sensitivity of wearable nanogenerators made of electrospun Eu^{3+} doped P(VDF-HFP)/graphene composite nanofibers for self-powered voice recognition. *Nanotechnology,* **2016**, *27*(49), 495501.
http://dx.doi.org/10.1088/0957-4484/27/49/495501 PMID: 27831929

[288] Zhai, Y.; Bai, X.; Cui, H.; Zhu, J.; Liu, W.; Zhang, T.; Dong, B.; Pan, G.; Xu, L.; Zhang, S.; Song, H. Carbon dot/polyvinylpyrrolidone hybrid nanofibers with efficient solid-state photoluminescence constructed using an electrospinning technique. *Nanotechnology,* **2018**, *29*(2), 025706.
http://dx.doi.org/10.1088/1361-6528/aa99be PMID: 29125471

[289] Alam, A.-M.; Liu, Y.; Park, M.; Park, S.-J.; Kim, H.-Y. Preparation and characterization of optically transparent and photoluminescent electrospun nanofiber composed of carbon quantum dots and polyacrylonitrile blend with polyacrylic acid. *Polymer (Guildf.),* **2015**, *59*, 35-41.
http://dx.doi.org/10.1016/j.polymer.2014.12.061

[290] Safaei, B.; Youssefi, M.; Rezaei, B.; Irannejad, N. Synthesis and properties of photoluminescent carbon quantum dot/polyacrylonitrile composite nanofibers. *Smart Sci.,* **2018**, *6*, 117-124.
http://dx.doi.org/10.1080/23080477.2017.1399318

[291] He, J.; He, Y.; Chen, Y.; Zhang, X.; Hu, C.; Zhuang, J.; Lei, B.; Liu, Y. Construction and multifunctional applications of carbon Dots/PVA nanofibers with phosphorescence and thermally activated delayed fluorescence. *Chem. Eng. J.,* **2018**, *347*, 505-513.
http://dx.doi.org/10.1016/j.cej.2018.04.110

[292] Zhai, Y.; Bai, X.; Zhu, J.; Sun, X.; Pan, G.; Dong, B.; Xu, L.; Xu, W.; Zhang, S.; Song, H. Luminescence carbon dot-based nanofibers for a water-insoluble drug release system and their monitoring of drug release. *J. Mater. Chem. B Mater. Biol. Med.,* **2018**, *6*, 3579-3585.
http://dx.doi.org/10.1039/C8TB00117K

[293] Lin, M.; Zou, H.Y.; Yang, T.; Liu, Z.X.; Liu, H.; Huang, C.Z. An inner filter effect based sensor of tetracycline hydrochloride as developed by loading photoluminescent carbon nanodots in the electrospun nanofibers. *Nanoscale,* **2016**, *8*(5), 2999-3007.
http://dx.doi.org/10.1039/C5NR08177G PMID: 26781447

[294] Li, S.; Zhou, S.; Xu, H.; Xiao, L.; Wang, Y.; Shen, H.; Wang, H.; Yuan, Q. Luminescent properties and sensing performance of a carbon quantum dot encapsulated mesoporous silica/polyacrylonitrile electrospun nanofibrous membrane. *J. Mater. Sci.,* **2016**, *51*, 6801-6811.
http://dx.doi.org/10.1007/s10853-016-9967-7

[295] Zhang, P.; Zhao, X.; Ji, Y.; Ouyang, Z.; Wen, X.; Li, J.; Su, Z.; Wei, G. Electrospinning graphene quantum dots into a nanofibrous membrane for dual-purpose fluorescent and electrochemical biosensors. *J. Mater. Chem. B Mater. Biol. Med.,* **2015**, *3*, 2487-2496.
http://dx.doi.org/10.1039/C4TB02092H

[296] Liao, B.; Wang, W.; Long, P.; Deng, X.; He, B.; Liu, Q.; Yi, S. The carbon nanoparticles grafted with copolymers of styrene and spiropyran with reversibly photoswitchable fluorescence. *Carbon,* **2015**, *91*, 30-37.
http://dx.doi.org/10.1016/j.carbon.2015.04.030

[297] Wang, Y.; Zhu, Y.; Huang, J.; Cai, J.; Zhu, J.; Yang, X.; Shen, J.; Li, C. Perovskite quantum dots encapsulated in electrospun fiber membranes as multifunctional supersensitive sensors for biomolecules, metal ions and pH. *Nanoscale Horiz.,* **2017**, *2*, 225-232.
http://dx.doi.org/10.1039/C7NH00057J

[298] Wang, Y.; Zhu, Y.; Huang, J.; Cai, J.; Zhu, J.; Yang, X.; Shen, J.; Jiang, H.; Li, C. CsPbBr3 perovskite quantum dots-based monolithic electrospun fiber membrane as an ultrastable and ultrasensitive fluorescent sensor in aqueous medium. *J. Phys. Chem. Lett.,* **2016**, *7*(21), 4253-4258.
http://dx.doi.org/10.1021/acs.jpclett.6b02045 PMID: 27734662

[299] Tsai, P.-C.; Chen, J.-Y.; Ercan, E.; Chueh, C.-C.; Tung, S.-H.; Chen, W.-C. Uniform luminous perovskite nanofibers with color-tunability and improved stability prepared by one-step core/shell electrospinning. *Small,* **2018**, *14*(22), e1704379.
http://dx.doi.org/10.1002/smll.201704379 PMID: 29709108

[300] Sultana, A.; Alam, M.M.; Sadhukhan, P.; Ghorai, U.K.; Das, S.; Middya, T.R.; Mandal, D. Organo-lead halide perovskite regulated green light emitting poly(vinylidene fluoride) electrospun nanofiber mat and its potential utility for ambient mechanical energy harvesting application. *Nano Energy,* **2018**, *49*, 380-392.
http://dx.doi.org/10.1016/j.nanoen.2018.04.057

[301] Abitbol, T.; Wilson, J.T.; Gray, D.G. Electrospinning of fluorescent fibers from CdSe/ZnS quantum dots in cellulose triacetate. *J. Appl. Polym. Sci.,* **2011**, *119*, 803-810. http://dx.doi.org/10.1002/app.32782

[302] Xiaoqiang, L.; Chen, S.; Hua, Q.; Hong, S.; Kenji, O. Fabrication of fluorescent poly(l-lactide-co-caprolactone) fibers with quantum-dot incorporation from emulsion electrospinning for chloramphenicol detection. *J. Appl. Polym. Sci.,* **2017**, *134*, 44584. http://dx.doi.org/10.1002/app.44584

[303] Zhu, L.; Yang, S.; Wang, J.; Wang, C.-F.; Chen, L.; Chen, S. Quantum-dot-embedded polymeric fiber films with photoluminescence and superhydrophobicity. *Mater. Lett.,* **2013**, *99*, 54-56. http://dx.doi.org/10.1016/j.matlet.2012.03.118

[304] Başlak, C.; Köysüren, Ö.; Kuş, M. *Electrospun Nanofibers with CdTe QDs, CdTeSe QDs and CdTe/CdS Core-Shell QDs* In: *Proceedings of the 2017 IEEE 7th International Conference, Nanomaterials: Application and Properties (NAP)*, Odessa, Ukraine, September 10-15, 2017; IEEE, **2017**; pp. 03NNSA39-1. http://dx.doi.org/10.1109/NAP.2017.8190290

[305] Demir, M.M.; Soyal, D.; Ünlü, C.; Kuş, M.; Özçelik, S. Controlling spontaneous emission of CdSe nanoparticles dispersed in electrospun fibers of polycarbonate urethane. *J. Phys. Chem. C,* **2009**, *113*, 11273-11278. http://dx.doi.org/10.1021/jp903899s

[306] Wang, H.; Lu, X.; Zhao, Y.; Wang, C. Preparation and characterization of ZnS:Cu/PVA composite nanofibers *via* electrospinning. *Mater. Lett.,* **2006**, *60*, 2480-2484. http://dx.doi.org/10.1016/j.matlet.2006.01.021

[307] Dhandayuthapani, B.; Poulose, A.C.; Nagaoka, Y.; Hasumura, T.; Yoshida, Y.; Maekawa, T.; Kumar, D.S. Biomimetic smart nanocomposite: *in vitro* biological evaluation of zein electrospun fluorescent nanofiber encapsulated CdS quantum dots. *Biofabrication,* **2012**, *4*(2), 025008. http://dx.doi.org/10.1088/1758-5082/4/2/025008 PMID: 22592161

[308] Kim, B.-S.; Song, H.-M.; Lee, C.-S.; Lee, S.-G.; Son, Y.-A. Preparation of luminescing nanocrystal and its application to electrospinning. *Fibers Polym.,* **2008**, *9*, 534-537. http://dx.doi.org/10.1007/s12221-008-0085-2

[309] Altıntas, Y.; Kiremitler, N.B.; Genç, S.; Onses, M.S.; Mutlugün, E. FRET enabled light harvesting within quantum dot loaded nanofibers. *J. Phys. D Appl. Phys.,* **2018**, *51*, 065111. http://dx.doi.org/10.1088/1361-6463/aaa55a

[310] Liu, H.; Edel, J.B.; Bellan, L.M.; Craighead, H.G. Electrospun polymer nanofibers as subwavelength optical waveguides incorporating quantum dots. *Small,* **2006**, *2*(4), 495-499. http://dx.doi.org/10.1002/smll.200500432 PMID: 17193073

[311] Zhu, J.; Wei, S.; Patil, R.; Rutman, D.; Kucknoor, A.S.; Wang, A.; Guo, Z. Ionic liquid assisted electrospinning of quantum dots/elastomer composite nanofibers. *Polymer (Guildf.),* **2011**, *52*, 1954-1962. http://dx.doi.org/10.1016/j.polymer.2011.02.051

[312] Liu, Y.; Wang, J.; Che, Q.; Yang, P.; Yue, Y. Hydrophobic and hydrophilic quantum dots embedded in poly(vinyl pyrrolidone) fibers with bright photoluminescence. *Nanosci. Nanotechnol. Lett.,* **2018**, *7*, 105-110. http://dx.doi.org/10.1166/nnl.2015.1911

[313] Saito, T.; Kimura, S.; Nishiyama, Y.; Isogai, A. Cellulose nanofibers prepared by TEMPO-mediated oxidation of native cellulose. *Biomacromolecules,* **2007**, *8*(8), 2485-2491. http://dx.doi.org/10.1021/bm0703970 PMID: 17630692

[314] Yao, J.; Ji, P.; Wang, B.; Wang, H.; Chen, S. Color-tunable luminescent macrofibers based on CdTe QDs-loaded bacterial cellulose nanofibers for pH and glucose sensing. *Sens. Actuators B Chem.,* **2018**, *254*, 110-119. http://dx.doi.org/10.1016/j.snb.2017.07.071

[315] Sui, X.; Shao, C.; Liu, Y. Photoluminescence of polyethylene oxide-ZnO composite electrospun fibers. *Polymer (Guildf.),* **2007**, *48*, 1459-1463. http://dx.doi.org/10.1016/j.polymer.2007.01.039

[316] Zhang, Z.; Shao, C.; Gao, F.; Li, X.; Liu, Y. Enhanced ultraviolet emission from highly dispersed ZnO quantum dots embedded in poly(vinyl pyrrolidone) electrospun nanofibers. *J. Colloid Interface Sci.,* **2010**, *347*(2), 215-220. http://dx.doi.org/10.1016/j.jcis.2010.03.052 PMID: 20400088

[317] Sui, X.M.; Shao, C.L.; Liu, Y.C. White-light emission of polyvinyl alcohol/ZnO hybrid nanofibers prepared by electrospinning. *Appl. Phys. Lett.,* **2005**, *87*, 113115. http://dx.doi.org/10.1063/1.2048808

[318] Wang, C.; Yan, E.; Huang, Z.; Zhao, Q.; Xin, Y. Fabrication of highly photoluminescent TiO_2/PPV hybrid nanoparticle-polymer fibers by electrospinning. *Macromol. Rapid Commun.,* **2007**, *28*, 205-209. http://dx.doi.org/10.1002/marc.200600626

[319] Liu, S.; Tan, L.; Li, X.; Fu, J.; Chronakis, I.S.; Ge, M. Gold nanoparticles-gelatin hybrid fibers with bright photoluminescence. *Mater. Lett.,* **2014**, *135*, 1-4. http://dx.doi.org/10.1016/j.matlet.2014.07.070

[320] Zhang, J.; Li, X.; Li, S.; Zhang, J.C.; Yan, X.; Yu, G.F.; Yang, D.P.; Long, Y.Z. Ultrasensitive fluorescence lifetime tuning in patterned polymer composite nanofibers with plasmonic nanostructures for multiplexing. *Macromol. Rapid Commun.,* **2018**, *40*(5), 1800022. http://dx.doi.org/10.1002/marc.201800022 PMID: 29675910

[321] Senthamizhan, A.; Celebioglu, A.; Uyar, T. Ultrafast on-site selective visual detection of TNT at sub-ppt level using fluorescent gold cluster incorporated single nanofiber. *Chem. Commun. (Camb.),* **2015**, *51*(26), 5590-5593. http://dx.doi.org/10.1039/C4CC01190B PMID: 24949681

[322] Baptista, A.C.; Botas, A.M.; Almeida, A.P.C.; Nicolau, A.T.; Falcão, B.P.; Soares, M.J.; Leitão, J.P.; Martins, R.; Borges, J.P.; Ferreira, I. Down conversion photoluminescence on PVP/Ag-nanoparticles electrospun composite fibers. *Opt. Mater.,* **2015**, *39*, 278-281. http://dx.doi.org/10.1016/j.optmat.2014.11.015

[323] Senthamizhan, A.; Celebioglu, A.; Uyar, T. Real-time selective visual monitoring of Hg(2+) detection at ppt level: An approach to lighting electrospun nanofibers using gold nanoclusters. *Sci. Rep.,* **2015**, *5*, 10403. http://dx.doi.org/10.1038/srep10403 PMID: 26020609

[324] Ortaç, B.; Kayaci, F.; Vural, H.A.; Deniz, A.E.; Uyar, T. Photoluminescent electrospun polymeric nanofibers incorporating germanium nanocrystals. *React. Funct. Polym.,* **2013**, *73*, 1262-1267. http://dx.doi.org/10.1016/j.reactfunctpolym.2013.06.007

[325] İncel, A.; Varlikli, C.; McMillen, C.D.; Demir, M.M. Triboluminescent electrospun mats with blue-green emission under mechanical force. *J. Phys. Chem. C,* **2017**, *121*, 11709-11716. http://dx.doi.org/10.1021/acs.jpcc.7b02875

[326] Lu, X.; Li, L.; Zhang, W.; Wang, C. Preparation and characterization of Ag(2)S nanoparticles embedded in polymer fibre matrices by electrospinning. *Nanotechnology,* **2005**, *16*(10), 2233-2237. http://dx.doi.org/10.1088/0957-4484/16/10/043 PMID: 20818001

[327] Di Benedetto, F.; Camposeo, A.; Persano, L.; Laera, A.M.; Piscopiello, E.; Cingolani, R.; Tapfer, L.; Pisignano, D. Light-emitting nanocomposite CdS-polymer electrospun fibres *via in situ* nanoparticle generation. *Nanoscale,* **2011**, *3*(10), 4234-4239. http://dx.doi.org/10.1039/c1nr10399g PMID: 21901210

[328] Bashouti, M.; Salalha, W.; Brumer, M.; Zussman, E.; Lifshitz, E. Alignment of colloidal CdS nanowires embedded in polymer nanofibers by electrospinning. *ChemPhysChem,* **2006**, *7*(1), 102-106. http://dx.doi.org/10.1002/cphc.200500428 PMID: 16363016

[329] Lu, X.; Zhao, Y.; Wang, C.; Wei, Y. Fabrication of CdS nanorods in PVP fiber matrices by electrospinning. *Macromol. Rapid Commun.,* **2005**, *26*, 1325-1329. http://dx.doi.org/10.1002/marc.200500300

[330] Wang, Q.; Chen, Y.; Liu, R.; Liu, H.; Li, Z. Fabrication and characterization of electrospun CdS-OH/Polyacrylonitrile hybrid nanofibers. *Compos. Part A Appl. Sci. Manuf.,* **2012**, *43*, 1869-1876. http://dx.doi.org/10.1016/j.compositesa.2012.07.023

[331] Yang, Y.; Wang, H.; Lu, X.; Zhao, Y.; Li, X.; Wang, C. Electrospinning of carbon/CdS coaxial nanofibers with photoluminescence and conductive properties. *Mater. Sci. Eng. B,* **2007**, *140*, 48-52. http://dx.doi.org/10.1016/j.mseb.2007.03.010

[332] Hernández-Martínez, D.; Nicho, M.E.; Hu, H.; León-Silva, U.; Arenas-Arrocena, M.C.; García-Escobar, C.H. Electrospinning of P3HT-PEO-CdS fibers by solution method and their properties. *Mater. Sci. Semicond. Process.,* **2017**, *61*, 50-56. http://dx.doi.org/10.1016/j.mssp.2016.12.039

[333] Lu, X.; Zhao, Y.; Wang, C. Fabrication of PbS nanoparticles in polymer-fiber matrices by electrospinning. *Adv. Mater.,* **2005**, *17*, 2485-2488.
http://dx.doi.org/10.1002/adma.200500196

[334] Ye, J.; Chen, Y.; Zhou, W.; Wang, X.; Guo, Z.; Hu, Y. Preparation of polymer@PbS hybrid nanofibers by surface-initiated atom transfer radical polymerization and acidolysis by H_2S. *Mater. Lett.,* **2009**, *63*, 1425-1427.
http://dx.doi.org/10.1016/j.matlet.2009.03.041

[335] Mthethwa, T.P.; Moloto, M.J.; De Vries, A.; Matabola, K.P. Properties of electrospun CdS and CdSe filled poly(methyl methacrylate) (PMMA) nanofibres. *Mater. Res. Bull.,* **2011**, *46*, 569-575.
http://dx.doi.org/10.1016/j.materresbull.2010.12.022

[336] Cao, Y.; Liu, N.; Yang, P.; Shi, R.; Ma, Q.; Zhang, A.; Zhu, Y.; Wang, J.; Wang, J. High luminescent fibers with hybrid SiO_2-coated CdTe nanocrystals fabricated by electrospinning technique. *Mater. Chem. Phys.,* **2015**, *149-150*, 51-58.
http://dx.doi.org/10.1016/j.matchemphys.2014.09.030

[337] Cho, K.; Kim, M.; Choi, J.; Kim, K.; Kim, S. Synthesis and characterization of electrospun polymer nanofibers incorporated with CdTe nanoparticles. *Synth. Met.,* **2010**, *160*, 888-891.
http://dx.doi.org/10.1016/j.synthmet.2010.01.041

[338] Wang, S.; Li, Y.; Wang, Y.; Yang, Q.; Wei, Y. Introducing CTAB into CdTe/PVP nanofibers enhances the photoluminescence intensity of CdTe nanoparticles. *Mater. Lett.,* **2007**, *61*, 4674-4678.
http://dx.doi.org/10.1016/j.matlet.2007.03.016

[339] Wang, S.; Li, Y.; Bai, J.; Yang, Q.; Song, Y.; Zhang, C. Characterization and photoluminescence studies of CdTe nanoparticles before and after transfer from liquid phase to polystyrene. *Bull. Mater. Sci.,* **2009**, *32*, 487-491.
http://dx.doi.org/10.1007/s12034-009-0072-2

[340] Sun, H.; Zhang, H.; Zhang, J.; Wei, H.; Ju, J.; Li, M.; Yang, B. White-light emission nanofibers obtained from assembling aqueous single-colored CdTe NCs into a PPV precursor and PVA matrix. *J. Mater. Chem.,* **2009**, *19*, 6740-6744.
http://dx.doi.org/10.1039/b909089d

[341] Nakhaei, O.; Shahtahmassebi, N.; Azhir, E. Co-precipitation synthesis of CaF_2:Er nanocomposites and photoluminescence characterizations of electrospun polyvinyl alcohol/CaF_2:Er nanofibers. *Indian J. Phys.,* **2014**, *88*, 1245-1250.
http://dx.doi.org/10.1007/s12648-014-0574-7

[342] Dong, G.; Liu, X.; Xiao, X.; Qian, B.; Ruan, J.; Ye, S.; Yang, H.; Chen, D.; Qiu, J. Photoluminescence of Ag nanoparticle embedded Tb^{3+}/Ce^{3+} codoped $NaYF_4$/PVP nanofibers prepared by electrospinning. *Nanotechnology,* **2009**, *20*(5), 055707.
http://dx.doi.org/10.1088/0957-4484/20/5/055707 PMID: 19417366

[343] Dong, B.; Song, H.; Yu, H.; Zhang, H.; Qin, R.; Bai, X.; Pan, G.; Lu, S.; Wang, F.; Fan, L.; Dai, Q. Upconversion properties of Ln^{3+} doped $NaYF_4$/Polymer composite fibers prepared by electrospinning. *J. Phys. Chem. C,* **2008**, *112*, 1435-1440.
http://dx.doi.org/10.1021/jp076958z

[344] Gangwar, A.K.; Gupta, A.; Kedawat, G.; Kumar, P.; Singh, B.P.; Singh, N.; Srivastava, A.K.; Dhakate, S.R.; Gupta, B.K. Highly luminescent dual mode polymeric nanofibers based flexible mat for white security paper and encrypted nanotaggants applications. *Chemistry,* **2018**, *24*(38), 9477-9484.
http://dx.doi.org/10.1002/chem.201800715 PMID: 29790610

[345] Liu, K.-C.; Zhang, Z.-Y.; Shan, C.-X.; Feng, Z.-Q.; Li, J.-S.; Song, C.-L.; Bao, Y.-N.; Qi, X.-H.; Dong, B. A flexible and superhydrophobic upconversion-luminescence membrane as an ultrasensitive fluorescence sensor for single droplet detection. *Light Sci. Appl.,* **2016**, *5*(8), e16136.
http://dx.doi.org/10.1038/lsa.2016.136 PMID: 30167183

[346] Bao, Y.; Luu, Q.A.N.; Zhao, Y.; Fong, H.; May, P.S.; Jiang, C. Upconversion polymeric nanofibers containing lanthanide-doped nanoparticles *via* electrospinning. *Nanoscale,* **2012**, *4*(23), 7369-7375.
http://dx.doi.org/10.1039/c2nr32204h PMID: 23026874

[347] Chen, Y.; Liu, S.; Hou, Z.; Ma, P.; Yang, D.; Li, C.; Lin, J. Multifunctional electrospinning composite fibers for orthotopic cancer treatment *in vivo. Nano Res.,* **2015**, *8*, 1917-1931.
http://dx.doi.org/10.1007/s12274-014-0701-y

[348] Hsu, C.-Y.; Liu, Y.-L. Rhodamine B-anchored silica nanoparticles displaying white-light photoluminescence and their uses in preparations of photoluminescent polymeric films and nanofibers. *J. Colloid Interface Sci.,* **2010**, *350*(1), 75-82.
http://dx.doi.org/10.1016/j.jcis.2010.06.011 PMID: 20599206

[349] Wang, Y.; Tang, J.; Huang, L.; Wang, Y.; Huang, Z.; Liu, J.; Xu, Q.; Shen, W.; Belfiroe, L.A. Enhanced emission of nano SiO_2-carried Eu^{3+} complexes and highly luminescent hybrid nanofibers. *Opt. Mater.,* **2013**, *35*, 1395-1403.
http://dx.doi.org/10.1016/j.optmat.2013.02.007

[350] Kamil, M.A.R.; Suhaimi, N.F.M.; Edwin, E.E.; Dian, W.; Abdul Halim, N.H. Optical characteristics of erbium-doped SiO_2/PVA electrospun nanofibers. *Adv. Mat. Res.,* **2015**, *1108*, 59-66.

[351] Jo, S.; Kim, J.; Noh, J.; Kim, D.; Jang, G.; Lee, N.; Lee, E.; Lee, T.S. Conjugated polymer dots-on-electrospun fibers as a fluorescent nanofibrous sensor for nerve gas stimulant. *ACS Appl. Mater. Interfaces,* **2014**, *6*(24), 22884-22893.
http://dx.doi.org/10.1021/am507206x PMID: 25431844

[352] Dong, G.; Liu, X.; Xiao, X.; Zhang, Q.; Lin, G.; Ma, Z.; Chen, D.; Qiu, J. Tunable emission of BCNO nanoparticle-embedded polymer electrospun nanofibers. *Electrochem. Solid-State Lett.,* **2009**, *12*, K53-K55.
http://dx.doi.org/10.1149/1.3137021

[353] de Melo, E.F.; Alves, K.G.B.; Junior, S.A.; de Melo, C.P. Synthesis of fluorescent PVA/polypyrrole-ZnO nanofibers. *J. Mater. Sci.,* **2013**, *48*, 3652-3658.
http://dx.doi.org/10.1007/s10853-013-7159-2

[354] Selvin, S.S.P.; Lee, J.; Kumar, S.; Radhika, N.; Merlin, J.P.; Lydia, I.S. Photocatalytic degradation of rhodamine B using cysteine capped ZnO/P(3HB-*co*-3HHx) fiber under UV and visible light irradiation. *React. Kinet. Mech. Catal.,* **2017**, *122*, 671-684.
http://dx.doi.org/10.1007/s11144-017-1232-9

[355] Naphade, R.; Jog, J. Electrospinning of PHBV/ZnO membranes: Structure and properties. *Fibers Polym.,* **2012**, *13*, 692-697.
http://dx.doi.org/10.1007/s12221-012-0692-9

[356] Turky, A.O.; Barhoum, A. Mohamed Rashad, M.; Bechlany, M. Enhanced the structure and optical properties for ZnO/PVP nanofibers fabricated *via* electrospinning technique. *J. Mater. Sci. Mater. Electron.,* **2017**, *28*, 17526-17532.
http://dx.doi.org/10.1007/s10854-017-7688-6

[357] Shehata, N.; Samir, E.; Gaballah, S.; Hamed, A.; Elrasheedy, A. Embedded ceria nanoparticles in crosslinked PVA electrospun nanofibers as optical sensors for radicals. *Sensors (Basel),* **2016**, *16*(9), 1371.
http://dx.doi.org/10.3390/s16091371 PMID: 27571083

[358] Hingwe, V.S.; Koparkar, K.A.; Bajaj, N.S.; Omanwar, S.K. Optical properties of one dimensional hybrid PVA/YVO_4:Eu^{3+} nanofibers synthesized by electrospining. *Optik (Stuttg.),* **2017**, *140*, 211-215.
http://dx.doi.org/10.1016/j.ijleo.2017.04.047

[359] Chigome, S.; Abiona, A.A.; Ajao, J.A.; Kana, J.B.K.; Guerbous, L.; Torto, N.; Maaza, M. Synthesis and characterization of electrospun poly(ethylene oxide)/europium-doped yttrium orthovanadate (PEO/YVO_4:Eu^{3+}) hybrid nanofibers. *Int. J. Polym. Mater. Polym. Biomater.,* **2010**, *59*, 863-872.
http://dx.doi.org/10.1080/00914037.2010.504146

[360] Yao, Y.; Zhou, Z.; Ye, F. Properties of a novel $Ba_5Si_8O_{21}$:Eu^{2+}, Nd^{3+} phosphor: Bulk and 1D nanostructure with PVP synthesized by sol-gel and electrospinning. *J. Alloys Compd.,* **2017**, *712*, 213-218.
http://dx.doi.org/10.1016/j.jallcom.2017.04.102

[361] Qin, C.; Gu, M.; Huang, Y.; Dai, L.; Chen, G.; Shi, L.; Qiao, X.; Seo, H.J. Preparation and luminescence properties of La_6MoO_{12}:Eu^{3+}/PVA nanofibers by Pechini/electrospinning process. *J. Nanosci. Nanotechnol.,* **2011**, *11*(11), 9570-9575.
http://dx.doi.org/10.1166/jnn.2011.5245 PMID: 22413249

[362] Erdem, R.; İlhan, M.; Ekmekçi, M.K.; Erdem, Ö. Electrospinning, preparation and photoluminescence properties of $CoNb_2O_6$:Dy^{3+} incorporated polyamide 6 composite fibers. *Appl. Surf. Sci.,* **2017**, *421*, 240-246.
http://dx.doi.org/10.1016/j.apsusc.2016.11.134

[363] Ye, F.; Dong, S.; Tian, Z.; Yao, S.; Zhou, Z.; Wang, S. Fabrication and characterization of long-persistent luminescence/polymer ($Ca_2MgSi_2O_7$:Eu^{2+}, Dy^{3+}/PLA) composite fibers by electrospinning. *Opt. Mater.,* **2015**, *45*, 64-68.

http://dx.doi.org/10.1016/j.optmat.2015.03.011

[364] Sepahvandi, A.; Eskandari, M.; Moztarzadeh, F. Fabrication and characterization of $SrAl_2O_4$: Eu(2+)Dy(3+)/CS-PCL electrospun nanocomposite scaffold for retinal tissue regeneration. *Mater. Sci. Eng. C,* **2016**, *66*, 306-314.
http://dx.doi.org/10.1016/j.msec.2016.03.028 PMID: 27207067

[365] Ma, Q.; Yu, W.; Dong, X.; Wang, J.; Liu, G.; Xu, J. Electrospinning preparation and properties of Fe_3O_4/Eu(BA)$_3$phen/PVP magnetic-photoluminescent bifunctional composite nanofibers. *J. Nanopart. Res.,* **2012**, *14*, 1203.
http://dx.doi.org/10.1007/s11051-012-1203-z

[366] Wang, H.; Li, Y.; Sun, L.; Li, Y.; Wang, W.; Wang, S.; Xu, S.; Yang, Q. Electrospun novel bifunctional magnetic-photoluminescent nanofibers based on Fe_2O_3 nanoparticles and europium complex. *J. Colloid Interface Sci.,* **2010**, *350*(2), 396-401.
http://dx.doi.org/10.1016/j.jcis.2010.06.068 PMID: 20650463

[367] Gai, G.; Wang, L.; Dong, X.; Xu, S. Electrospun Fe_3O_4/PVP//Tb(BA)$_3$phen/PVP magnetic-photoluminescent bifunctional bistrand aligned composite nanofibers bundles. *J. Mater. Sci.,* **2013**, *48*, 5140-5147.
http://dx.doi.org/10.1007/s10853-013-7299-4

[368] Ma, Q.; Wang, J.; Dong, X.; Yu, W.; Liu, G. Electrospinning fabrication of high-performance magnetic@photoluminescent bifunctional coaxial nanocables. *Chem. Eng. J.,* **2013**, *222*, 16-22.
http://dx.doi.org/10.1016/j.cej.2013.02.063

[369] Gai, G.; Wang, L.; Dong, X.; Zheng, C.; Yu, W.; Wang, J.; Xiao, X. Electrospinning preparation and properties of magnetic-photoluminescent bifunctional bistrand-aligned composite nanofibers bundles. *J. Nanopart. Res.,* **2013**, *15*, 1539.
http://dx.doi.org/10.1007/s11051-013-1539-z

[370] Ma, Q.; Wang, J.; Dong, X.; Yu, W.; Liu, G.; Xu, J. Electrospinning preparation and properties of magnetic-photoluminescent bifunctional coaxial nanofibers. *J. Mater. Chem.,* **2012**, *22*, 14438-14442.
http://dx.doi.org/10.1039/c2jm32043f

[371] Ma, Q.; Wang, J.; Dong, X.; Yu, W.; Liu, G. Magnetic-upconversion luminescent bifunctional flexible coaxial nanoribbon and janus nanoribbon: One-pot electrospinning preparation, structure and enhanced upconversion luminescent characteristics. *Chem. Eng. J.,* **2015**, *260*, 222-230.
http://dx.doi.org/10.1016/j.cej.2014.09.033

[372] Xi, X.; Ma, Q.; Dong, X.; Li, D.; Yu, W.; Wang, J.; Liu, G. Flexible special-structured janus nanofiber synchronously endued with tunable trifunctionality of enhanced photoluminescence, electrical conductivity and superparamagnetism. *J. Mater. Sci. Mater. Electron.,* **2018**, *29*, 7119-7129.
http://dx.doi.org/10.1007/s10854-018-8700-5

[373] Xi, X.; Ma, Q.; Dong, X.; Li, D.; Yu, W.; Wang, J.; Liu, G. Peculiarly structured janus nanofibers display synchronous and tuned trifunctionality of enhanced luminescence, electrical conduction, and superparamagnetism. *ChemPlusChem,* **2018**, *83*(3), 108-116.
http://dx.doi.org/10.1002/cplu.201800030 PMID: 31957338

[374] Tian, J.; Ma, Q.; Yu, W.; Dong, X.; Yang, Y.; Zhao, B.; Wang, J.; Liu, G. An electrospun flexible janus nanoribbon array endowed with simultaneously tuned trifunctionality of electrically conductive anisotropy, photoluminescence and magnetism. *New J. Chem.,* **2017**, *41*, 13983-13992.
http://dx.doi.org/10.1039/C7NJ03090H

[375] Camposeo, A.; Jurga, R.; Moffa, M.; Portone, A.; Cardarelli, F.; Della Sala, F.; Ciracì, C.; Pisignano, D. Nanowire-intensified metal-enhanced fluorescence in hybrid polymer-plasmonic electrospun filaments. *Small,* **2018**, *14*(19), e1800187.
http://dx.doi.org/10.1002/smll.201800187 PMID: 29655227

[376] Li, L.; Wang, F.; Lv, Y.; Liu, J.; Bian, H.; Wang, W.; Li, Y.; Shao, Z. CQDs-doped magnetic electrospun nanofibers: Fluorescence self-display and adsorption removal of mercury(II). *ACS Omega,* **2018**, *3*(4), 4220-4230.
http://dx.doi.org/10.1021/acsomega.7b01969 PMID: 31458655

[377] Yang, L.; Ma, Q.; Xi, X.; Li, D.; Liu, J.; Dong, X.; Yu, W.; Wang, J.; Liu, G. Novel sandwich-structured composite pellicle displays high and tuned electrically conductive anisotropy, magnetism and photoluminescence. *Chem. Eng. J.,* **2019**, *361*, 713-724.
http://dx.doi.org/10.1016/j.cej.2018.12.125

[378] Zhou, X.; Ma, Q.; Yu, W.; Wang, T.; Dong, X.; Wang, J.; Liu, G. Magnetism and white-light-emission bifunctionality simultaneously assembled into flexible janus nanofiber *via* electrospinning. *J. Mater. Sci.,* **2015**, *50*, 7884-7895.
http://dx.doi.org/10.1007/s10853-015-9313-5

[379] Guo, D.; Sun, Z.; Xu, L.; Gao, Y.; Dai, M.; Wang, S.; Chang, Q.; Wang, C.; Ma, D. Water-soluble luminescent-electrical-magnetic trifunctional composite nanofibers prepared *via* electrospinning technique. *Mater. Lett.,* **2015**, *159*, 159-162.
http://dx.doi.org/10.1016/j.matlet.2015.06.005

[380] Lv, N.; Ma, Q.; Dong, X.; Wang, J.; Yu, W.; Liu, G. Parallel spinnerets electrospinning fabrication of novel flexible luminescent-electrical-magnetic trifunctional bistrand-aligned nanobundles. *Chem. Eng. J.,* **2014**, *243*, 500-508.
http://dx.doi.org/10.1016/j.cej.2014.01.022

[381] Xi, X.; Wang, J.; Dong, X.; Ma, Q.; Yu, W.; Liu, G. Flexible janus nanofiber: A new tactics to realize tunable and enhanced magnetic-luminescent bifunction. *Chem. Eng. J.,* **2014**, *254*, 259-267.
http://dx.doi.org/10.1016/j.cej.2014.05.142

[382] Ma, Q.; Wang, J.; Dong, X.; Yu, W.; Liu, G. Electrospinning fabrication and characterization of magnetic-upconversion fluorescent bifunctional core–shell nanofibers. *J. Nanopart. Res.,* **2014**, *16*, 2239.
http://dx.doi.org/10.1007/s11051-013-2239-4

[383] Schaer, M.; Crittin, M.; Kasmi, L.; Pierzchala, K.; Calderone, C.; Digigow, R.G.; Fink, A.; Forró, L.; Sienkiewicz, A. Multifunctional magnetic photoluminescent photocatalytic polystyrene-based micro- and nano-fibers obtained by electrospinning. *Fibers (Basel),* **2014**, *2*, 75-91.
http://dx.doi.org/10.3390/fib2010075

[384] Yu, W.; Ma, Q.; Li, X.; Dong, X.; Wang, J.; Liu, G. One-pot coaxial electrospinning fabrication and properties of magnetic-luminescent bifunctional flexible hollow nanofibers. *Mater. Lett.,* **2014**, *120*, 126-129.
http://dx.doi.org/10.1016/j.matlet.2014.01.076

[385] Sheng, S.; Ma, Q.; Dong, X.; Lv, N.; Wang, J.; Yu, W.; Liu, G. Photoluminescence-electricity-magnetism trifunction simultaneously assembled into one flexible nanofiber. *J. Mater. Sci. Mater. Electron.,* **2014**, *25*, 1309-1316.
http://dx.doi.org/10.1007/s10854-014-1728-2

[386] Xi, X.; Ma, Q.; Yang, M.; Dong, X.; Wang, J.; Yu, W.; Liu, G. Janus nanofiber: A new strategy to achieve simultaneous enhanced magnetic-photoluminescent bifunction. *J. Mater. Sci. Mater. Electron.,* **2014**, *25*, 4024-4032.
http://dx.doi.org/10.1007/s10854-014-2124-7

[387] Guo, R.; Wang, J.; Dong, X.; Ma, Q.; Yu, W.; Song, C.; Liu, G. A new strategy to assemble enhanced magnetic-photoluminescent bifunction into a flexible nanofiber. *J. Mater. Sci.,* **2014**, *49*, 5418-5426.
http://dx.doi.org/10.1007/s10853-014-8253-9

[388] Bi, F.; Dong, X.; Wang, J.; Liu, G. Flexible janus nanofiber to acquire tuned and enhanced simultaneous magnetism-luminescence bifunctionality. *J. Mater. Sci.,* **2014**, *49*, 7244-7252.
http://dx.doi.org/10.1007/s10853-014-8431-9

[389] Xue, H.; Sun, X.; Bi, J.; Wang, T.; Han, J.; Ma, Q.; Han, L.; Dong, X. Facile electrospinning construction and characteristics of coaxial nanobelts with simultaneously tunable magnetism and color-tuned photoluminescence bifunctionality. *J. Mater. Sci. Mater. Electron.,* **2015**, *26*, 8774-8783.
http://dx.doi.org/10.1007/s10854-015-3557-3

[390] Wang, L.; Gai, G.; Xiao, X.; Gao, S. Fabrication of magnetic-luminescent bifunctional composite nanofibers *via* facile electrospinning. *J. Mater. Sci. Mater. Electron.,* **2014**, *25*, 3147-3153.
http://dx.doi.org/10.1007/s10854-014-1996-x

[391] Sheng, S.; Ma, Q.; Dong, X.; Lv, N.; Wang, J.; Yu, W.; Liu, G. A single nanobelt to achieve simultaneous photoluminescence-electricity-magnetism trifunction. *J. Mater. Sci. Mater. Electron.,* **2014**, *25*, 2279-2286.
http://dx.doi.org/10.1007/s10854-014-1872-8

[392] Lun, K.; Ma, Q.; Yang, M.; Dong, X.; Yang, Y.; Wang, J.; Yu, W.; Liu, G. Electricity-magnetism and color-tunable trifunction simultaneously assembled into one strip of flexible microbelt *via* electrospinning. *Chem. Eng. J.,* **2015**, *279*, 231-240.
http://dx.doi.org/10.1016/j.cej.2015.05.022

[393] Lv, N.; Ma, Q.; Dong, X.; Wang, J.; Yu, W.; Liu, G. Flexible Janus nanofibers: Facile electrospinning construction and enhanced luminescent-electrical-magnetic trifunctionality. *ChemPlusChem,* **2014**, *79*, 690-697.
http://dx.doi.org/10.1002/cplu.201300404

[394] Song, G.; Li, Z.; Li, K.; Zhang, L.; Meng, A. SiO_2/ZnO composite hollow sub-micron fibers: Fabrication from facile single capillary electrospinning and their photoluminescence properties. *Nanomaterials (Basel),* **2017**, *7*(3), 53.
http://dx.doi.org/10.3390/nano7030053 PMID: 28336887

[395] Zhou, J.; Sun, G.; Zhao, H.; Pan, X.; Zhang, Z.; Fu, Y.; Mao, Y.; Xie, E. Tunable white light emission by variation of composition and defects of electrospun Al_2O_3-SiO_2 nanofibers. *Beilstein J. Nanotechnol.,* **2015**, *6*, 313-320.
http://dx.doi.org/10.3762/bjnano.6.29 PMID: 25821669

[396] Yousef, A.; Barakat, N.A.M.; Amna, T.; Unnithan, A.R.; Al-Deyab, S.S.; Yong Kim, H. Influence of CdO-doping on the photoluminescence properties of ZnO nanofibers: Effective visible light photocatalyst for waste water treatment. *J. Lumin.,* **2012**, *132*, 1668-1677.
http://dx.doi.org/10.1016/j.jlumin.2012.02.031

[397] Han, W.; Ding, B.; Park, M.; Cui, F.; Ghouri, Z.K.; Saud, P.S.; Kim, H.-Y. Facile synthesis of luminescent and amorphous La_2O_3-ZrO_2:Eu^{3+} nanofibrous membranes with robust softness. *Nanoscale,* **2015**, *7*(34), 14248-14253.
http://dx.doi.org/10.1039/C5NR02173A PMID: 26139103

[398] Xia, Z.; Fu, Y.; Gu, T.; Li, Y.; Liu, H.; Ren, Z.; Li, X.; Han, G. Fibrous CaF_2:Yb,Er@SiO_2-PAA 'tumor patch' with NIR-triggered and trackable DOX release. *Mater. Des.,* **2017**, *119*, 85-92.
http://dx.doi.org/10.1016/j.matdes.2017.01.022

[399] Bao, Y.N.; Xu, X.S.; Wu, J.L.; Liu, K.C.; Zhang, Z.Y.; Cao, B.S.; Dong, B. Thermal-induced local phase transfer on Ln^{3+}-doped $NaYF_4$ nanoparticles in electrospun ZnO nanofibers: Enhanced upconversion luminescence for temperature sensing. *Ceram. Int.,* **2016**, *42*, 12525-12530.
http://dx.doi.org/10.1016/j.ceramint.2016.04.156

[400] Liu, M.; Liu, H.; Sun, S.; Li, X.; Zhou, Y.; Hou, Z.; Lin, J. Multifunctional hydroxyapatite/Na(Y/Gd)F_4:Yb^{3+},Er^{3+} composite fibers for drug delivery and dual modal imaging. *Langmuir,* **2014**, *30*(4), 1176-1182.
http://dx.doi.org/10.1021/la500131d PMID: 24432899

[401] Hou, Z.; Li, C.; Ma, P.; Li, G.; Cheng, Z.; Peng, C.; Yang, D.; Yang, P.; Lin, J. Electrospinning preparation and drug-delivery properties of an up-conversion luminescent porous $NaYF_4$:Yb^{3+}, Er^{3+}@silica fiber nanocomposite. *Adv. Funct. Mater.,* **2011**, *21*, 2356-2365.
http://dx.doi.org/10.1002/adfm.201100193

[402] Li, X.; Li, Y.; Chen, X.; Li, B.; Gao, B.; Ren, Z.; Han, G.; Mao, C. Optically monitoring mineralization and demineralization on photoluminescent bioactive nanofibers. *Langmuir,* **2016**, *32*(13), 3226-3233.
http://dx.doi.org/10.1021/acs.langmuir.6b00290 PMID: 27010624

[403] Liu, L.; Zhang, H.; Wang, Y.; Su, Y.; Ma, Z.; Xie, Y.; Zhao, H.; Chen, C.; Liu, Y.; Guo, X.; Su, Q.; Xie, E. Synthesis and white-light emission of ZnO/HfO_2: Eu nanocables. *Nanoscale Res. Lett.,* **2010**, *5*(9), 1418-1423.
http://dx.doi.org/10.1007/s11671-010-9655-5 PMID: 20730130

[404] Bi, F.; Dong, X.; Wang, J.; Liu, G. Coaxial electrospinning preparation and properties of magnetic-photoluminescent bifunctional $CoFe_2O_4$@Y_2O_3:Eu^{3+} coaxial nanofibers. *J. Mater. Sci. Mater. Electron.,* **2014**, *25*, 4259-4267.
http://dx.doi.org/10.1007/s10854-014-2158-x

[405] Zhou, J.-Y.; Chen, Z.-Y.; Zhou, M.; Gao, X.-P.; Xie, E.-Q. SiC nanorods grown on electrospun nanofibers using Tb as catalyst: fabrication, characterization, and photoluminescence properties. *Nanoscale Res. Lett.,* **2009**, *4*(8), 814-819.
http://dx.doi.org/10.1007/s11671-009-9320-z PMID: 20596383

[406] Li, D.; Pan, C. Fabrication and characterization of electrospun TiO_2/CuS micro-nano-scaled composite fibers. *Prog. Nat. Sci. Mater. Int.,* **2012**, *22*, 59-63.
http://dx.doi.org/10.1016/j.pnsc.2011.12.010

[407] Li, X.H.; Shao, C.L.; Liu, Y.C.; Zhang, X.T.; Hark, S.K. Preparation, structure and photoluminescence properties of SiO_2/ZnO nanocables *via* electrospinning and vapor transport deposition. *Mater. Lett.,* **2008**, *62*, 2088-2091.
http://dx.doi.org/10.1016/j.matlet.2007.11.021